Sial, Sara Baber, 2013. Communicating simulated emotional states of robots by expressive movements. Available from Middlesex University's Research Repository.

Communicating Simulated Emotional States of Robots by Expressive Movements

A thesis submitted to Middlesex University in partial fulfilment of the requirements for the degree of Master of Science (by Research)

Sara Baber Sial (Masters by Research)

School of Science and Technology

Middlesex University

September 2013

This work is dedicated to
Mr Muhammad Baber Sial- my husband

Abstract:

This research focuses on the non-verbal emotional communication of a non-android robotic arm used for Human Robot Interaction (HRI). It investigates whether products, by moving in a life-like way, can communicate their emotions and intentions to humans or not. The research focuses mainly on the mechanoid robot (IGUS Robolink) whether it is able to communicate its emotions to the user or not. It further inspects about the motion parameters that are important to change the behaviour of mechanoid robot used.

In this study, a relationship is developed between the motion of the robot and the perceived emotion. The validity of the perceived emotion by the user is later checked using three different emotional models: Russell’s circumplex model of affect, Tellegen-Watson-Clark model and PAD scale. The motion characteristics such as velocity and acceleration are changed systematically to observe the change in the perception of affect caused by the robotic motion. The perceived affect is then marked by the user on all three emotional behaviour models.

The novelty of the research lies in two facts: Firstly the robotic embodiment used does not have any anthropomorphic or zoomorphic features. Secondly the embodiment is programmed to adopt the smooth human motion profile unlike traditional trapezoidal motion used in industrial robots.

From the results produced it can be concluded that the selected motion parameters of velocity and acceleration are linked with the changed of perceived emotions. The emotions at low values of motion parameters are perceived as sad and unhappy. As the values for motion parameters are increased the perceived emotion changes from sad to happy and then to excited. Moreover the validity of perceived emotions is proved as the emotion marked by the user is same on all the three scales, also confirming the reliability of all the three emotional scale models. Another major finding of this research is that mechanoid robots are also able to communicate their emotions to the user successfully. These findings for Human-Robot interaction on user’s perception of emotions are important if robots are to co-exist with humans in various environments, such as co-workers in industry or care-workers in domestic settings.

Acknowledgments:

I would like to thank Prof. Mehmet Karamanoglu, Head of Department of Design Engineering and Mathematics, who helped me in getting through all the process of finalizing my admission and introducing me to this project as well as Dr Aleksandar Zivanovic, my supervisor, who has helped me in achieving all the objectives that were needed to complete this project.

Thanks to all other who are not mentioned here but have supported me in this project and my stay over here. They will be always in my memories.

Last but not the least I would like to thank my husband, Muhammad Baber Sial, my Parents and Dr.Irtiza Ali Shah (NUST), for constant support and making me believe that everything can be achieved if you just put your sincere efforts into it.

Table of contents

APPENDICES

List of figures

List of tables

CHAPTER 1

Introduction

Currently, most robots in industry work independently of humans, due to safety concerns. Robots typically operate in work cells with safety fences surrounding them which shut down the robot if a person enters.

Researchers are now trying to develop effective interaction of robots with humans for different purposes such as entertainment, medical diagnosis, exchange of information and much more. As the robots can move anywhere around offices, hospitals and homes, they need to interact safely with humans rather than being an obstruction or a danger.

In a situation where a robot can choose one of multiple options to achieve its goal, the next movement of that robot might not be clear to a human. For this reason it may cause an accident or it might not be safe to work with robots if a human is not aware of its intentions for the next move. For this reason human-robot interaction is important as one can infer the intention of the robot if the motion is interactive.

The central focus of this thesis is to develop safe human-robot interaction in social environments. This thesis also discusses various emotional models that are relevant for HRI. A design algorithm is proposed for interaction of IGUS robot and guidelines to improve this algorithm for interaction. Several results are presented based upon the experimentation keeping in view the various factors that affect HRI.

1.1 Definition of HRI

M. A. Goodrich and A. C. Schultz (2007) define Human-robot interaction as "A field of study dedicated to understanding, designing, and evaluating robotic systems for use by or with humans".

This human-machine interaction is usually non-verbal communication. As by definition "Non-verbal communication serves as a rich source of information in inter human communication" (Saerbeck and Bartneck, 2010). As the motion in itself contains a lot of information, one can easily predict the physical state intention from the robot's motion. One can relate this non-verbal human-robot interaction with human-animal interaction. Although animals cannot speak human language, or cannot interact with them verbally, but from their gestures and motion they can tell humans their different states of emotions that include happiness, anger, sadness, boredom, hunger and many more.

The "Success of a robotic platform depends upon more than mere task performance." (Saerbeck and Bartneck, 2010). For example, if the robot is programmed for speedy cleaning with fast performance, humans might perceive it as angry or aggressive. So in order for successful and complete interaction with robots, it is necessary to understand how humans perceive their motion and behaviour. The research described in this dissertation focuses on designing an algorithm in LabVIEW that helps the robot to develop and produce expressive and interactive movements to communicate with humans.

Robots now in the market are introduced as co-workers such as KUKA Roboter GmbH (Haddadin et al., 2011) and Baxter (Anandan, 2013) etc. The rapid growing market of HRI give rise to different types of robots. Some developers and researchers believe that humanoid robots are important for natural and effective interaction. As defined by (Bartneck et al., 2006) that "Designing androids with anthropomorphized appearance for more natural communication encourages a fantasy that interaction with robots is thoroughly human like and promotes emotional or sentimental attachments".

Anthropomorphism is a term that is widely used in the robotics world. "Anthropomorphism refers to the attribution of a human form, human characteristics, or human behaviour to non-human things such as robots, computers and animals", (Bartneck et al., 2009). Research has shown that if the interface is humanoid the expectations of humans increases tremendously such that the robot might not be able to fulfil them, while for the machine interface, the level of expectations from robots is lowered (Bartneck et al., 2006). The possible explanation for this situation could be that people look with different aspects towards human and robots. According to the Mori's Uncanny valley theory (Mori, 2005) the degree of empathy increases as the robot becomes more human-like.

1.2 Types of robots

- Android
- Machine robots

These are two main kinds of robots used in the industry and for research. The robots that look like a machine without any anthropomorphic or zoomorphic features are called as machine robots. Robots, especially androids, are being developed as a helpers and co-workers as well for commercial purpose where they are used as toys and for other household purposes. These robots look like humans or animals. They are further divided in the categories of anthropomorphic and zoomorphic robots that are explained below:

Anthropomorphic robots have human like appearance like facial expressions, humanoid head mounted on a neck with eyes and ears, skin etc. These are also known as humanoid robots. Some popular anthropomorphic robots are: PKD, Tron-X, TOPIO ("TOSY Ping Pong Playing Robot") and many more. These robots are shown in Fig. 1.1

(a) (b) (c)

Figure1. 1 : PKD, Tron-X, TOPIO android robots (dick, 2013)
Fig. 1.1(a) shows a PKD robots sitting and staring, Fig. 1.1(b) shows Tron-X interacting with environment and Fig. 1.1(c) shows TOPIO playing table tennis

Another type of android robot are one that looks like animals (Boris, 2003). Zoomorphism refers to the shape of something in form of animals. These robots raise the level of expectations because of their appearance as compared with machine interface robots. Some of the famous zoomorphic robots are: Sony AIBO, Lamprey etc. These can be seen below in Fig. 1.2.

Research and questionnaires have shown that people look differently towards anthropomorphic and zoomorphic robots. Bartneck et al., (2006) have carried out research in which they have concluded that "Because ABIO is a zoomorphic robot, not a humanoid, we believe that people did not expect it to demonstrate a very good performance on task".


(a) (b)

Figure1. 2: Famous zoomorphic robots (Gizmag, 2002)
Fig.1.2 (a) represents AIBO that resembles a dog and Fig.1.2 (b) represents a zoomorphic robot that resembles a snake

1.3 Socially evocative robots

Traditionally the term 'social robots' was used for multiple robots working together. There are a lot of challenges that are faced in the research of Human-Robot interaction in terms of nature of interaction and social behaviour (Dautenhahn, 2007). In today's research world this term is usually used to differentiate between human-interactive anthropomorphic robots from other type of robots (Breazeal, 2003). Recent commercial and industrial applications are emerging where human robot interaction is an important aspect of robotics.

There are several subclasses of social robots such as anthropomorphic, zoomorphic, caricatured and functional (Fong et al, 2003). Entertainment robots like AIBO, Furby etc. are well-known. Similarly Lego Mind-storm kits are popular but are aimed more at the educational market.

The interactive capabilities of these robots are limited, but this is quite motivational for carrying out further research in this area. These are socially evocative, socially communicative, socially responsive, and sociable as described by Breazeal in her paper (Breazeal, 2003).

1.4 Natural movements in human versus industrial robots

Most industrial robots focus only at the high precision of the end effector reaching the target position and typically, use a trapezoidal velocity profile (see Fig. 1.3).

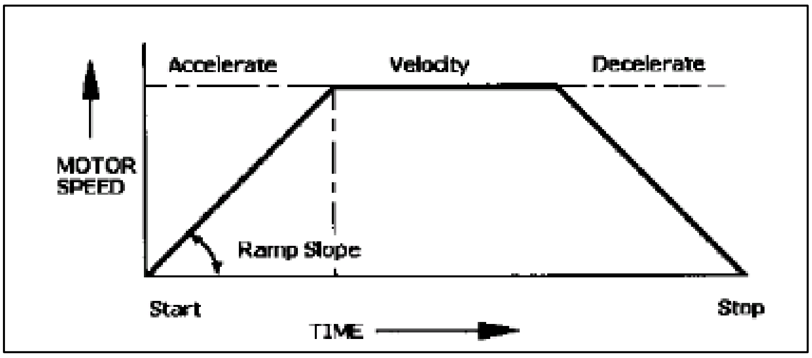

Figure1. 3: Typical motion of industrial robot (Sandin, 2003)

Fig. 1.3 shows that the robot motion profile is quite sharp. So if the robots have to work as co-workers with humans in industry, the motion is quite unpredictable, because it appears jerky and “un-natural” (Flanagan et al., 1990). It is proposed that if a robotic system adopted a human profile for its motion, it would appear to move more “naturally”, which might make it safer to work together with humans (Gaertner et al., 2010). The velocity motion profile of human limb movement is a bell shaped-smooth curve without the sharp edges seen in the profile of industrial robots. Natural human movements for position, velocity and acceleration profile are shown in Fig. 1.4(Gaveau and Papaxanthis, 2011).

The process of trajectory formation in human arm movements is more complex than simply alerting between the equilibrium positions. For example it is proved that if the arm is displaced from its normal trajectory during movements, it will not return to initial or final equilibrium positions but will move to points intermediate between them (Bizzi et al., 1984).

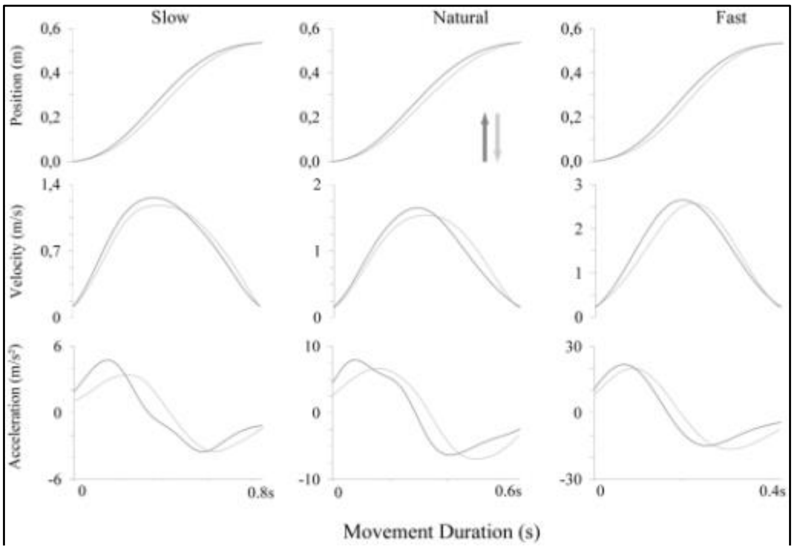

Figure1. 4: Natural human movements (Gaveau and Papaxanthis, 2011)

The aim of this research is to program a low-level control system for the given robotic platform in order to develop a motion profile that resembles human's motion as in Fig. 1.4.

1.5 Commercial applications of robots

Commercial robotic applications are now widely using robot-robot and human-robot interaction technologies (Koeppe et al., 2003). Although the capability of android robots is restricted in terms of interaction with humans, it is a rapidly growing field of research. These robots are not only used for entertainment purposes but also have several other applications in industry. Some of the popular interactive robots are as shown in Fig. 1.5 to 1.8.

1.5.1 MINERVA museum tour-guide robot

This is a popular interactive tour-guide robot used in the Smithsonian museum. During the interaction of two weeks, it met thousands of different people traversing more than 44 km at speeds of up to 163 cm/sec (Thrun et al., 1999). The purpose of robot was to describe the exhibits to visitors.

Figure1. 5: MINERVA famous tour guide robot (Thrun et al., 1999)

1.5.2 Nursing robots

Robots are now increasingly used for nursing and caring applications. The tasks of these robots include helping the elderly to move around in a room, taking them to toilets, helping them to lay down etc. RIBA is one of the well-known examples of nursing robots which resembles a friendly bear.

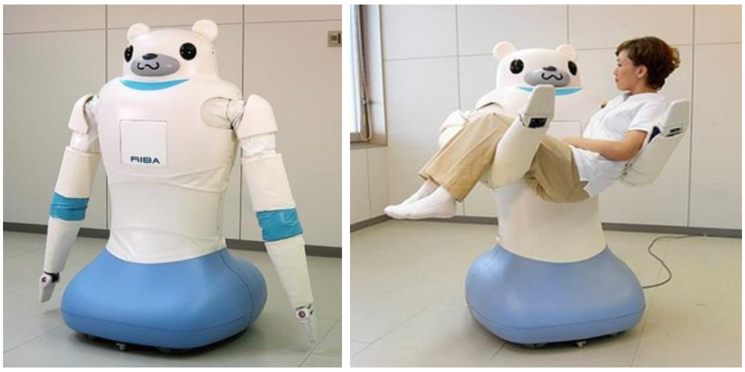

Figure1. 6: RIBA- a famous nursing robot (Uno, 2009)

1.5.3 NASA humanoid robot

NASA developed a humanoid robot which acts as an assistant for astronauts. The fame of these robots is not only because of their ability for carrying out their task but also in the fact of how they interact and behave with people around them. Fig. 1.7 shows NASA humanoid robot.

Figure1. 7: NASA humanoid robot (NASA, 2013)

1.5.4 KISMET

Kismet (see Fig. 1.8) is a robot that is used for human-robot interaction. It has got various input features for interacting with human beings. It can produce several facial expressions, voices and other actions. To produce facial expressions it has got eyebrows, lips, jaws and various other features.

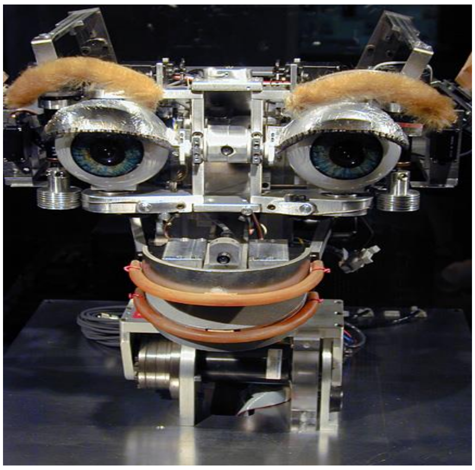

Figure1. 8: KISMET used for HRI research (Menzel, 2013)

1.6 Comparison of different robots

There are different kinds of robots available for various purposes. The usefulness of the robot depends on how they interact and sense the environment and surroundings around them (Jason, 2007).The design of robot influences the human-robot interaction significantly (Forlizzi and DiSalvo, 2006). Table 1.1 shows different kinds of robots that are used in industry, entertainment and in several other fields.

Robots	Type of robot	Use
KISMET	Android	Used for HRI, produce various facial expressions
NASA	Humanoid	Acts as an assistant for astronauts
Geminoid TMF	Humanoid	Mimics a person's facial expressions
MOTOMAN	Robotic arm	Industrial robot used for painting
AIBO	Zoomorphic	Used for interaction and entertainment
SCARA	Robotic arm	Used for industrial purposes
Micro Flying Robot	Mechanoid	Used as a flying camera
MINERVA	Mobile	Used as a tour guide in museum
PUMA	Robotic arm	Used for industrial purposes
RIBA	Zoomorphic	Used for nursing purposes
Robocup	Humanoid	Used for playing football

Table1. 1: Comparison of different robots

1.7 Summary of the chapter

This chapter reviews the robots that are socially interactive and highlights the importance of human-robot interaction in today's world. There are several types of robots discussed in this chapter. It discusses how a robot can have "natural" movements that can be anticipated by the humans. It then compares various different types of robots and there use in industry as well as domestic fields.

The next chapter discusses how these robots can be used for the effective communication by their expressive movements.

CHAPTER 2

AFFECTIVE EXPRESSIONS OF MACHINES

2.1 Expression of emotion

Recent research in human-robot interaction has shown that emotions play an important role in designing any interface, as the machines are now perceived as social actors (Nass, 1996). As explained by (Picard, 1997b), people are usually seen expressing their frustration to computers when they are not working by shouting or yelling at them.

However, the distinctness of the expression depends strongly on the type of embodiment. So if the embodiment is a humanoid rather than machine interface robot, it will express its emotions more prominently. Research in the field of HRI shows that these emotional capabilities play a significant role in decision making (Barnes, 1996) and problem solving (Fesit, 1994).

2.2 Types of communication

There are mainly two kinds of communication:

- Verbal communication
- Non-verbal communication

Communication that involves speech is called verbal communication and is a natural way for humans to express their emotions. Thrun et al., (1999) states that "The most influential parameters for emotional expression in speech is pitch (level, range and variability)". Humanoid robots are usually capable of verbal communication, but what if the robots cannot express their emotion by speech? Body language and gestures are considered to be an important aspect for expression of emotion (Thrun et al., 1999).

The main emphasis of this thesis is on non-verbal and behavioural communication, as the type of embodiment used for this project is a robotic arm without the capability of verbal communication. Mime artists are good example of non-verbal communication through their body gestures and facial expressions. Body gestures are an important aspect as the embodiment used in this research does not have any anthropomorphic or zoomorphic features for expressing its emotions.

2.3 How machines express emotions

The main focus of this research is on designing expressive behaviours of robots that have machine interface like IGUS robotic arm shown in Fig. 2.1. The reason for choosing this specific platform of mechanoid robot rather than some industrial embodiment is because one can get into the low level programming of this kind of robot and make it move in a way that is natural and closely resembles with human movements. The robots are now widely used to express their emotions by movement (Matsumaru, 2009). Physical movements hold great importance for the emotional interaction between humans and products (Qassem at el., 2010).

Figure2. 1: IGUS robotic arm (Fontys, 2013)

The feature of being interactive for this robotic arm actually means that it should exhibit some expressive movements based on various parameters, as expressive movements are the main content for non-verbal communication. People usually interpret motion pattern based on emotions (Heider and Simmel, 1944). The motion pattern and movement trajectory of the robot plays a substantial role in how a user perceives its emotions. This movement of the robot is actually interpreted as an emotional behaviour. There are several motion features that are the cause of expressing emotions (Saerbeck and Van Breemen, 2007). According to the hypothesis if we change these motion parameters, the perceived emotions for the particular embodiment is also changed.

2.4 User Perception of emotions

User perceptions of the emotions of robots depend on several factors. Research in the field of HRI has introduced several models that are used for perception of emotions. An evolutionary model suggests that the ability to correctly judge the emotions and to perceive intentions correctly is important in order to integrate robots effectively in everyday life (Saerbeck and Bartneck, 2010). For example one can easily tell the emotions of a mountain lion by observing it and say whether it is angry, hungry for prey, relaxed, mating or wandering (Blythe et al., 1999). According to another model, social reasoning also contributes a lot towards the emotional behaviour (Wondolowski and Davis, 1991).

However, anthropomorphism also contributes towards the perception of emotions. If the robot has high anthropomorphism (i.e. very close resemblance to humans), the expectations of the user are high for this robot as compared to zoomorphic. However comparing a zoomorphic and machine like robot, the expectations are further lowered with a robot that looks like a machine. This behaviour of user perception for emotions is explained by the Uncanny Valley theory (Mori, 2005). The factors used in this research to animate various emotions are mainly velocity, acceleration and spline motion of the joints of the robot. These features and the scales used for them will be discussed in later chapters.

2.5 Summary of the chapter

This chapter discusses how a robot can use it's movements to express the emotions and describes the reason for choosing a mechanoid platform rather than an industrial robot. Effect of motion parameters on the perceived behaviour is discussed in this chapter. It highlights the fact that how a user will perceive the emotions in machines according to Uncanny Valley theory and how the level of expectation is linked with the type of embodiment.

The next chapter will focus in detail on the hardware and software platform that is used for expressing the emotional behaviour of machines for this research.

CHAPTER 3

HARDWARE AND SOFTWARE PLATFORM FOR RESEARCH

3.1 Introduction of hardware "IGUS-Robolink"

IGUS is a German company specializing in plastic bearings and cable management systems etc. One of their products is the Robolink system, which is a range of configurable joints and links that allows customers to specify the number of joints, lengths of links, etc. The joints are actuated by flexible cables which are routed through the hollow links (IGUS, 2012a). They produce four different types of joints. Optionally, incremental encoders may be specified that are used for tracking the position of joint. The system is not supplied with end effectors, but different types of end effectors can be fitted at the end of the last plastic link, like cameras, grippers, light actuators etc. The articulated arm is designed in a way that the cables for these actuators can be routed through the body of robot.

The Robolink system is basically a toolbox of mechanical components that can be put together to make a robotic arm. This product was launched three years ago and the first mechanical component of this toolbox was a plastic link with tendon drive (IGUS, 2009).

The main parts of this robotic arm are: stepper drives, drive units for these motors, a cable system to deliver motion in the articulated arm, incremental encoders, plastic joints and rigid links. The features and working of each of these will be discussed in detail.

The particular articulated arm that was used for this project had 5DOFs, with three rotational and two pivot joints. It had three link rods and also had incremental encoders. Fig. 3.1 represents the different parts of the IGUS articulated robotic arm.

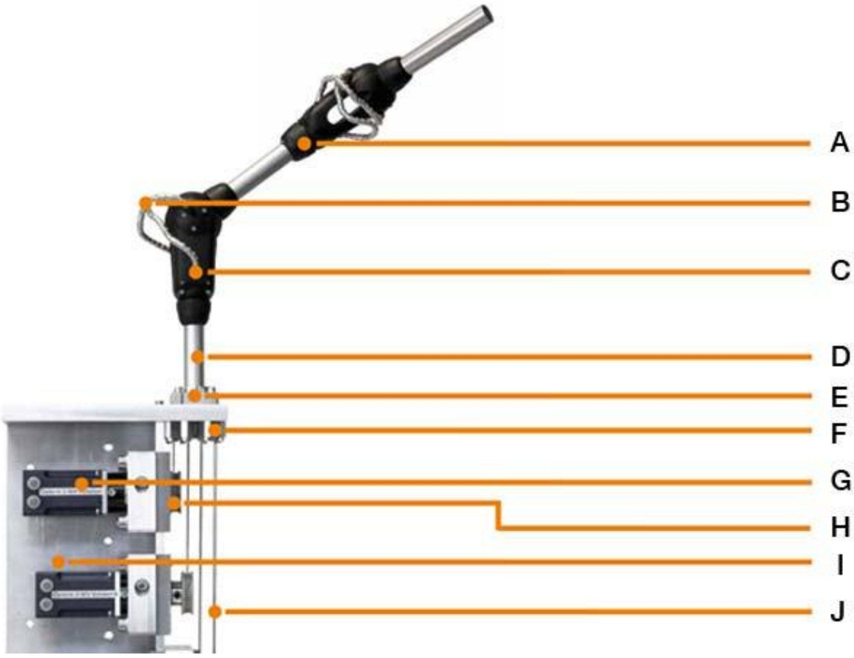

Figure3. 1: IGUS articulated arm with labelling of different parts (IGUS, 2013)

A. Joint

B. Robolink bowden cable

C. Robolink multi axis joint

D. Robolink connecting tubes

E. Robolink flange shaft support

F. Movement through pulleys

G. IGUS stepper motor

H. Robolink drive wheel

I. Housing drive unit

J. Dyneema ropes

3.2 Features of IGUS-Robolink used for HRI

There are several features of the Robolink system that makes them suitable for the reasearch described in this dissertation.

The joints in these articulated arms are made of polymers. The reason for using plastic is that it is light in weight (only 350 grams), the joints do not need any kind of lubrication, they are low in price and have longer life.

These arms are compact because each joint unit has 2 DOF, one pivoting and one rotational. Also the link length is configurable because the links are simple tubes.

The tendon drive system for these robotic arms makes it easy for the designer to choose the drive and control elements freely. For position accuracy and precision, angular positioning indicators can also be ordered with these arms that have a precision of 0.07 degrees.

Another feature of this robotic arm is that the drive system is freely selectable. The joints are driven by a flexible sinews (rope) system. The tightness of these ropes drive is adjustable. Moreover alternate drive or control systems are very easy to introduce in these articulated arms. Stepper motors were used in the system used for this research. The detail on mechanical parts and joint types of the IGUS-Robolink are attached in appendix M.

3.3 Specification of robotic arm used

The weight of the arm is 350g including the plastic joints, connecting tubes and ropes. The joint is made up of fine polyamide 2200 (IGUS, 2013.). The specific arm used in this research has a part number of RL-50-DOF5-28-WS. The component number for this robotic arm is TL-002-001. 001 and 002 represents the joint versions. Rl-50-002 WS is the one with angle sensors and rotation allowed by this is +130/-50°. Whereas for Rl-50-001 the rotation allowed is +/-90°. WS in the product code indicates that the joints are equipped with angle sensors. DOF5 represents that it has 5 degrees of freedom, with the base joint as a rotational. Of the remaining joints, two are pivot and two are rotational joints. There are three 0.4m links. The specifications of particular arm that is used for research is stated below.

The arm that is used in the research of this project has 5 DOFs. Fig. 3.2 represents the DOF for specific arm that is being used:

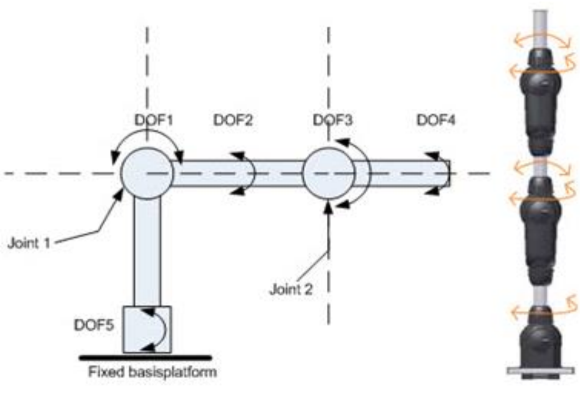

Figure3. 2: Research platform used (Fontys, 2013)

3.4 Kinematics of robot

Denavit-Hartenberg method was used for calculating the kinematics of the IGUS robot that is used in the research. This method is widely used to determine the direct kinematics of robot by specifying some of the parameters. According to DH conventions the coordinate frame of link i+1 with respect to the coordinate frame of link i can be represented by following matrix (NI, 2013).

$$ {}^{i-1}A_i = \begin{bmatrix} \cos\theta_i & -\sin\theta_i \cos\alpha_i & \sin\theta_i \sin\alpha_i & a_i \cos\theta_i \\ \sin\theta_i & \cos\theta_i \cos\alpha_i & -\cos\theta_i \sin\alpha_i & a_i \sin\theta_i \\ 0 & \sin\alpha_i & \cos\alpha_i & d_i \\ 0 & 0 & 0 & 1 \end{bmatrix} $$

DH parameters calculated for IGUS robot are shown in Table 3.1 below:

Link Number	Length (meters)	Twist angle (radians)	Offset distance (meters)
1	0.4	0	0
2	0	-1.5	0
3	0.4	0	0
4	0	1.5	0
5	0.4	0	0

Table3. 1: DH parameters of IGUS robot 5DOF

3.5 Introduction to LabVIEW

LabVIEW stands for Laboratory Instrument Engineering Workbench. This system was developed when National instruments started to look for some way by which they could reduce the time that is required to program instrumentation systems (Travis and Kring, 2013).This graphical programming language is used in academic, research, industry and many more fields.

It is multi-purpose software that can be used for testing and measurement, monitoring, simulation and for process control and automation. Its popularity is due to unparalleled connectivity to instruments, powerful data acquisition capabilities, natural dataflow based graphical programming interface, scalability, and overall function completeness (NI, 2011a).

LabVIEW has the capability of running on multiple devices. The coding is done by the user in an environment provided by LabVIEW software and then it is deployed on the target. Some of the commonly used targets in LabVIEW are CompactRIO which are basically programmable automation controllers, programmable device arrays (PDA's), real time operating system (PXI), microcontrollers, or field programmable gate arrays (FPGAs)(Folea,2011).

There are many built-in libraries, examples, software drivers for data acquisition that are available in LabVIEW. LabVIEW has toolkits used for signal processing, data analysis, mathematics, real-time programming, simulation, robotics and many more. The popularity and expansion of LabVIEW in market, academics, research and other fields for engineering, design, simulation, and testing etc. can be seen in Fig. 3.3.

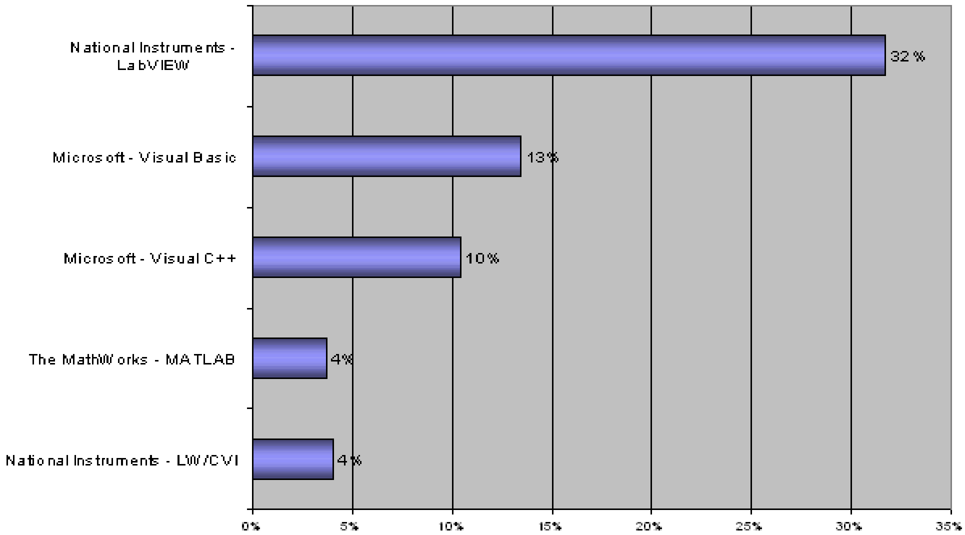

Figure3. 3: Usage popularity of LabVIEW compared with other software (NI, 2013b)

According to the research by the producers of LabVIEW (NI, 2009) "In 2004, National Instruments measurement hardware provided customers with more than 6,000,000 virtual instrumentation measurement channels. From low cost USB data acquisition, to process control vision systems and image acquisition, to RF measurement at 2.7GHz, to GIPB bus communication, National Instruments has shown more than 25,000 companies that it offers the measurement hardware and scalable hardware platform required to complete virtual instruments"

3.5.1 Reasons for using LabVIEW

Some of the reasons why this software is chosen over others for research purposes are: (Ertugrul, 1999):

- It allows the user to develop his/her own virtual environment for programming and provides a user-friendly interface that is economical and adaptable

- It has some multimedia ability which makes it even more friendly (e.g. adding voices, warnings etc.)
- It generates a report file at the end in notepad format that is easy to understand by the user
- Its capable of printing a specific part of the program that user wants
- Capability of placing access limitations for others on different parts of the code
- Can link to other popular software like Pro-E etc.
- Provides many examples, tutorials and test programs

Beside all these, it provides the user with the option of thousands of modules and toolkits of robotics, instrument and measurement, kinematics etc.

3.6 Selection of NI hardware platform

There are many hardware platforms available from National Instruments that can be used for the purpose of research for connecting with IGUS-Robolink. The one selected is CompactRIO 9074, which is a high performance programmable automation controller (PAC).

3.6.1 CompactRIO

"CompactRIO is a reconfigurable embedded control and acquisition system" (NI, 2013a). The hardware platform of CompactRIO contains slots for various input/output modules, a reconfigurable FPGA chassis, with an embedded controller. It can be used with LabVIEW for a variety of different applications like measurement and testing, robotics, embedded control etc.

Figure3. 4: CompactRIO platform (NI, 2013a)

The specific CompactRIO used for this research is cRIO 9074 see Fig. 3.5, with the following features (NI, 2012a) as stated below. The datasheet is attached in the appendix H:

Figure3. 5: CompactRIO 9074 (NI, 2012c)

This is an integrated system that combines a real time processor and a reconfigurable Field Programmable Gate Array (FPGA) within the same chassis. The real time processor is 400MHz with 2M gate FPGA. There are eight slots available in the chassis for different input output modules. The DRAM provided by the system is 128MB for embedded operations and 256MB of non-volatile memory for data logging. For network programming, communication it is provided by two 10/100 Mb/s Ethernet ports. Properties of the CompactRIO used in this research are in appendix J.

3.6.2 Stepper drivers 9501

NI 9501 is a C-series stepper driver that can be used with cRIO 9074 to operate stepper motors used in the IGUS Robolink. The datasheet for this module is in appendix G.

Figure3. 6: Stepper driver 9501(NI, 2012c)

This driver is equipped with all of the features to control and power the stepper motor. It is capable of interfacing with the FPGA in the chassis, and then controlling the stepper motors by step and direction in programming. Fig. 3.7 shows the complete architecture of NI 9501 with CompactRIO.

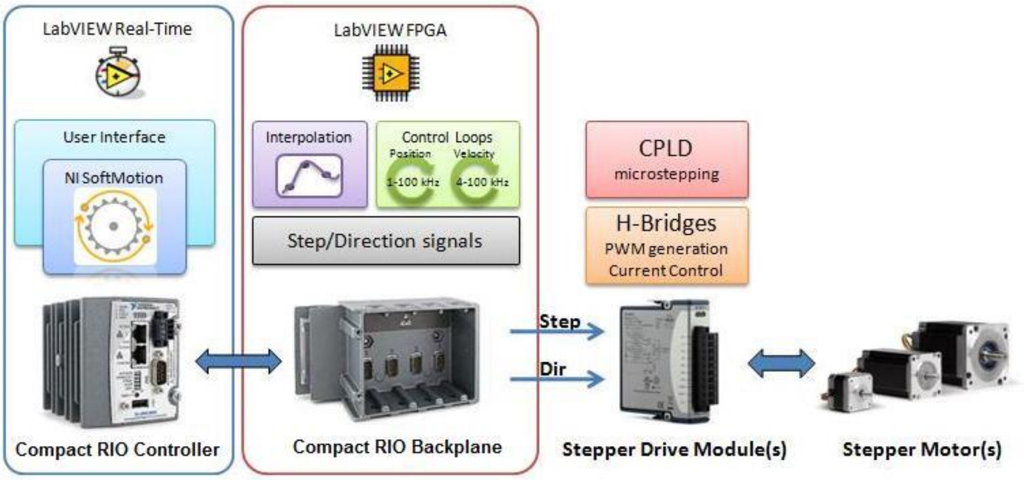

Figure3. 7: Complete architecture with NI 9501 (NI, 2011b)

The user will be sending command from the LabVIEW software and the code will be deployed on FPGA controller. This will send signals to the stepper modules inserted in the backplane of cRIO 9074 that in return sends the direction and step signals to the motors attached with IGUS-Robolink. This allows the motors to move independently to their respective positions.

3.7 Connecting cRIO 9074 and IGUS-Robolink

For setting up and configuring the cRIO 9074 for this research project, specific hardware and software were installed. The process for wiring the chassis and connecting to cRIO is in appendix L. The hardware and software setup required for this is listed below:

3.7.1 Hardware required

The following hardware was required to be installed:

- Power supply for the controller
- Ethernet connection cable or cross over cable
- C Series stepper drives modules. Datasheet is attached in the appendix G
- 8 Channel, 5V/TTL high speed bidirectional digital input/output module. Datasheet is attached in the appendix I

- Power supplies for the connection of robotic arm and drivers

3.7.2 Software required

The following software was required:

- NI LabVIEW 12.0 (or any version 8.6 or later)
- NI LabVIEW Real time module 12.0 (or any version 8.6 or later)
- NI LabVIEW FPGA module 12.0 (or any version form 8.6 or later)
- NI-RIO 12.0 (or any version 8.6 or later)

3.7.3Hardware connection

Once the controller is configured successfully by installing the specific hardware and software as mentioned above, IGUS-Robolink was connected with NI hardware then. There were a total of 8 slots available on the chassis, of which 5 were used by NI 9501 stepper motor drivers, one for each joint of the robotic arm. The pin configuration for connecting the motors with the drive modules is in appendix K.

All the joints of the robotic arm used in this research were provided with incremental encoders as discussed earlier, in order to keep track of the position of the joints. The module used for the connecting this incremental encoder to the CompactRIO was NI 9401 shown in Fig. 3.8. The datasheet of this module is attached in the appendix I. This is an 8 channels, 5V/TTL high-speed bidirectional digital input/output module connected with the encoder wires of IGUS-Robolink. The whole hardware i.e. NI hardware and IGUS-Robolink is then interfaced with LabVIEW software in order to develop an algorithm that would be able to move the robot in a natural manner to express various emotions to the user.

Figure3. 8: NI module 9401 (NI, 2012d)

3.8 Summary of the chapter

This chapter discusses in detail about the hardware and the software platform that is used for this research. The NI hardware used is cRIO 9074, stepper driver modules 9501 and an encoder module 9401. The reason for choosing this hardware and connecting this with IGUS-Robolink is described in detail. Method of how to interface the whole hardware with the software of LabVIEW is also mentioned. It also highlights the DH parameters used for this specific robot.

The next chapter will discuss the modules and methods used for designing of the algorithm for this specific platform.

CHAPTER 4

DESGIN OF ALGORITHM USING LABVIEW

4.1 Introduction to design of algorithm

There are basically two main code files that are programmed. One is called the FPGA VI, which is deployed on the hardware of the cRIO by compiling the code and generating results. The other VI is the Real Time (RT) VI. This VI serves an interactive panel for the user to operate the platform.

There are several main modules used for programming of both of these VIs as named below:

- NI LabVIEW FPGA Module
- NI LabVIEW Real Time Module
- NI LabVIEW SoftMotion Module
- NI LabVIEW Robotics Module

These modules will be discussed in detail one by one in this chapter.

4.2 NI LabVIEW FPGA module

The main purpose of using FPGA is to achieve the parallelism in dataflow. NI offers the FPGA based reconfigurable input/output hardware cRIO to achieve this concept of parallelism using graphical programming.

The same graphical interface is used for programming real-time as well as FPGA targets. For this purpose LabVIEW takes its graphical code diagram to different compilers to create an executable file suitable for specific type of hardware. LabVIEW offers FPGAs with millions of gates for complex programming with inherent capacity of parallel programming. The software module used is shown in Fig. 4.1.

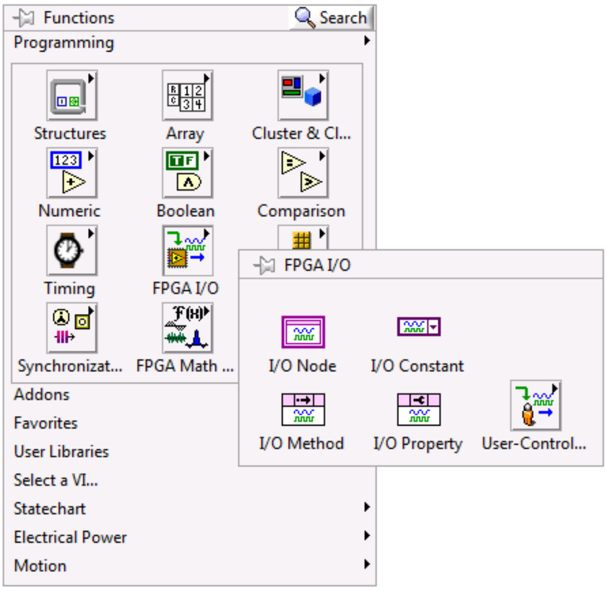

Figure4. 1: FPGA programming palette

Communication of this FPGA VI with the real time host VI is another important aspect of FPGA programming. For this LabVIEW provides different host interfaces. NI offers PC, PXIs, PCIs, and Ethernet enabled hardware that takes care of all the functions and does not require any custom work by the user. The user can focus on algorithm design, whereas the hardware takes cares of things like data communications, direct memory access, registers, bus communication, analog and digital outputs, clocks, interrupts etc.

The current targets for LabVIEW FPGA include the following hardware shown in Fig. 4.2. The rugged platform of cRIO is perfect for standalone and network applications.

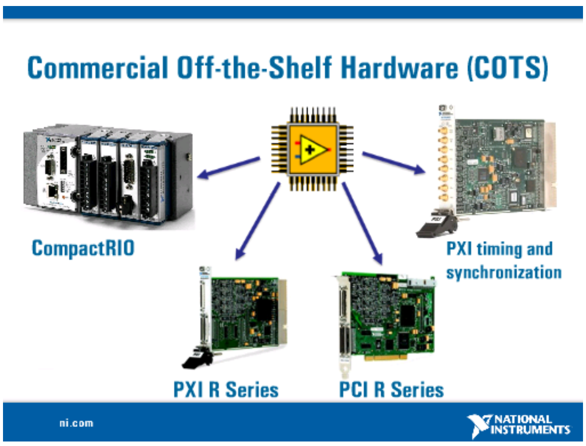

Figure4. 2: FPGA based hardware offered by NI (Kuhlman, 2013)

Some of the common applications of LabVIEW FPGA systems are as follow (Kuhlman, 2013.):

- High speed control
- Smart Data acquisition system DAQ
- Digital communication protocols
- Sensor simulation
- On board processing and data reduction
- Co-processing

The block diagram in Fig. 4.3 explains the deployment and creation of bitmap file for FPGA code:

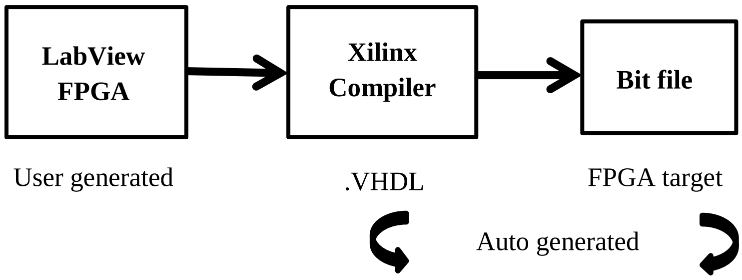

Figure4. 3: Process of code deployment on FPGA

4.3 NI LabVIEW Real-Time module

The operating system is mainly responsible for managing hardware and hosting applications on the computer. The real time operating system does these tasks with high reliability and very precise timings.

NI Real-Time modules give the user the ability to develop a complete and reliable embedded system that is run by the graphical programming platform of LabVIEW (NI, 2013c). The real time hardware systems introduced by LabVIEW are NI CompactRIO, NI Single-Board RIO, PXI, PC and various others.

There are several reasons for using real time system for this project:

- The graphical interface of LabVIEW allows the user to program their tasks more quickly and easily. The same graphical programming platform is used with LabVIEW real-time module to create stand-alone systems.
- The common LabVIEW programming system uses the windows operating system which is not optimized to handle tasks for critical timings over an extended

period of time. This module provides the real time operating system for high reliability and precise timings for the tasks.

○ With this module the user can take advantage of various LabVIEW libraries (e.g. PID, FFT)

4.3.1 Basic Real-Time architecture

Fig. 4.4 shows the basic architecture for real-time module of LabVIEW. The host program develops the network communication with the target program and then executes it on the basis of priority given to the loops by user.

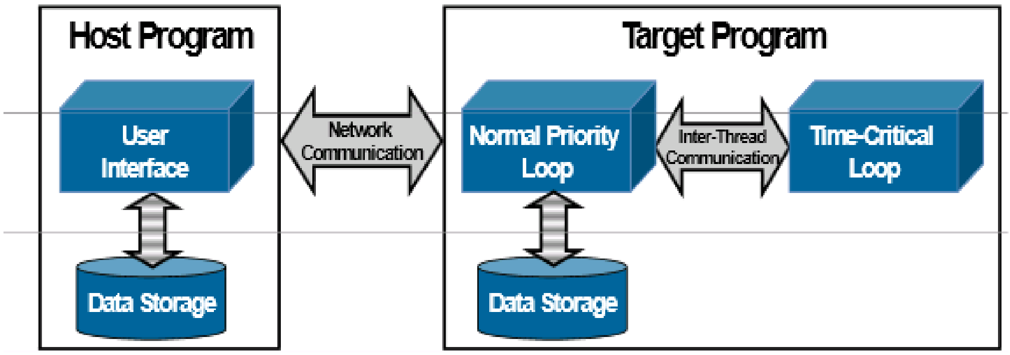

Figure4. 4: Basic architecture (NI, 2013a)

4.3.2 Basic Real-Time toolkits

There are several built-in libraries and toolkits available for real-time programming of LabVIEW that allows the user to concentrate on its logic and make programming much easier. The Fig. 4.5 shows the toolkit used for real-time programming.

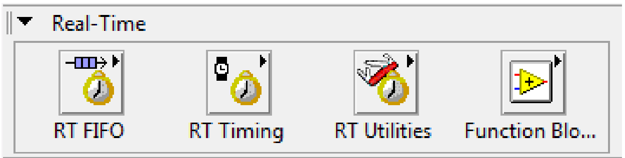

Figure4. 5: RT toolkit

4.3.3 Steps for the development of the Real-time system

The three main steps for developing of the real-time system include (NI, 2013a):

- Development of the application on the host computer i.e. graphical coding for the system
- Downloading of the code to the real-time hardware target

- Execution of the code

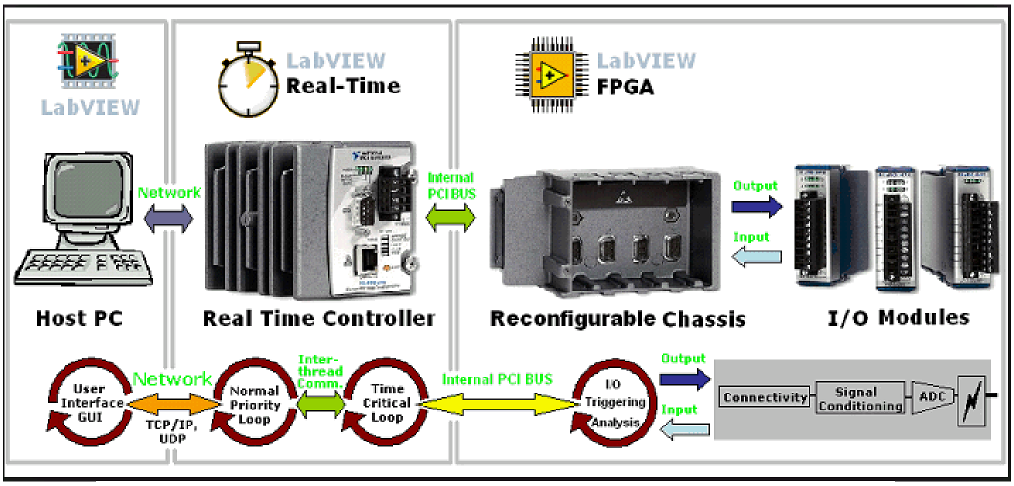

Figure4. 6: Summary of development process (NI, 2013e)

4.4 NI LabVIEW SoftMotion Module

NI has introduced another module called SoftMotion that is compatible with the RT module and FPGA module. This module helps build custom motion control applications by providing functions such as path planning, trajectory generation, position velocity control for various different kinds of steppers as well as servo motors.

The C-Series driver discussed in the chapters above is used for the motion control of stepper motors in this research. This module provides various interactive tools for high level motion functions for simplified development (NI, 2012e).

In this research the main reason for using this module is to create the spline motion for the stepper motors using the 9501driver. The programming palette for soft motion module is shown in Fig. 4.7.

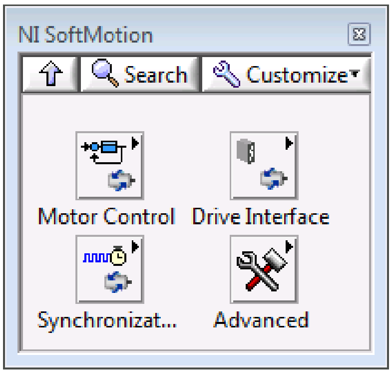

Figure4. 7: SoftMotion palette for programming

In order to control the motion of the stepper motors there is a sub-palette called stepper available inside the motor control. From there the spline motion generation function is used for the motion control of stepper motors. Fig. 4.8 shows the specific palette that is used:

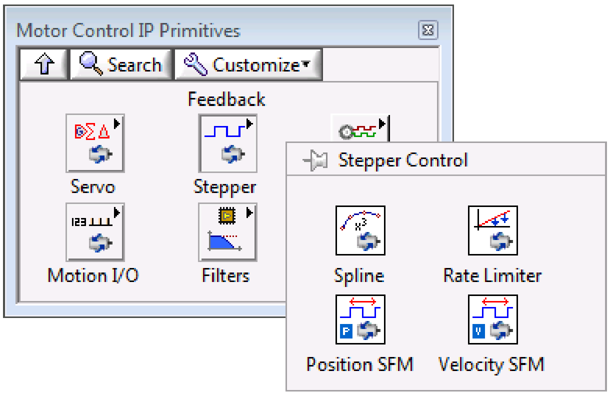

Figure4. 8: Spline generation function

The spline function is used to smooth the motion of the motor. This takes data from spline function and return the step and direction for the operation of motor. Various types of interpolations are available to generate splines like linear interpolation, cubic B spline, and Catmull-Rom spline. Cubic B spline interpolation was used in this research.

Fig. 4.9 shows the stepwise execution of this module. The spline engine and trajectory generation processes are done on the FPGA side whereas the supervisory control is done on the RT side.

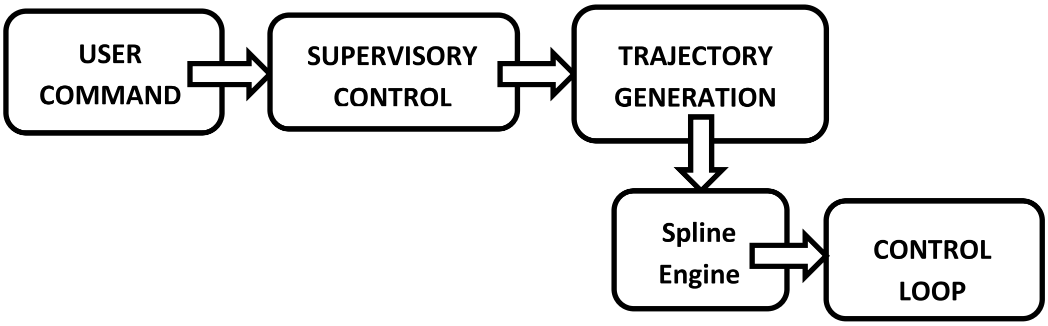

Figure4. 9: Spline generation loop

The user gives commands to the supervisory control loop that is actually the main loop for motion control. This loop monitors inputs/outputs and faults. This part of the code is executed on the RT side. This sends commands to the trajectory generation loop that is actually the path planner. It creates the set points that are used to calculate the interpolated position by the spline engine which results in smooth motion. The control loop then creates a command signal based on the set points generated by the trajectory generation as shown in Fig. 4.10. The user specifies the command from user interface that goes to RT side in supervisory control loop. This sends the signal to FPGA side where trajectory generation process is done and points are interpolated. This sends the command and direction signal to driver modules of the stepper motors and operates the robot.

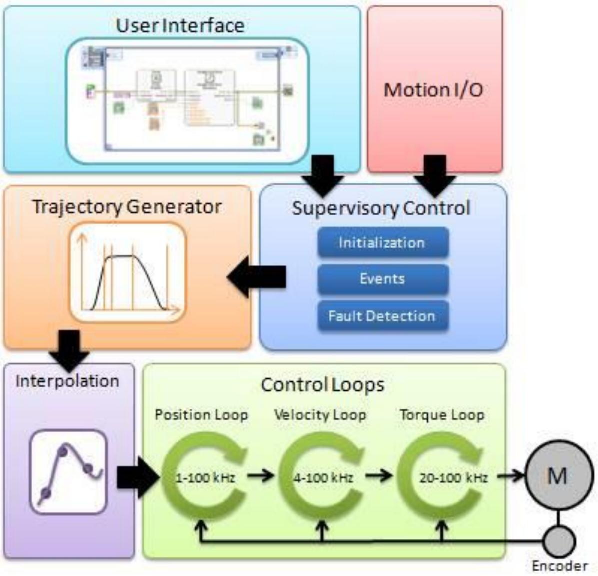

Figure4. 10: Detailed process for Spline generation (NI, 2013f)

4.5 NI LabVIEW Robotics Module

Another important module used for the programming of this project is the Robotics module. This module uses software tools to design autonomous and semi-autonomous systems (NI, 2012f). It includes the following features as shown in Fig. 4.11.

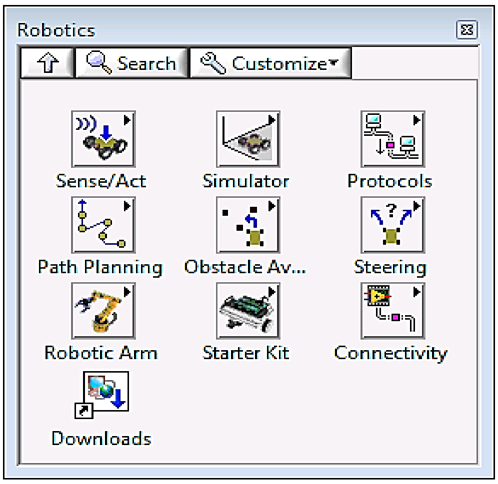

Figure4. 11: Robotics toolkit

The main purpose of the robotics module in this research was to use the inverse kinematics function to generate point-point motion of the robotic arm. The robot moves automatically to the X, Y, and Z coordinates given by the user provided it is reachable and within the joint limits of the robotic arm. Fig. 4.12 shows the function of inverse kinematics in the robotics module.

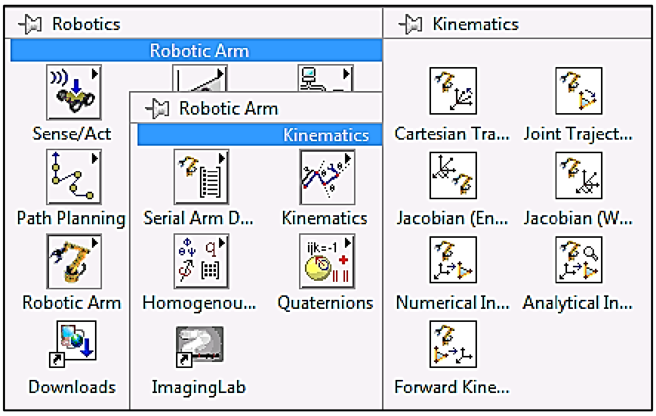

Figure4. 12: Function of inverse kinematics

Fig. 4.13 shows the front panel for setting the parameters for the inverse kinematics. The parameters shown in the figure are for the specific robot that was used in this project.

The joints types are set to be revolute as all five of the joints of the robot are revolute. The twist angle between the first two and last two joints is -1.5radians or 90°. The length of the links for each of them is 4000mm or 0.4m. For a random point using these parameters, Fig. 4.14 is generated by the inverse kinematics module.

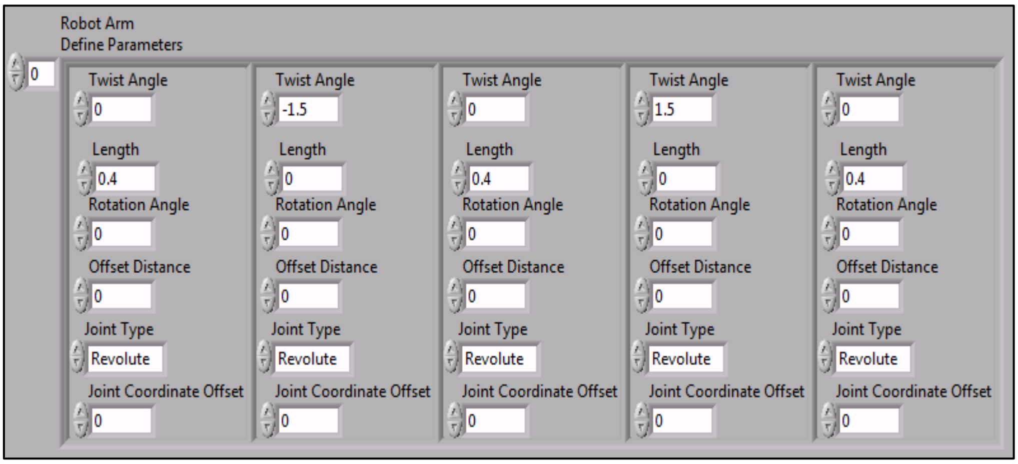

Figure4. 13: Parameters for inverse kinematics of robot

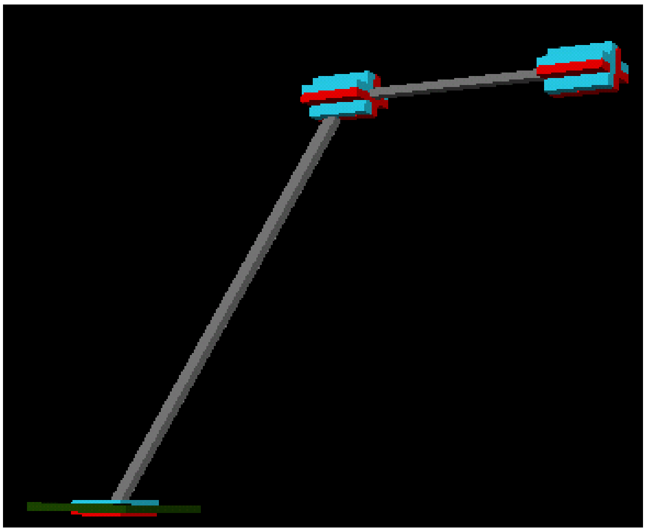

Figure4. 14: Serial arm with 5 revolute joints

This part of code is later integrated in main code that is attached in the appendix J. Thus, using the inverse kinematics module of LabVIEW it allows the user to input the spatial coordinates so that the robot moves to the position specified by the user based on the constraints applied.

4.5.1 Stages involved in implementing inverse kinematics

The code development for the research initiated from building up the logic for forward kinematics of the robot. The logic was developed so that user will be entering 5 different angles for each of the motor. The motors will move to the respective positions as entered by the user independently. However the motion obtained out of this was a typical trapezoidal motion with sharp edges. The aim was to smooth down the motion so that the robot moves in a natural way. For this reason SoftMotion module of LabVIEW was used. However another approach of PID was also considered before applying the SoftMotion module.

Later for getting on to the inverse kinematics of the robot, the model as shown in Fig. 6.17 was developed in “Robot simulation model builder” in LabVIEW keeping in regard the original parameters. However the problem of Direct Memory Access (DMA) channels was encountered while developing logic for inverse kinematics. As cRIO 9074 offers only 3 DMA channels for the transfer of data between RT to FPGA side. To move 5 motors independently, either 5 DMA channels were required or a logic should be developed that can send data from same DMA channel but independently for different motors. Different methods that include interleaving and decimating of data, join-split function for data, 2D array approach and clusters etc. were used. The first two methods failed as they were not moving motors independently. As soon as the array data of one motors finishes the other motor stops. However the methods mentioned later were not supported on FPGA side.

Therefore logic was developed so that the smaller array would be sending '0' as its data elements till the larger array is completely transferred to FPGA side. Thus making the motors move independently to different positions.

Another major problem encountered was the space on FPGA controller after developing the correct logic for inverse kinematics. This was resolved by optimizing area on FPGA before compiling the code and changing the virtual RAM of computer. Later the Robotics and SoftMotion were integrated in the main code.

4.6 Summary of the chapter

This chapter highlights the modules that were used for the logic development of this research. It explains about the spline engine generation and the trajectory loop process that is done on FPGA side. It discusses how the forward and inverse kinematics for point-point motion was developed and the problems involved in developing the logic for inverse kinematics. The code for the process is attached in appendix O.

The next chapter will discuss in detail the core research methodologies that were used for user's perception of emotions for specific gestures of the robot. The reasons for choosing those specific models are also discussed in next chapter.

CHAPTER 5

CORE RESEARCH METHODOLOGY FOR PERCEPTION OF ROBOT EMOTIONS

5.1 Core concept for research

There are various different emotional models that are introduced by psychologists for verbal as well as non-verbal communication of machines e.g. Russell's circumplex model of affect, PANAS, PANAS-X, PAD scale, SAM scale, Schimmack and Grob model etc. (Tuomas at el, 2011). Most of these models interpret the emotions of the machines based on the subjective opinion of people looking at them.

Affectionate robotic pets, household robots, nursing robots and many other are creeping in our lives very fast. The future is crowded with emotive humanoid robot companions (Dautenhahn at el., 2009). Because of this growing importance of human interaction with robots and the idea of perceiving these robots as social actors (Dautenhahn K., 1999)., it is important to define this human-robot interaction in terms of robots working with humans. The focus of this research is how humans perceive the emotions of robots which look like machines (as opposed to anthropomorphic robots). It uses three different models to describe the emotional state of the IGUS robotic platform. These three models will be discussed later in this chapter. Participants were invited to observe three different gestures of the robot in three states, and afterwards they had to fill in a questionnaire that would tell how they have perceived the emotional state of robot for a particular gesture at that time.

The perception of emotions by the participants greatly depends on the type of embodiment used in the research. According to Mori's Uncanny Valley theory the degree of expectation towards the robot increases as it becomes more human-looking. However in his theory there is a point on the anthropomorphic scale where the robot's appearance becomes confusing and it is difficult to distinguish between humans and robots (Mori, 2005). This was proved in the research carried by Bartneck et al. in which all the robots were not treated as the same by the participants because of their anthropomorphic or zoomorphic appearance which differed from each other (Bartneck et al., 2006).

In this particular research the robot is not from the anthropomorphic or zoomorphic family of robots. It looks like a machine, so the expectations from the participants are lowered because of the type of embodiment. Moreover as the robot cannot exhibit as many moods as an anthropomorphic or zoomorphic robot can, the moods are measured on wide zones on the standard scales used for this research.

5.2 Modelling machine emotions

Emotions in machines are very important in today's world of research. People may use an emotionless machine as a tool but not a reliable partner or companion to work with them in industry and various other fields. So emotions are important aspect in human-machine communication. Although even with high-level programming techniques it will be difficult for the machines to express emotions like humans do. According to research even simple machines can express or can display emotional feelings (Braitenberg, 1984). The example of two vehicles controlled by sensors as shown in Fig. 5.1 clearly explain the concept.

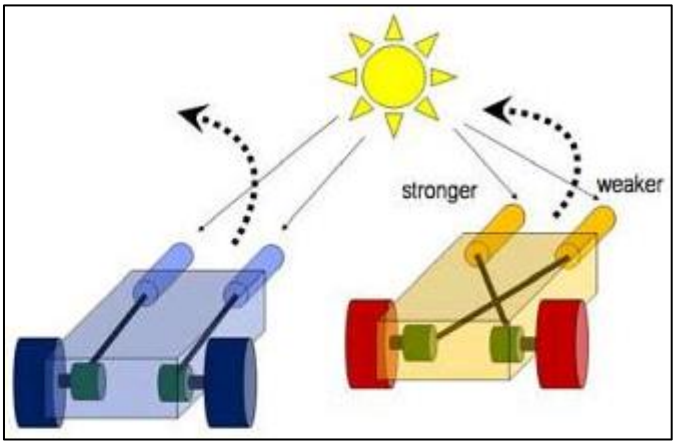

Figure5. 1: Emotional vehicles responding to light (Nishida et al., 2010)

Both of these are connected with the sensors that respond to a light source. When these vehicles are exposed to light, the one on right moves towards the light source and the left away from the source. This difference is because of the way sensors are connected to motors. The left cart will move away as its right sensor is receiving stronger light then left, thus producing more torque on right wheel than left. This motion can be translated in terms of emotional feeling that as the right vehicle does not like the light source so it is moving away; whereas the other cart is attracted towards the light source (Nishida et al., 2010). The computational model for these emotional vehicles is shown in Fig. 5.2

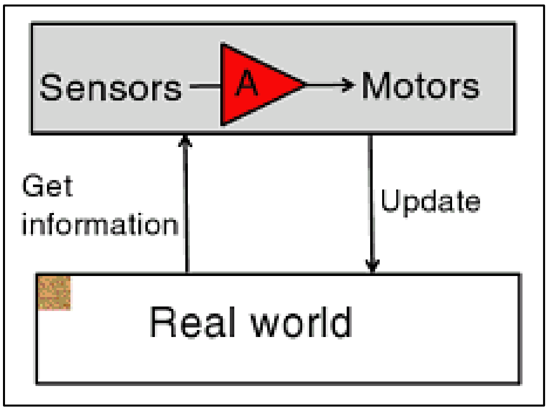

Figure5. 2: Computational model for emotional vehicle (Nishida et al., 2010)

5.3 Emotional models for research

There are many different models for categorising the emotions of robot by the user. Detailed study for mutual co-relation among different kinds of emotions is being done. The research is carried out by using different statistical approaches, for example, multidimensional scaling, and factor analysis of individual reports of different emotional experiences. The research consistently resulted in 2-D models of affective emotional experiences, with different attributes for the two dimensions such as valence and arousal by Russell, dimensions of PANAS by Watson, tension and energy by Thayer and various others (Posner et al., 2005). The ones that are used in this research are:

- Russell's circumplex Model
- Tellegen-Watson-Clark model
- PAD scale

The reason for selecting these models is because these are well-known and renowned one's that are used for research of HRI. The models will be discussed and explained one by one.

5.3.1 Russell's circumplex model of affect

There are two basic models used for measuring the emotional state of machines that have found wide acceptance and support. These are Ekman's and Russell's model. Russell's model is used for this research as from the Ekman's model "it is not clear which emotions make the basic set of which all other emotions can be constructed" (Saerbeck and Bartneck, 2010).

Russell proposed the basic circumplex model of emotions (Russell, 1980). This model described emotion in two axis space. The vertical axis represents the arousal in the observed emotion and the horizontal axis represents valence. The center where both axes meet was neutral emotions. This model was usually used for testing stimuli of emotion words, emotional facial expressions and affective states (Remington et al., 2000).

Most psychologists believe that emotions are independent from each other and have their own dimensions such as distress, depression and anxiety etc. However Russell proposed that all these affective emotional states are interlinked and dependent on each other (Russell, 1980). He proposed a circular model in a two dimensional bi-polar space of valence and arousal rather than as a mono-polar space that are independent of each other. Later, the model was extended for 28 different feelings that are interlinked and sometimes synonymous. The particular Russell's model used in this research is shown in Fig. 5.3:

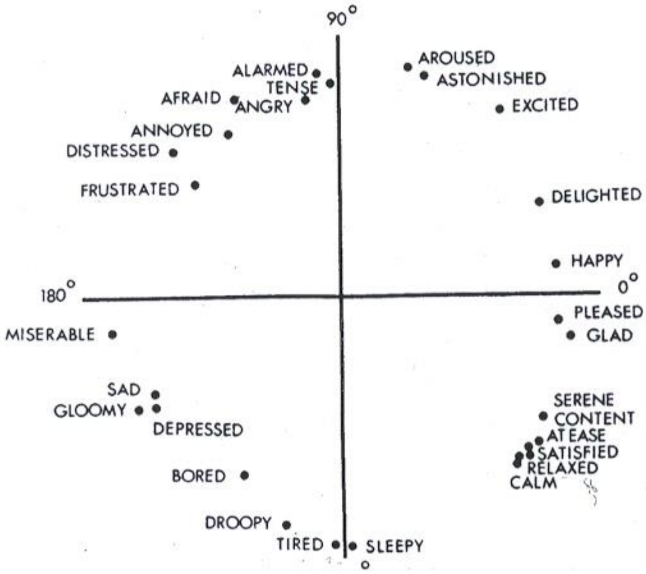

Figure5. 3: Russell's circumplex model of emotions (Russell, 1980)

Because there are no distinct boundaries between emotions like "happiness" and "being pleased", "relaxed" and "clam", "sad" and "gloomy" etc. emotions that overlap each other are placed close together making a cluster in this scale (Russell, 1980). Fig. 7.3 shows 28 emotional states distributed in four different quadrants following core concept of two main axes of valence and arousal. As defined by

(Kensinger, 2004) "The dimension of valence ranges from highly positive to highly negative whereas the dimension of arousal ranges from calming or soothing to exciting and agitating." The valence axis can be defined in terms of unpleasant-pleasant axis and the arousal can be defined as deactivation-activation in the emotions (Junghyun et al., 2010). Thus there can be various different events that can be negative and agitating or positive, calming and soothing. In this scale the Table 5.1 represents the emotions with respect to degrees in this circular arrangement.

EMOTIONS	DEGREES
Pleasure	0°
Excitement	45°
Arousal	90°
Distress	135°
Misery	180°
Depression	225°
Sleepiness	270°
Contentment	315°

Table5. 1: Location of emotion on circular graph (Russell, 1980)

All these emotions are placed on the circular pattern graph keeping in view the relation of these with arousal and valence. For example "delighted" is placed at 24.9° indicating that it has both factors of arousal as well as pleasure (Russell et al., 1989). Similarly, looking at the emotion of being "excited" at 48.6° involves higher arousal. Furthermore, looking at the behaviour of being "astonished" we can see less pleasure and more arousal (Russell et al., 1989). Words that are close to each other on the graph describe similar emotions, whereas being apart on scale and further from each other indicates the difference in emotional states. This scale with 28 different emotions in two bipolar spaces was used in the questionnaire for interpreting the emotional state of the robotic platform.

There were two other more or less similar scales that were proposed by Russell, but experimentation for quantitative comparison among the scales showed that these produce equivalent results. All of the scales look almost the same and produce similar results (Russell, 1980). The one used in this research is shown in Fig. 5.3

The reason for not using the basic model is that it "accounts for the substantial proportion, but not all, of the variance in self-reported affective state" (Russell, 1980).

5.3.1.1 Example of affective interaction

There is a SMS-service called eMOTO that sends text messages in addition to different colourful and animated shapes in the background that express the emotions of the person sending text. The expression is chosen on the basis of set of gestures using stylus pen that comes with sensors that would know about the pressure and the shakiness in movements. Thus the background would be representing the emotions of person sending the text. It also allows the user to build their own gestures as they are not limited to specific set of gestures only. Pressure and shaking movements is the main constituent for expressing these emotions (Höök, 2013).

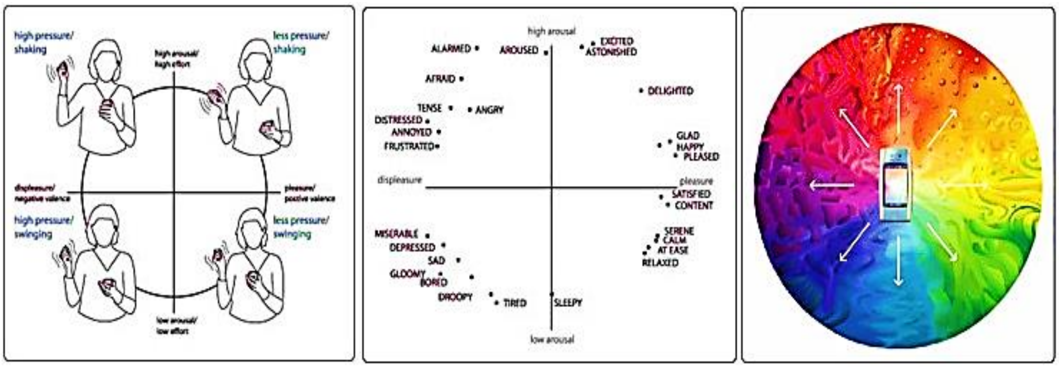

(a) (b) (c)

Figure5. 4: Russell's circumplex model for affective interaction (Höök, 2013)

Fig. 5.4 (a) shows various physical movements that have different pressure and shakiness in them. These can be related with the affective experiences of Russell's circumplex model of affect shown in Fig. 5.4 (b). These emotions are then mapped to colourful expressions in Fig. 5.4 (c).

5.3.2 Tellegen-Watson-Clark model

Another model used for the analysis of emotional moods by perceiving the motion of the robot is Tellegen-Watson-Clark model. This model is shown in the Fig. 5.5:

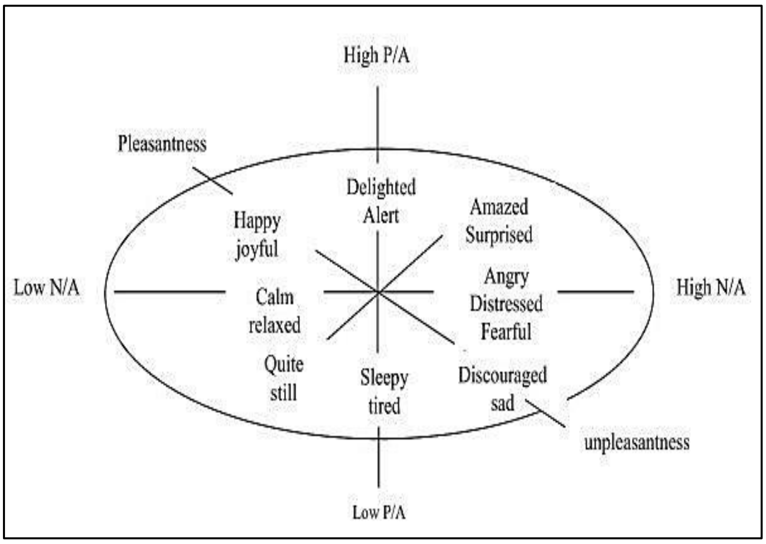

Figure5. 5: Tellegen-Watson-Clark model (Trohidis et al., 2011)

This model is another way of rating the emotions that eventually emerged as prominent criteria. The two main dimensional ratings in this scale are PA and NA. PA is an abbreviation for positive affect and is the degree of positive emotions that are being felt like "being cheerful" and "enthusiastic" etc. Whereas the Negative affect (NA), is the extent of experiencing negative moods like anger, rage, guilt etc. (Coan and Allen, 2007).

The wide scope of these terms includes many emotions in them. PA includes all those feelings that are pleasant like being enthusiastic, confident, interested, healthy etc. High positive effects reflect the state of full energy and full concentration whereas low PA is taken to be in the state of calmness and serenity.

On the other hand, NA includes all the negative feeling and emotions and moods of being guilty, feeling angry, fearful, distressed etc. Low NA is to be sad and being in a lethargic mood etc. However according to (Yang and Lee, 2004) NA is difficult to distinguish from each other as they are very closely related unlike PA. An example of anger and guilt is explained in his paper. Both of these are highly NA and are placed together, however taking the emotions of sadness and guilt, they are separated from each other, as sadness is also towards PA. Although PA and NA is highly uncorrelated and it is easy to distinguish between these two emotions yet to distinguish among the emotions in each category is difficult. "Happiness and sadness form a largely unidimensional bipolar structure, but PA and NA are relatively independent" (Tellegen et al., 1999).

This model represents the emotional state with more clarity from another new perspective of PA and NA as two independent emotional axes. Mainly two pairs of dimensions are being mapped by this model. Firstly PA and NA and the other dimension rotated to 45° showing the emotions of pleasantness VS unpleasantness. Including this dimension, give rises to the circular shape of model.

There was a great deal of research addressing the question whether these PA and NA are independent or not. But research has shown that these have emerged as two independent and consistent scales for categorising emotions (Watson et al., 1988).

However this model was renamed to avoid the ambiguity of terminology later on. PA and NA were later called Positive Activation and Negative Activation (Tellegen et al., 1999). Watson et al. concludes on the basis of their research that PA and NA are reliable and efficient ways of measuring two important dimensions of moods (Watson et al., 1988).

5.3.3 PAD scale :

The third scale used for measuring the emotional state is PAD shown in Fig. 5.6. This scale was developed by Albert Mehrabian to describe the different states of emotions in terms of Pleasure, Arousal and Dominance as three independent orthogonal features. It uses these three independent dimensions to describe all the emotional states (Mehrabian, 1980). This scale is used for non-verbal communication such as body language etc., in psychology (Mehrabian, 1977). There are three main dimensions for this scale in terms of which emotions are measured:

- **The Pleasure-Displeasure scale**: This particular dimension of the scale measures how pleasant or unpleasant an emotion is. For example happy and excited both comes under the category of pleasant emotions. However anger comes under displeasure.
- **The Arousal-Nonarousal scale**: This is another independent dimension of the PAD scale to measure the Arousal or Nonarousal aspect in the emotions.

It basically measures the intensity of emotions. The emotions that fall in the same category of either being pleasant or unpleasant can be further categorized on the basis of their intensity. For example, talking about two unpleasant emotions of anger and rage, the intensity for both of them is different although both come under the feeling of unpleasantness. Anger has less arousal than that of rage. Similarly, being happy and excited is another example from the pleasant category of emotions. Though both fall under same index but being happy contains less amount of arousal than that of being excited.

- **The Dominance-Submissiveness scale**: The third dimension of the PAD scale measures the factor of being dominant or submissive in its emotions. For example taking two pleasant emotions of happy and excited. Excitement contains more dominance. Similarly anger is more dominant than fear although both are under the list of unpleasant feelings.

For this research these three independent parameters were used to evaluate the emotions. A table was created and for each motion of the robotic arm, people were asked to mark all of the three factors of Pleasure, Arousal and Dominance in terms of being high, low or medium and then marking the overall affect they are getting from the motion. Before start filling in the questionnaire, people were clearly explained what these scales mean.

These three independent orthogonal dimensions of the PAD scale provide detailed information about the emotional state. The foundations for this PAD scales involve the differentiation between the emotions and temperament (Mehrabian, 1996). According to this scale any point in the space of PAD scale represents the emotion.

Rather than measuring it in terms of values ranging between 0-1, this research adopts another method of marking the emotional state in terms of High, Medium and Low states of Pleasure, Arousal and Dominance. This is because there are only three emotional states that are tested for three different gestures. Moreover it becomes easy for the participant to mark it in this way. For the validity of this scale, it is compared with the results of other two scales.

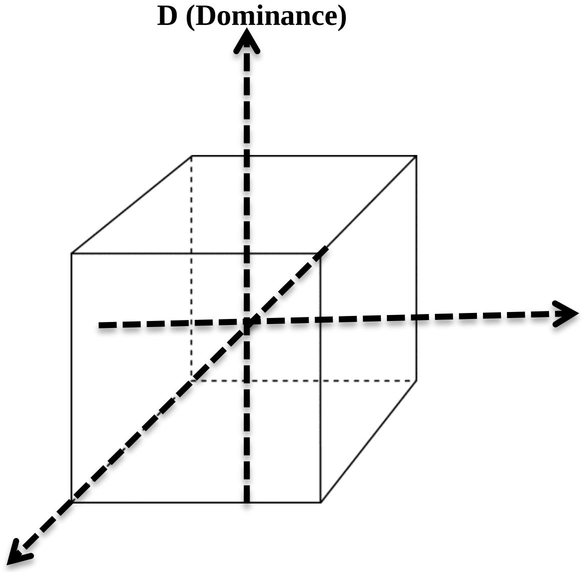

Figure5. 6: PAD model

People were also asked to judge the overall effect for the perceived emotion. The overall affect is categorised in three main groups of sad/tired---unpleasant, happy/pleased---pleasant, and excited---aroused. The overall emotion is then compared with the individual factors marked by the participants.

5.4 Selection of gestures

For all of the scales there were three different gestures. The emotions for all these three gestures were measured on these scales by dividing the quadrants according to the emotional state. The three gestures selected were:

- Point-Point motion
- Waving of the robotic arm
- Bowing down to welcome

5.4.1 Graphical illustration of gestures :

The point-point motion is the most basic and general kind of movement in the world of robotics. Fig. 5.7 represents point-point motion of robot from home position to three different points. This is done using the concept of inverse kinematics. The robot moves in a smooth spline trajectory as explained in earlier chapters.

Figure5. 7: Graphical representation of point-point motion

Fig. 5.8 represents the graphical illustration of waving of robot in a clockwise pattern. This gesture was selected as it is a basic human gesture in the form of a repetitive movement.

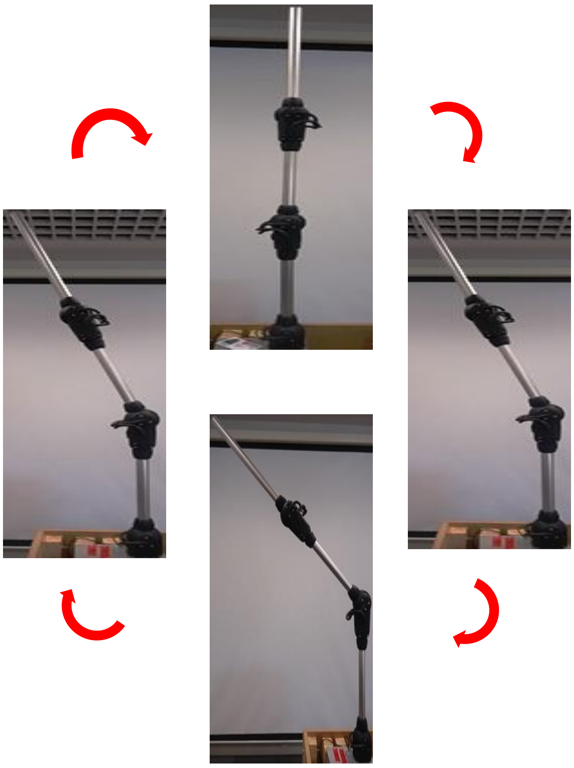

Figure5. 8: Graphical representation of waving of robot

Fig. 5.9 represents the graphical illustration of bowing down of the robot form right to left. The reason for choosing this gesture was as it is a universal cultural gesture that people can recognize quickly and easily. The robot can be seen bowing from straight position to almost 90 degrees for its last joint in Fig. 7.10.

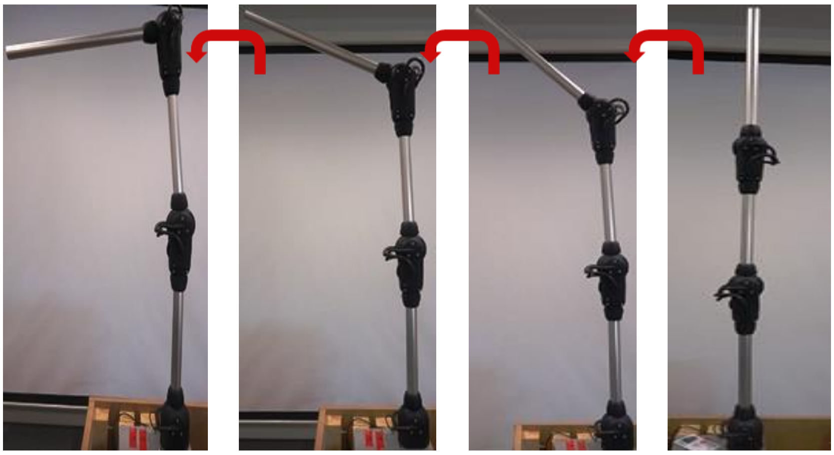

Figure5. 9: Graphical representation of bowing of robot

5.5 Motion characteristics

The motion characteristics that were used to change the emotional state of the robot were velocity and acceleration. Because of the change of these two parameters the robot changed its speed, trajectory, time consumed and curvatures (Saerbeck and Bartneck, 2010). The changing values of the velocity and acceleration shows the prominent change in emotional effect perceived by the user.

The effect can also be observed in the spline motion graph that is generated in the LabVIEW code.

However there were physical constraints when choosing the values such as, if the values were too high the wires could be pulled off the drive wheel. Similarly, if the velocity and acceleration were too low slippage occurred and the motor did not rotate properly.

Fig. 5.10 to 5.15 shows that as the motion parameters are changed spline shown on the graph is also changed. The splines for Point-Point motion of robotic arm that is for Gesture1 for all three parameters are shown in Fig. 5.10 to 5.12.

- **Gesture 1: At V=250, A=10**

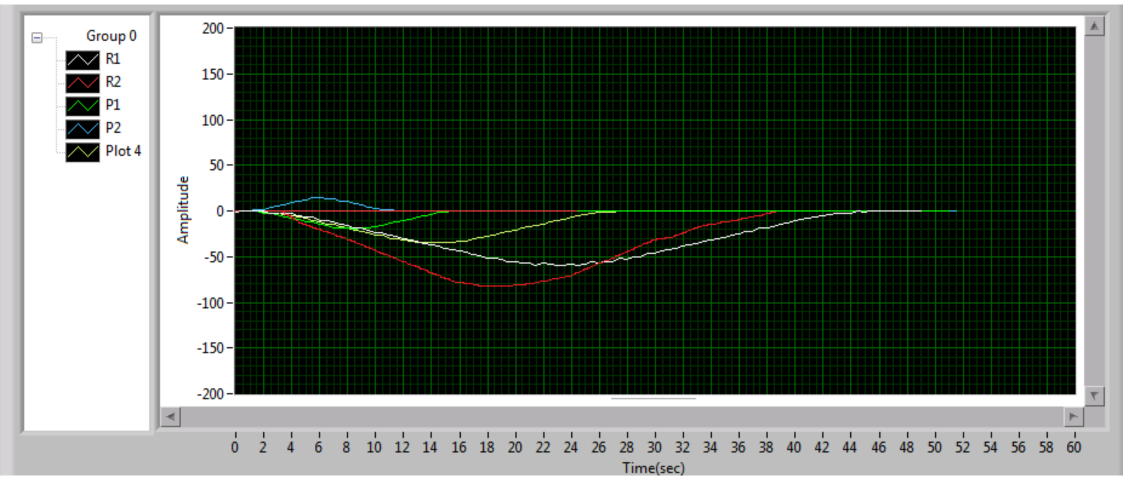

Figure5. 10: Spline curve for G1 at V=250

- **Gesture 1: At V=800, A=50**

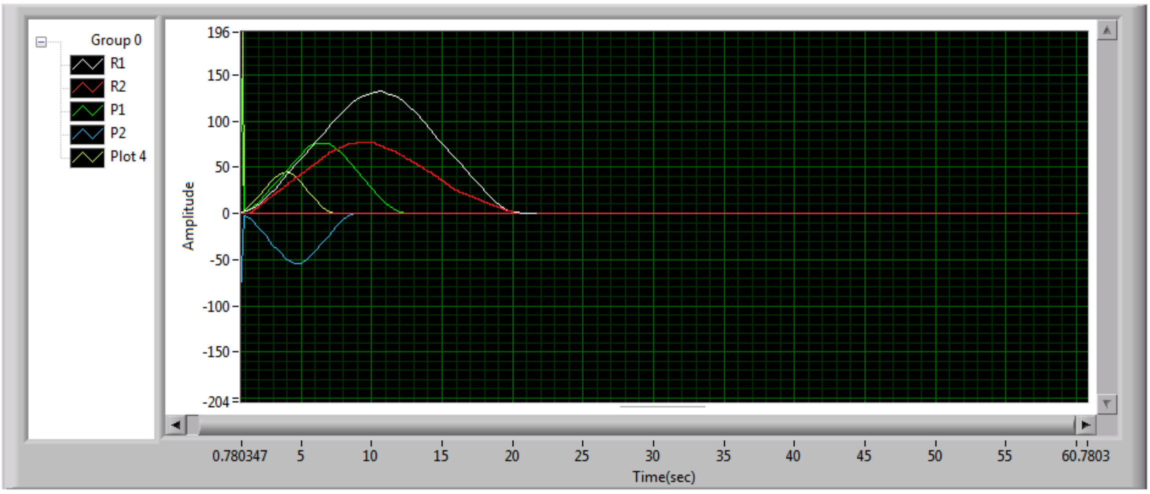

Figure5. 11: Spline curve for G1 at V=800

- **Gesture 1: At V=2000, A=300**

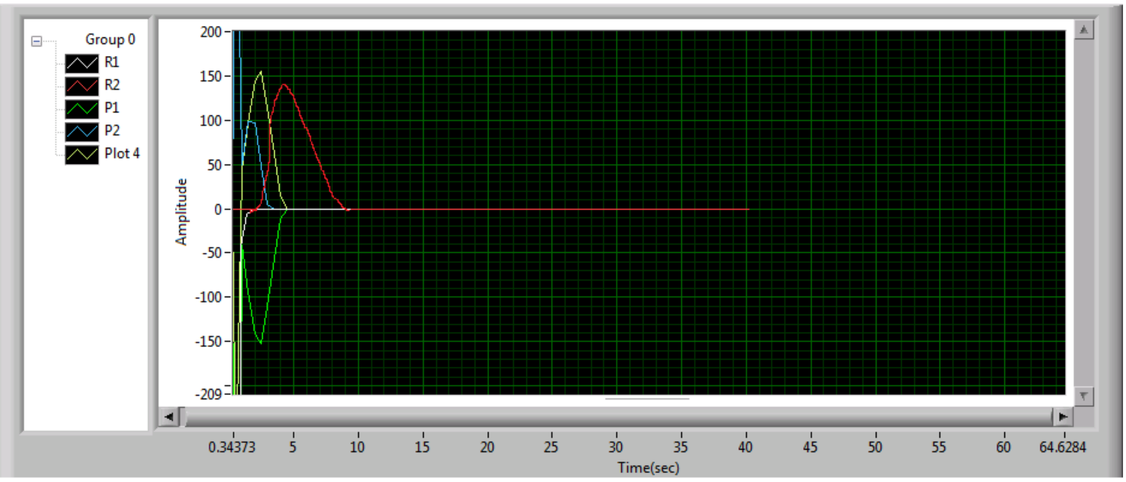

Figure5. 12: Spline curve for G1 at V=2000

The spline curves for Gesture 2 that is waving of the robotic arm, considering all the three set of parameters are shown in Fig. 5.13 to 5.15:

- **Gesture 2: At V=100, A=15**

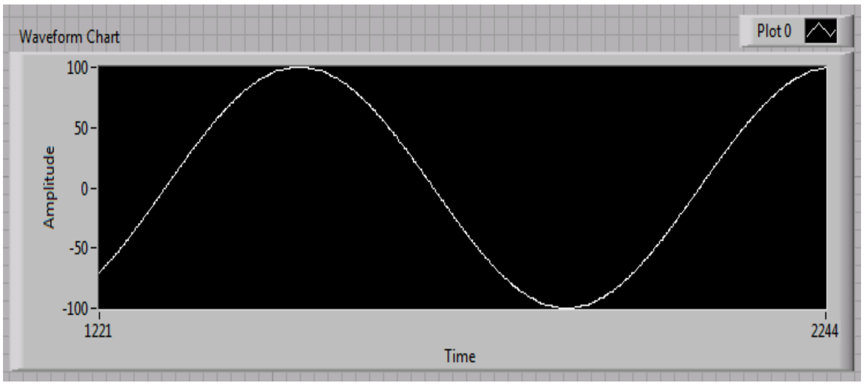

Figure5. 13: Spline curve for G2 at A=15

- **Gesture 2: At V=100, A=5:**

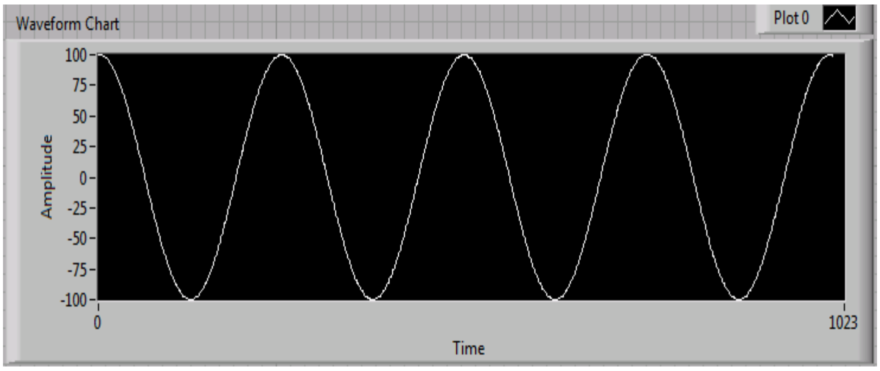

Figure5. 14: Spline curve for G2 at A=5

- **Gesture 2: At V=100, A=1.5:**

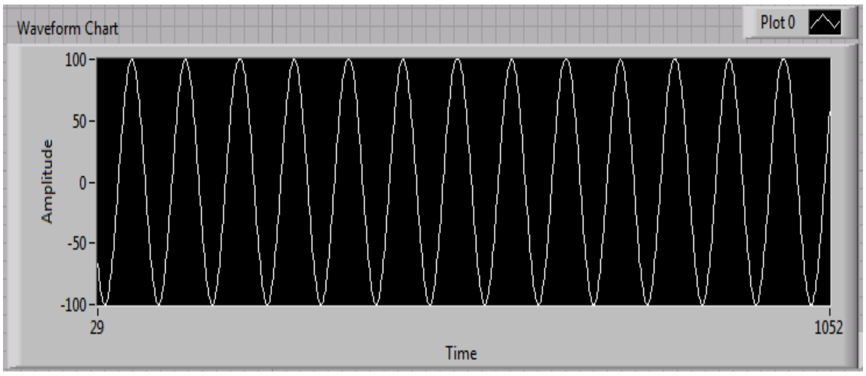

Figure5. 15: Spline curve for G2 at A=1.5

5.6 Summary of the chapter

This chapter explains the emotional models and reasons for choosing the specific models. It focuses on the fact of how three different emotional models i.e. Russell's circumplex model of affect, Tellegen-Watson-Clark model and PAD scale can be used by the user to mark the perceived emotion of a mechanoid robot. The gestures and motion parameters chosen to change these gestures are also explained in detail.

The next chapter discusses the experiments performed using these emotional models and gestures and the results collected. The discussion on how these models give the user flexibility of marking the perceived emotions for particular gestures in certain set of range are covered in next chapter.

CHAPTER 6

EXPERIMENTS AND RESULTS

6.1 Experiments for emotional communication

Several experiments were designed to investigate the emotional communication of the robot. These experiments were based on the emotional scales discussed above. The robot exhibited a variety of gestures, with changing motion characteristics and the participants had to judge the emotional state by marking the questionnaire given to them. The ethical approval and the consent form for this research is attached in appendix N.

6.1.1 Experiment procedure

Fig. 8.1, 8.2 and 8.3 shows the participant sheet that they were given in the experiment. The complete data was collected from 18 participants including males and females that fall in the age group of 17-50 years. The experiment took approximately 20 minutes.

Each session was started with a brief introduction of the project and an explanation of how the participant would have to mark the perceived emotions on the given scale. Participants were told what the individual terms mean. After this introductory session, the participants were given the consent form to sign before they start observing the robot.

In total 3 gestures, each with 3 different sets of velocity and acceleration were shown to each of the participants. This setup resulted in 3x3 emotions marked independently on each of the scales. So in total of 3x (3x3) emotion were marked by each of the participants for all of the three scales i.e. three models each with three different gestures, each with three different subsets of velocity and acceleration. For Russell's model, arousal and valence were the two independent axes. For the Tellegen-Watson-Clark model PA and NA were the main independent parameters and for the PAD scale Pleasure, Arousal and Dominance were used as a set of independent parameters to measure the emotions reflected in the motion of robot.

To have some reference for the comparison of different motions, the participants were shown the specific gesture for all the three different values of velocity and acceleration and then were asked to mark the perceived emotions for each set of velocity and acceleration. If requested, the participants were shown the motion with specific parameters again.

Participants marked a circle on the specific emotion that was perceived for that motion on the model graph. Some of the participants marked more than one emotion for the same motion. However they were in the same quadrant and closely resembled each other. In other words they can be termed as overlapping emotions.

6.2 Questionnaires for measuring perception of emotions

There were three different questionnaires based on the different scales that each of the participants had to fill in. The questionnaires for three different scales and gestures presented to the participants are shown in Fig. 6.1 to 6.3.

Fig. 6.4 to 6.6 shows the sample of filled questionnaire by the same participant for Russell's model, Tellegen-Watson-Clark model and PAD scale respectively at different velocities and accelerations for three different gestures.

The units used for velocity and acceleration are counts/revolutions and counts/revolutions^2 respectively for all three gestures and scales.

6.2.1Questionnaires for Russell’s model

Russell’s model of mood QUESTIONNAIRE

✓ **GESTURE: 1 POINT –POINT MOTION:**

VELOCITY (Counts/rev)	ACCELARATION (Counts/rev^2)	REPRESENTATION ON GRAPH
250	10	1A
800	50	1B
2000	300	1C

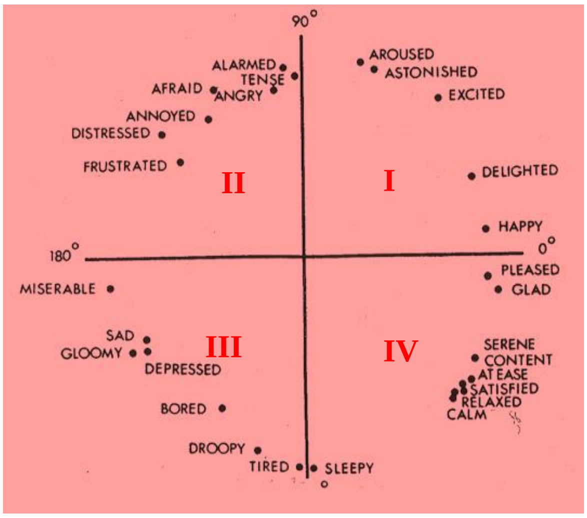

✓ **GESTURE: 2 WAVING OF ROBOTIC ARM:**

VELOCITY (Counts/rev)	ACCELARATION (Counts/rev^2)	REPRESENTATION ON GRAPH
100	15	2A
100	5	2B
100	1.5	2C

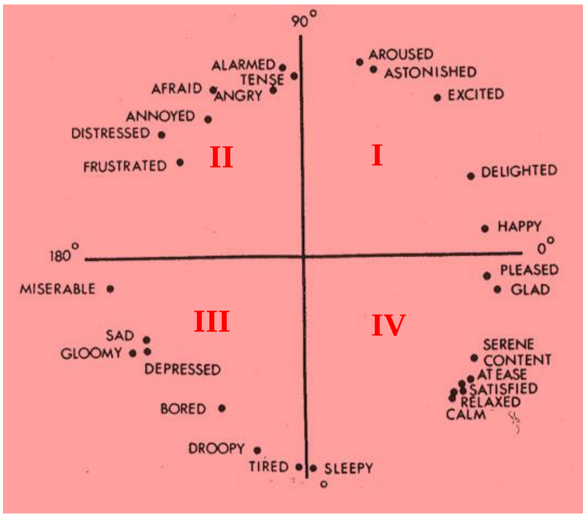

○ **GESTURE: 3 BOWING TO WELCOME:**

VELOCITY (Counts/rev)	ACCELARATION (Counts/rev^2)	REPRESENTATI-ON ON GRAPH
30	30	3A
50	50	3B
100	100	3C

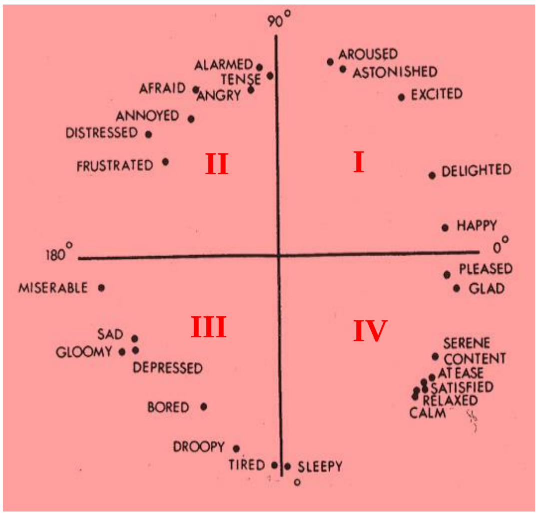

Figure6. 1: Russell's model questionnaire

6.2.2 Questionnaires for Tellegen-Watson-Clark model

Tellegen-Watson-Clark model of mood QUESTIONNAIRE

✓ **GESTURE: 1 POINT –POINT MOTION**:

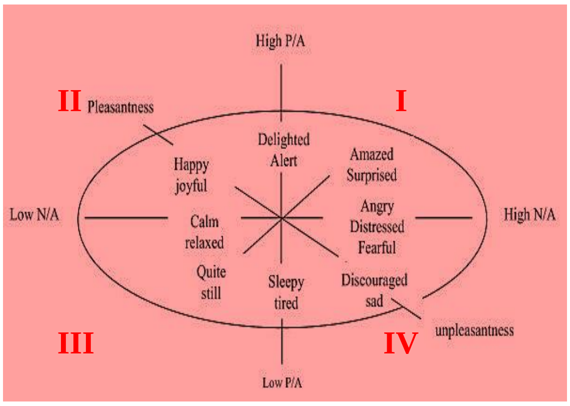

VELOCITY (Counts/rev)	ACCELARATION (Counts/rev^2)	REPRESENTATI-ON ON GRAPH
250	10	1A
800	50	1B
2000	300	1C

✓ **GESTURE: 2 WAVING OF ROBOTIC ARM**

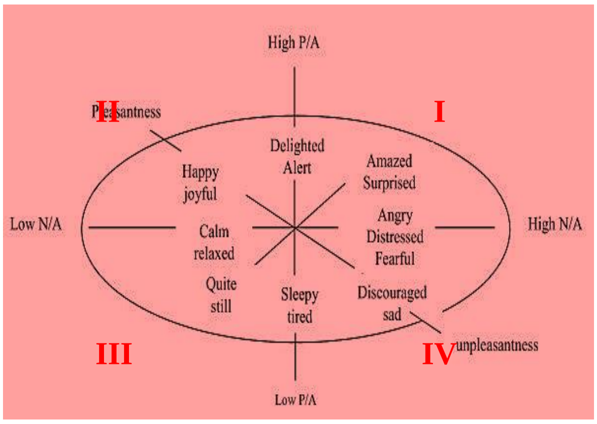

VELOCITY (Counts/rev)	ACCELARATION (Counts/rev^2)	REPRESENTATI-ON ON GRAPH
100	15	2A
100	5	2B
100	1.5	2C

✓ **GESTURE: 3 BOWING TO WELCOME**:

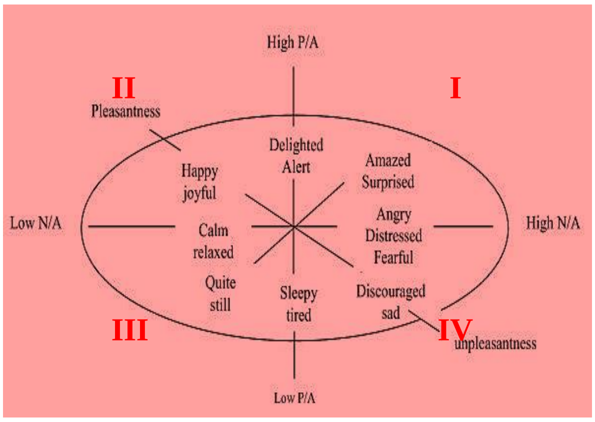

VELOCITY (Counts/rev)	ACCELARATION (Counts/rev^2)	REPRESENTATI-ON ON GRAPH
30	30	3A
50	50	3B
100	100	3C

Figure6. 2: Tellegen-Watson-Clark model questionnaire

6.2.3 Questionnaires for PAD model

PAD QUESTIONNAIRE

Explanation of terms:

Pleasure-how pleasant an emotion is like happy unhappy.
Arousal- how intense an emotion is like rage has more arousal factor than anger though both are unpleasant.
Dominance- measures submissiveness and dominant factor of expression.

✓ **GESTURE: 1 POINT –POINT MOTION:**

VELOCITY	ACCELARATION
250	10

	HIGH	MEDIUM	LOW
PLEASURE			
AROUSAL			
DOMINANCE			

Overall effect	Sad/Tired-unpleasant	Happy/ pleased-pleasant	Excited/ aroused-alert

VELOCITY	ACCELARATION
800	50

	HIGH	MEDIUM	LOW
PLEASURE			
AROUSAL			
DOMINANCE			

Overall effect	Sad/Tired-unpleasant	Happy/ pleased-pleasant	Excited/ aroused-alert

VELOCITY	ACCELARATION
2000	300

	HIGH	MEDIUM	LOW
PLEASURE			
AROUSAL			
DOMINANCE			

Overall effect	Sad/Tired-unpleasant	Happy/ pleased-pleasant	Excited/ aroused-alert

GESTURE: 2 WAVING OF ROBOTIC ARM:

VELOCITY	ACCELARATION
100	1.5

	HIGH	MEDIUM	LOW
PLEASURE			
AROUSAL			
DOMINANCE			

Overall effect	Sad/Tired-unpleasant	Happy/ pleased-pleasant	Excited/ aroused-alert

VELOCITY	ACCELARATION
100	5

	HIGH	MEDIUM	LOW
PLEASURE			
AROUSAL			
DOMINANCE			

Overall effect	Sad/Tired-unpleasant	Happy/ pleased-pleasant	Excited/ aroused-alert

VELOCITY	ACCELARATION
100	15

	HIGH	MEDIUM	LOW
PLEASURE			
AROUSAL			
DOMINANCE			

Overall effect	Sad/Tired-unpleasant	Happy/ pleased-pleasant	Excited/ aroused-alert

✓ **GESTURE: 3 BOWING TO WELCOME:**

VELOCITY	ACCELARATION
30	30

	HIGH	MEDIUM	LOW
PLEASURE			
AROUSAL			
DOMINANCE			

Overall effect	Sad/Tired-unpleasant	Happy/ pleased-pleasant	Excited/ aroused-alert

VELOCITY	ACCELARATION
50	50

	HIGH	MEDIUM	LOW
PLEASURE			
AROUSAL			
DOMINANCE			

Overall effect	Sad/Tired-unpleasant	Happy/ pleased-pleasant	Excited/ aroused-alert

VELOCITY	ACCELARATION
100	100

	HIGH	MEDIUM	LOW
PLEASURE			
AROUSAL			
DOMINANCE			

Overall effect	Sad/Tired-unpleasant	Happy/ pleased-pleasant	Excited/ aroused-alert

Figure6. 3: PAD questionnaire

6.2.4 Measurement of emotions by participants

Filled sample questionnaire for Russell's circumplex model of affect

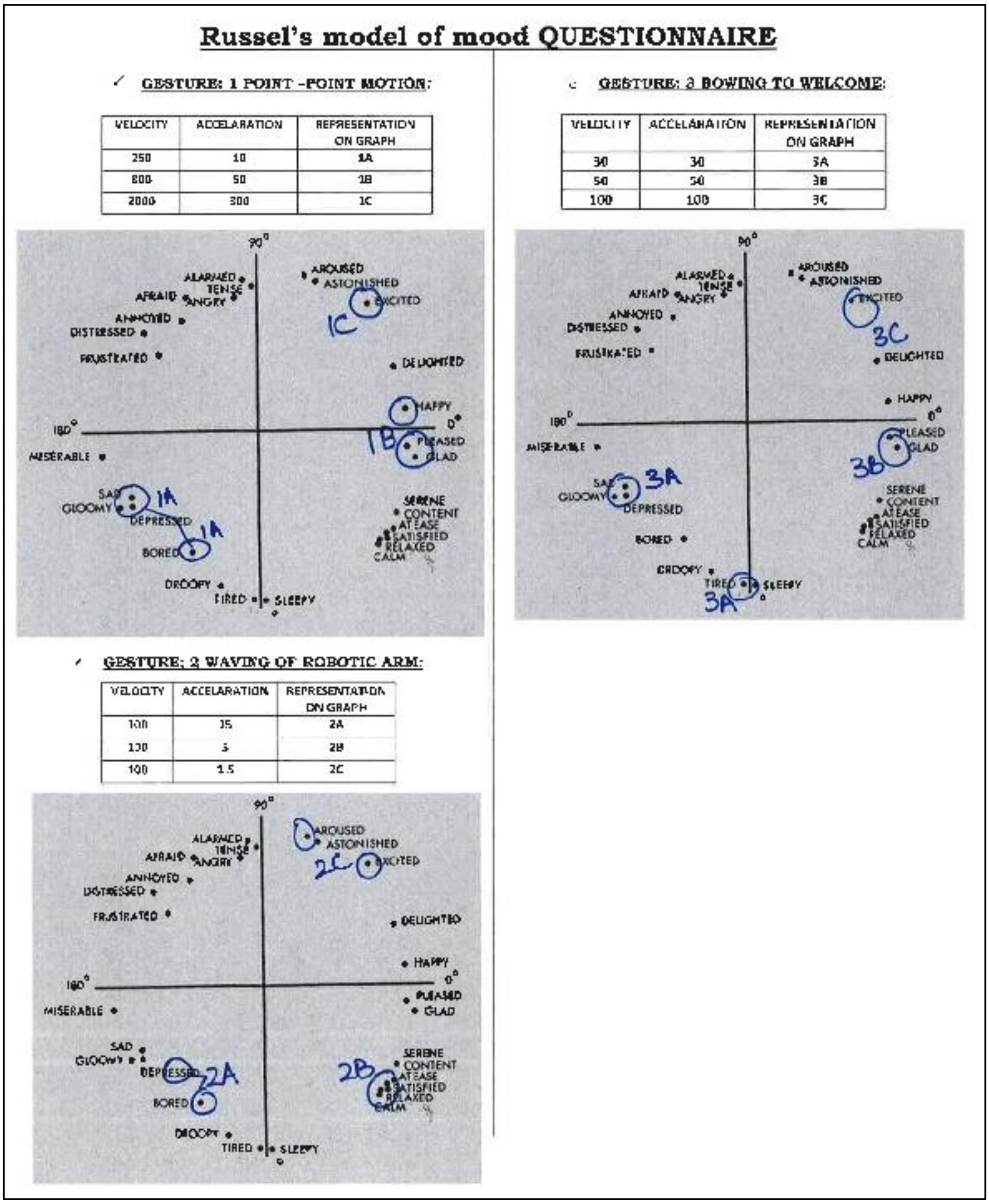

VELOCITY	ACCELARATION	REPRESENTATION ON GRAPH
250	10	1A
800	50	1B
2000	300	1C

VELOCITY	ACCELARATION	REPRESENTATION ON GRAPH
30	30	3A
50	50	3B
100	100	3C

VELOCITY	ACCELARATION	REPRESENTATION ON GRAPH
100	15	2A
130	5	2B
100	1.5	2C

Figure6. 4: Russell's questionnaire filled by the participant

Here is an example of the questionnaire filled by the same participant for the Tellegen-Watson-Clark model at different velocities and accelerations for three different gestures:

Tellegen-Watson-Clark model of mood QUESTIONNAIRE

✓ **GESTURE: 1 POINT –POINT MOTION:**

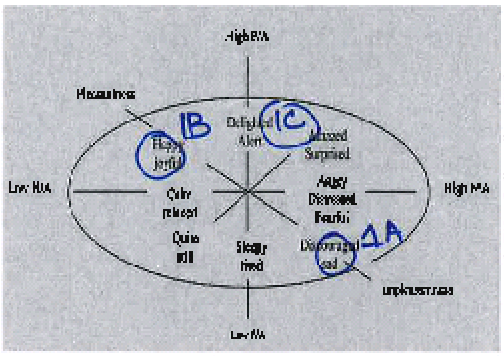

VELOCITY	ACCELARATION	REPRESENTATION ON GRAPH
250	10	1A
800	50	1B
2000	300	1C

✓ **GESTURE: 2 WAVING OF ROBOTIC ARM:**

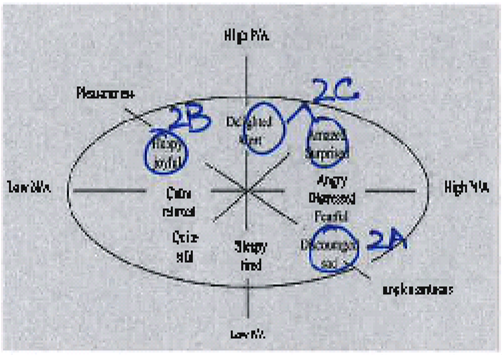

VELOCITY	ACCELARATION	REPRESENTATION ON GRAPH
100	15	2A
100	5	2B
100	1.5	2C

✓ **GESTURE: 3 BOWING TO WELCOME:**

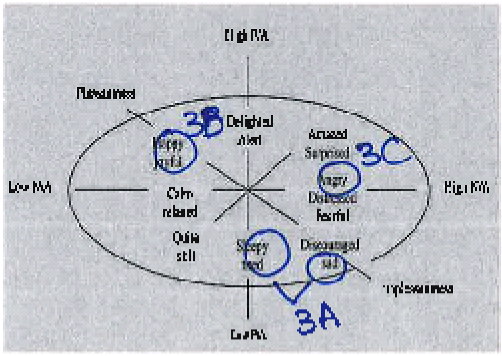

VELOCITY	ACCELARATION	REPRESENTATION ON GRAPH
30	30	3A
50	50	3B
100	100	3C

Figure6. 5: Tellegen-Watson-Clark questionnaire filled by the participant

Here is an example of the questionnaire filled by the same participant for the PAD model at different velocities and accelerations for three different gestures:

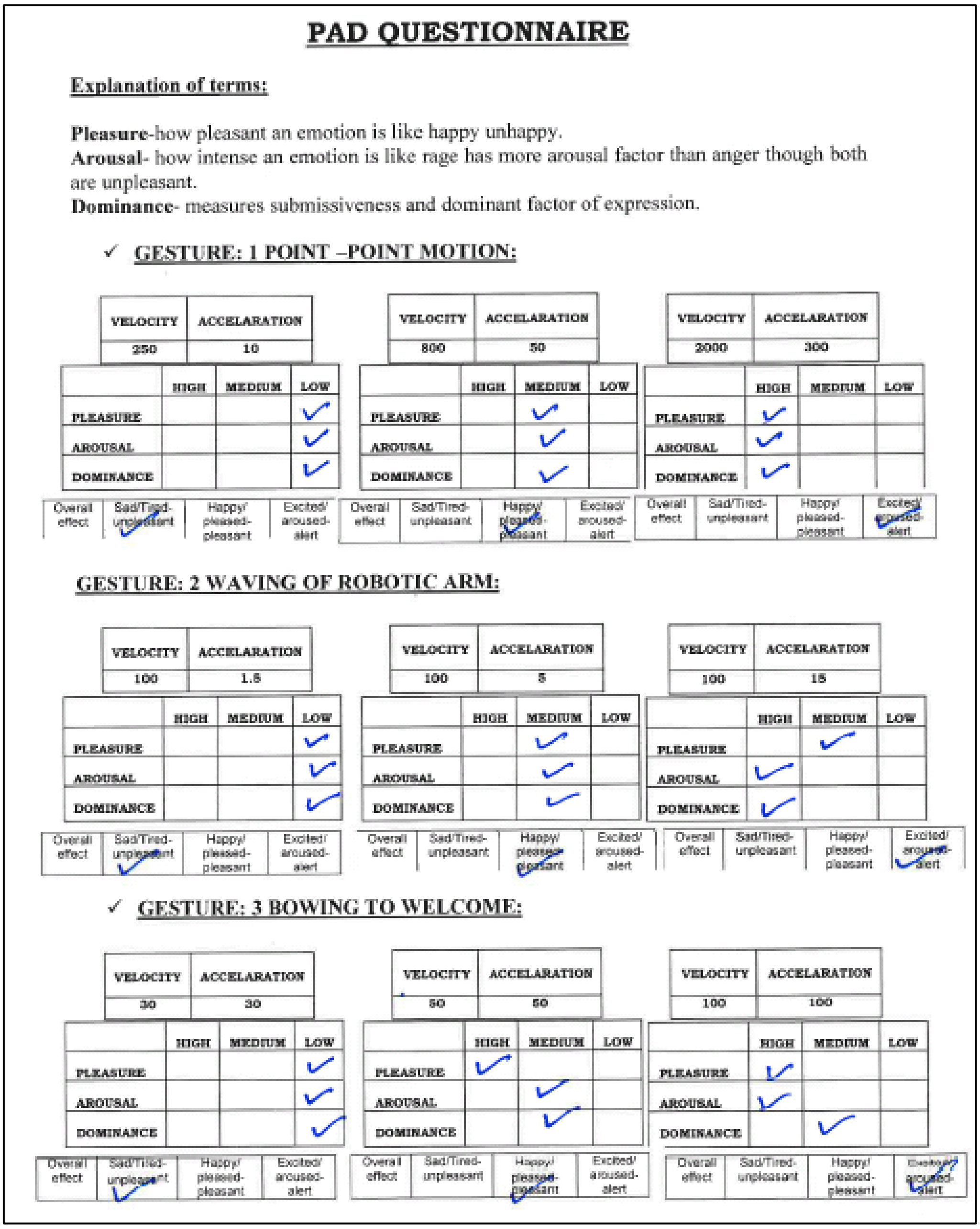

PAD QUESTIONNAIRE

Explanation of terms:

Pleasure-how pleasant an emotion is like happy unhappy.
Arousal- how intense an emotion is like rage has more arousal factor than anger though both are unpleasant.
Dominance- measures submissiveness and dominant factor of expression.

✓ GESTURE: 1 POINT –POINT MOTION:

VELOCITY	ACCELARATION
250	10

	HIGH	MEDIUM	LOW
PLEASURE			✓
AROUSAL			✓
DOMINANCE			✓

Overall effect	Sad/Tired-unpleasant	Happy/ pleased-pleasant	Excited/ aroused-alert
	✓		

VELOCITY	ACCELARATION
800	50

	HIGH	MEDIUM	LOW
PLEASURE		✓	
AROUSAL		✓	
DOMINANCE		✓	

Overall effect	Sad/Tired-unpleasant	Happy/ pleased-pleasant	Excited/ aroused-alert
		✓	

VELOCITY	ACCELARATION
2000	300

	HIGH	MEDIUM	LOW
PLEASURE	✓		
AROUSAL	✓		
DOMINANCE	✓		

Overall effect	Sad/Tired-unpleasant	Happy/ pleased-pleasant	Excited/ aroused-alert
			✓

GESTURE: 2 WAVING OF ROBOTIC ARM:

VELOCITY	ACCELARATION
100	1.5

	HIGH	MEDIUM	LOW
PLEASURE			✓
AROUSAL			✓
DOMINANCE			✓

Overall effect	Sad/Tired-unpleasant	Happy/ pleased-pleasant	Excited/ aroused-alert
	✓		

VELOCITY	ACCELARATION
100	5

	HIGH	MEDIUM	LOW
PLEASURE		✓	
AROUSAL		✓	
DOMINANCE		✓	

Overall effect	Sad/Tired-unpleasant	Happy/ pleased-pleasant	Excited/ aroused-alert
		✓	

VELOCITY	ACCELARATION
100	15

	HIGH	MEDIUM	LOW
PLEASURE		✓	
AROUSAL	✓		
DOMINANCE	✓		

Overall effect	Sad/Tired-unpleasant	Happy/ pleased-pleasant	Excited/ aroused-alert
			✓

✓ GESTURE: 3 BOWING TO WELCOME:

VELOCITY	ACCELARATION
30	30

	HIGH	MEDIUM	LOW
PLEASURE			✓
AROUSAL			✓
DOMINANCE			✓

Overall effect	Sad/Tired-unpleasant	Happy/ pleased-pleasant	Excited/ aroused-alert
	✓		

VELOCITY	ACCELARATION
50	50

	HIGH	MEDIUM	LOW
PLEASURE	✓		
AROUSAL		✓	
DOMINANCE		✓	

Overall effect	Sad/Tired-unpleasant	Happy/ pleased-pleasant	Excited/ aroused-alert
		✓	

VELOCITY	ACCELARATION
100	100

	HIGH	MEDIUM	LOW
PLEASURE	✓		
AROUSAL	✓		
DOMINANCE		✓	

Overall effect	Sad/Tired-unpleasant	Happy/ pleased-pleasant	Excited/ aroused-alert
			✓

Figure6. 6: PAD questionnaire filled by the participant

6.3 Emotion recognition based on scales

The emotions for each of the gestures were marked by the participants based on the perceived affect. The first two scales were divided into four different quadrants based on the range of emotions. So, the participants marked the emotions quadrant-wise for each of the gestures for both Russell's and Tellegen-Watson-Clark models of emotions.

Emotional ranges for each quadrant for both scales are given below:

- ✓ **For Russell's model**

Q1: Excited---Aroused

Q2: Tense---Annoyed---Miserable

Q3: Tired---Sad---Miserable

Q4: Calm---Content---Pleased

- ✓ **For Tellegen-Watson-Clark model**

Q1: Alert/Delighted--- Amazed/Surprized

Q2: Pleasant---Happy/Joyful

Q3: Sleepy---Calm/Relaxed

Q4: Unpleasant---Sad/Tired

The third scale that is PAD is actually based on measuring the pleasure, arousal and dominance in the emotions. Thus this scale cannot be divided into quadrants. So another approach of measuring the overall effect was implemented. The participants were asked to mark from the range of three different overall effects of the emotions that they perceived from the motion of embodiment after marking the three individual factors of pleasure, arousal and dominance. The overall emotional range for this scale used is given below:

- ✓ **For PAD model**

1. Sad/Tired---Unpleasant
2. Happy/Pleased---Pleasant
3. Excited/Aroused---Alert

This overall result is then compared with the individual effects marked on the scale that is shown in the results.

6.4 Models results

6.4.1 Results for Russell's model

Gesture:1	Q1	Q2	Q3	Q4
V=250 & A=10	0	0	17	1
V=800 & A=50	4	6	1	7
V=2000 & A=300	12	5	0	1
Q1: Excited/Delighted ---- Aroused **Q2**: Tense/Annoyed --- Miserable **Q3**: Tired/Sleepy --- Sad/Miserable **Q4**: Calm/Content --- Pleased				

Table6. 1: Response of participants for Russell's model G1

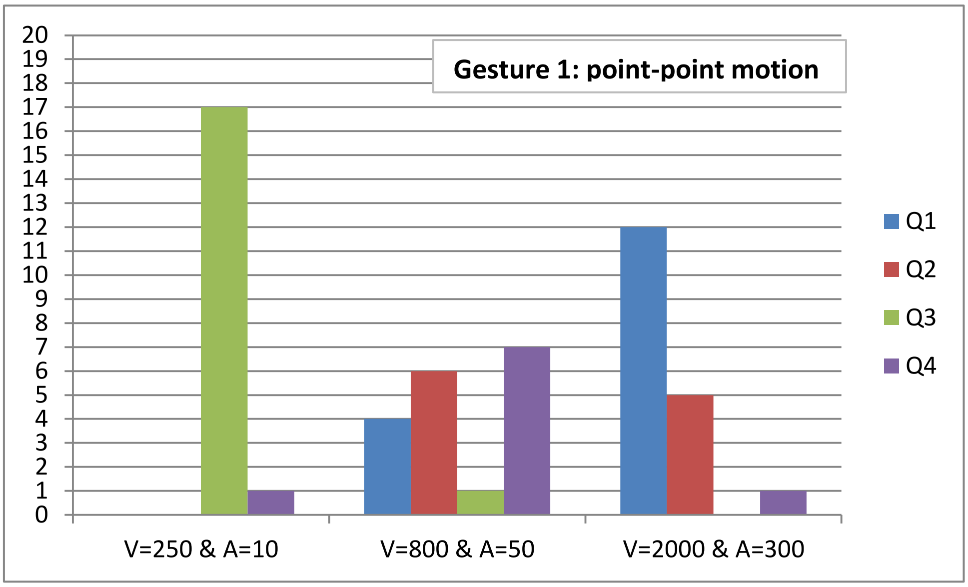

Figure6. 7: Russell's model graph for 3 sets of parameters for G1

The graph in Fig. 6.7 shows that at low velocity and acceleration 17/18 people have marked it in Q3 shown by green bar that says the perceived emotion is Tired/Sleepy --- Sad/Miserable. For medium level of velocity and acceleration 7/18 participants marked it in Q4 shown by purple bar saying that the robot is Calm/Content --- Pleased and at high velocity and acceleration majority i.e. 12/18 people have marked it in Q1 i.e. Excited/Delighted ---- Aroused.

Gesture:2	Q1	Q2	Q3	Q4
V=100 & A=15	0	2	15	1
V=100 & A=5	1	6	4	7
V=100 & A=1.5	13	5	0	0
Q1: Excited/Delighted ---- Aroused **Q2**: Tense/Annoyed --- Miserable **Q3**: Tired/Sleepy --- Sad/Miserable **Q4**: Calm/Content --- Pleased				

Table6. 2: Response of participants for Russell's model G2

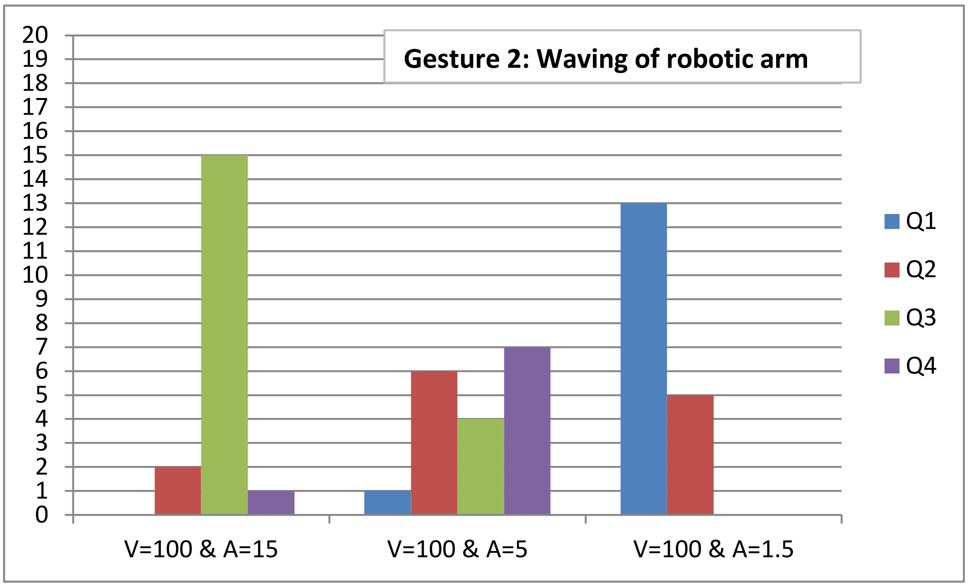

Figure6. 8: Russell's model graph for 3 sets of parameters for G2

The graph in Fig. 6.8 shows that 15/18 people have marked the gesture of waving in category Q3 represented by green bar, falling under the emotions of Tired/Sleepy --- Sad/Miserable. At medium level of velocity and acceleration 7/18 people marked it as Calm/Content --- Pleased shown by purple bar. For highest values of velocity and acceleration majority i.e. 13/18 perceived it as Excited/Delighted ---- Aroused shown by blue bar.

Gesture:3	Q1	Q2	Q3	Q4
V=30 & A=30	0	1	15	2
V=50 & A=50	2	3	4	9
V=100 & A=100	11	2	0	5
Q1: Excited/Delighted ---- Aroused **Q2**: Tense/Annoyed --- Miserable **Q3**: Tired/Sleepy --- Sad/Miserable **Q4**: Calm/Content --- Pleased				

Table6. 3: Response of participants for Russell's model G3

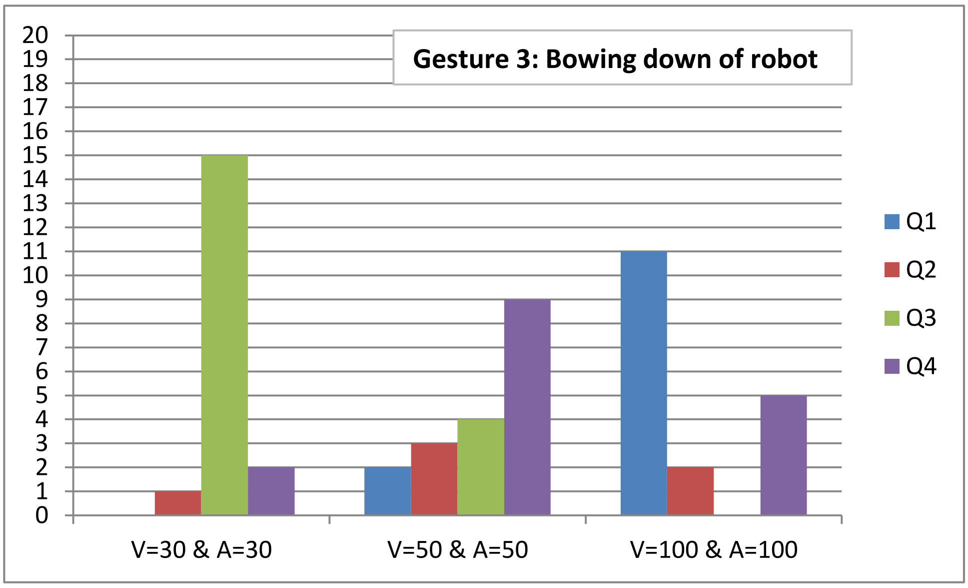

Figure6. 9: Russell's model graph for 3 sets of parameters for G3

The graph in Fig. 6.9 shows that 15/18 people have marked the gesture of waving in category Q3 represented by green bar, falling under the emotions of Tired/Sleepy --- Sad/Miserable. At medium level of velocity and acceleration 9/18 people marked it as Calm/Content --- Pleased shown by purple bar. For highest values of velocity and acceleration majority i.e. 11/18 perceived it as Excited/Delighted ---- Aroused shown by blue bar.

6.4.2 Results for Tellegen-Watson-Clark model

Gesture:1	Q1	Q2	Q3	Q4
V=250 & A=10	0	1	2	15
V=800 & A=50	2	11	1	4
V=2000 & A=300	9	1	6	2
Q1: Alert/Delighted---- Amazed/Surprized **Q2**: Pleasant --- happy/Joyful **Q3**: Sleepy --- Calm/Relaxed **Q4**: Unpleasant --- Sad/Tired				

Table6. 4: Response of participants for Tellegen-Watson-Clark model G1

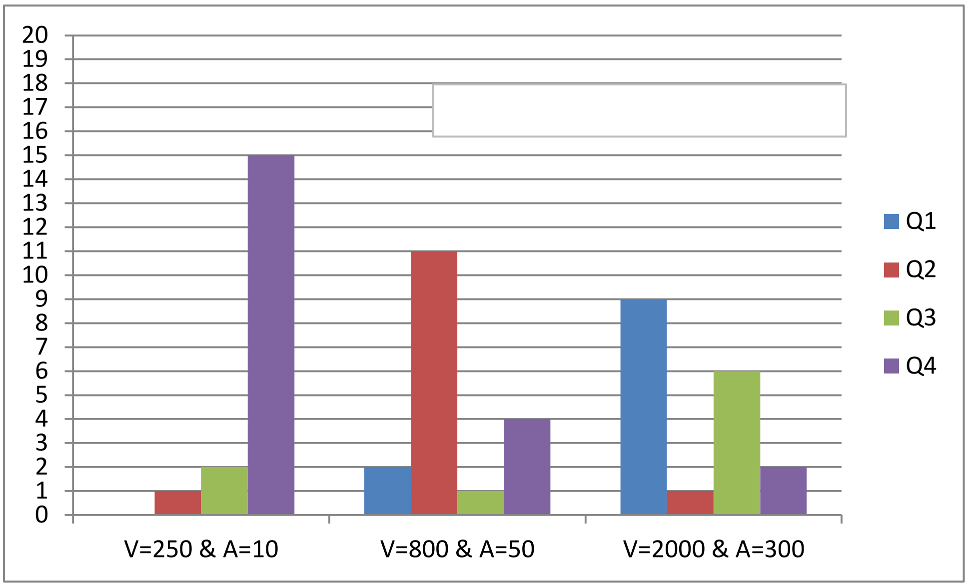

Figure6. 10: Tellegen-Watson-Clark model graph for 3 sets of parameters for G1

The graph in Fig. 6.10 shows that for point-point motion of robot according to Tellegen-Watson-Clark model 15/18 people have marked the gesture of waving in category Q4 represented by purple bar, falling under the emotions of Unpleasant --- Sad/Tired. At medium level of velocity and acceleration 11/18 people marked it as Pleasant --- happy/Joyful shown by red bar. For highest values of velocity and acceleration majority i.e. 9/18 perceived it as Alert/Delighted----Amazed/Surprized shown by blue bar.

Gesture:2	Q1	Q2	Q3	Q4
V=100 & A=15	1	0	2	15
V=100 & A=5	5	11	2	0
V=100 & A=1.5	12	6	0	0
Q1: Alert/Delighted---- Amazed/Surprized **Q2**: Pleasant --- happy/Joyful **Q3**: Sleepy --- Calm/Relaxed **Q4**: Unpleasant --- Sad/Tired				

Table6. 5: Response of participants for Tellegen-Watson-Clark model G2

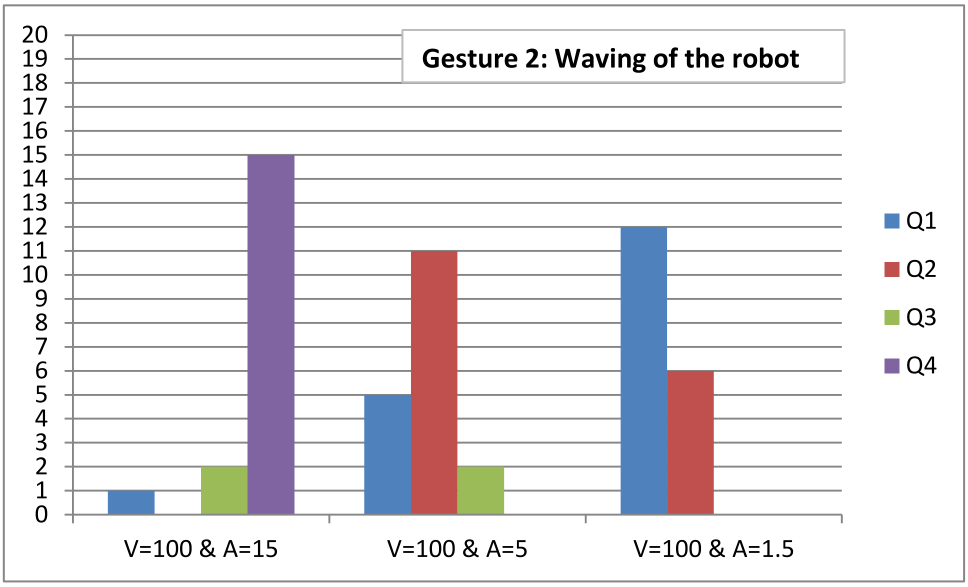

Figure6. 11: Tellegen-Watson-Clark model graph for 3 sets of parameters for G2

The graph in Fig. 6.11 shows that for waving of robot according to Tellegen-Watson-Clark model 15/18 people have marked the gesture of waving in category Q4 represented by purple bar, falling under the emotions of Unpleasant --- Sad/Tired. At medium level of velocity and acceleration 11/18 people marked it as Pleasant --- happy/Joyful shown by red bar. For highest values of velocity and acceleration majority i.e. 12/18 perceived it as Alert/Delighted----Amazed/Surprized shown by blue bar.

Gesture:3	Q1	Q2	Q3	Q4
V=30 & A=30	1	2	2	13
V=50 & A=50	2	14	1	1
V=100 & A=100	11	7	0	0
Q1: Alert/Delighted---- Amazed/Surprized **Q2**: Pleasant --- happy/Joyful **Q3**: Sleepy --- Calm/Relaxed **Q4**: Unpleasant --- Sad/Tired				

Table6. 6: Response of participants for Tellegen-Watson-Clark model G3

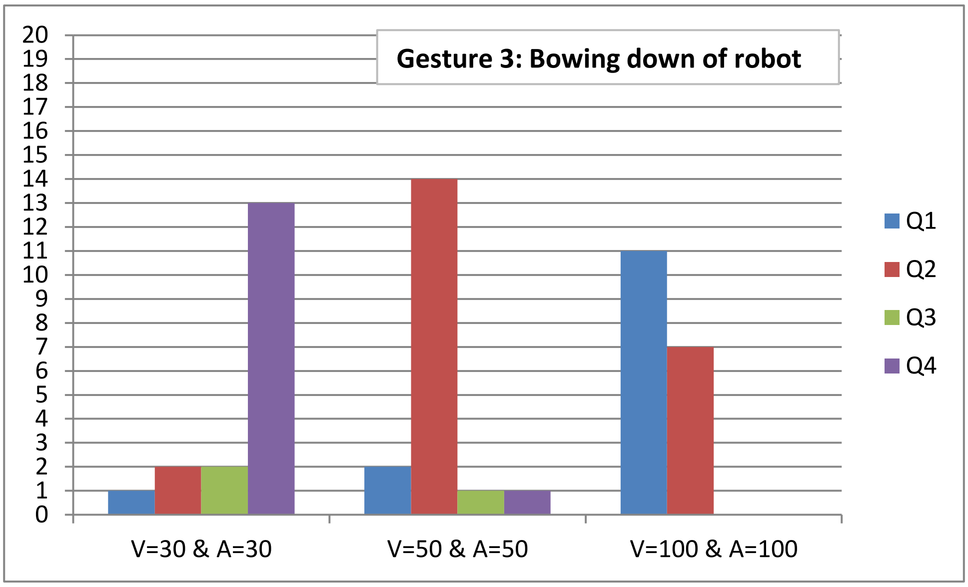

Figure6. 12: Tellegen-Watson-Clark model graph for 3 sets of parameters for G3

The graph in Fig. 6.12 shows that for bowing down of robot according to Tellegen-Watson-Clark model 13/18 people have marked the gesture of bowing in category Q4 represented by purple bar, falling under the emotions of Unpleasant ---Sad/Tired. At medium level of velocity and acceleration 14/18 people marked it as Pleasant ---happy/Joyful shown by red bar. For highest values of velocity and acceleration majority i.e. 11/18 perceived it as Alert/Delighted----Amazed/Surprized shown by blue bar.

6.4.3 Results for PAD model

Gesture: Point-point motion		Pleasure	Arousal	Dominance
V=250 & A=10	LOW	17	17	14
	MED	1	0	4
	HIGH	0	1	0
overall				
Range 1: R1	sad/tired-unpleasant	18		
Range 2: R2	happy/pleased-pleasant	0		
Range 3: R3	excited-aroused	0		
V=800 & A=50	LOW	4	3	2
	MED	13	14	15
	HIGH	1	1	1
Overall				
Range 1: R1	sad/tired-unpleasant	3		
Range 2: R2	happy/pleased-pleasant	11		
Range 3: R3	excited-aroused	4		
V=2000 & A=300	LOW	4	3	2
	MED	4	5	3
	HIGH	10	10	13
overall				
Range 1: R1	sad/tired-unpleasant	1		
Range 2: R2	happy/pleased-pleasant	12		
Range 3: R3	excited-aroused	5		

Table6. 7: Response of participants for PAD model G1

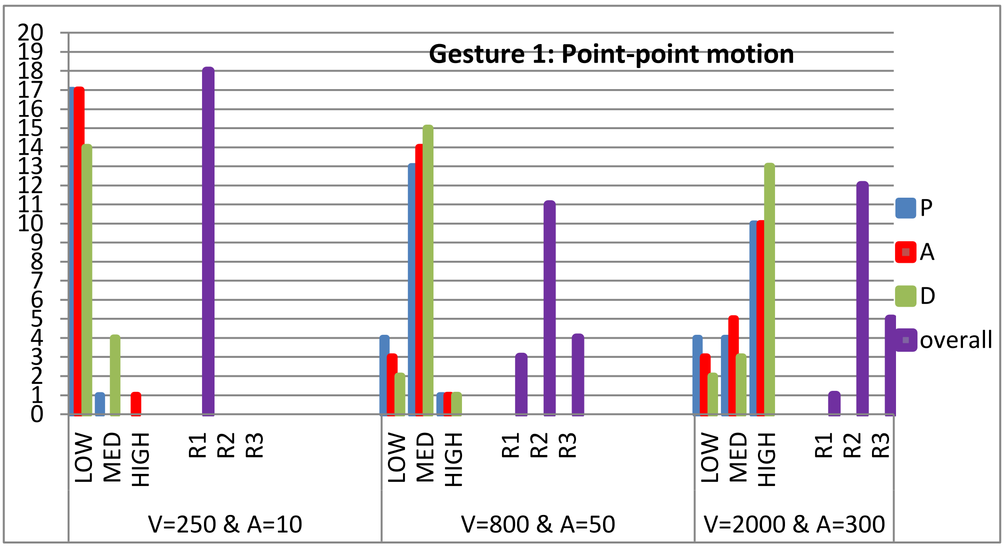

Figure6. 13: PAD model graph for 3 sets of parameters for G1

The graph in Fig. 6.13 shows that for point-point motion of robot according to PAD scale 18/18 people have marked the gesture in category R1 represented by purple bar, falling under the emotions of sad/tired-unpleasant. At medium level of velocity and acceleration 11/18 people marked it in R2 as Pleasant --- happy/Joyful shown by purple bar. For highest values of velocity and acceleration majority i.e. 12/18 perceived it as Pleasant --- happy/Joyful shown by purple bar.

	Gesture2: Waving of robot		**Pleasure**	**Arousal**	**Dominance**
V=100 & A=15	LOW		17	15	15
	MED		1	1	3
	HIGH		0	2	0
overall					
Range 1: R1	sad/tired-unpleasant	17			
Range 2: R2	happy/pleased-pleasant	1			
Range3 :R3	excited-aroused	0			
V=100 & A=5	LOW		2	3	4
	MED		16	14	12
	HIGH		0	1	2
overall					
Range 1: R1	sad/tired-unpleasant	3			
Range 2: R2	happy/pleased-pleasant	14			
Range3 :R3	excited-aroused	1			
V=100 & A=1.5	LOW		3	2	0
	MED		5	6	5
	HIGH		10	10	13
overall					
Range 1: R1	sad/tired-unpleasant	0			
Range 2: R2	happy/pleased-pleasant	4			
Range3 :R3	excited-aroused	14			

Table6. 8: Response of participants for PAD model G2

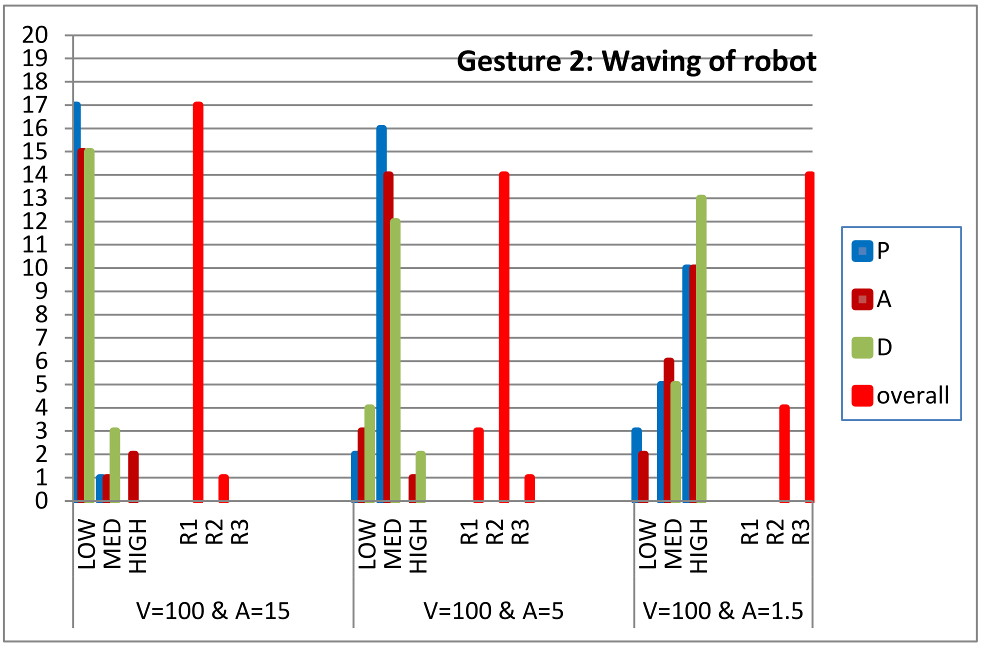

Figure6. 14: PAD model graph for 3 sets of parameters for G2

The graph in Fig. 6.14 shows that for waving of robot according to PAD scale 17/18 people have marked the gesture in category R1 represented by red bar, falling under the emotions of sad/tired-unpleasant. At medium level of velocity and acceleration 14/18 people marked it in R2 as Pleasant --- happy/Joyful shown by red bar. For highest values of velocity and acceleration majority i.e. 14/18 perceived it as excited-aroused shown by red bar.

	Gesture3: Bowing down of robot		Pleasure	Arousal	Dominance
V=30 & A=30	LOW		16	16	16
	MED		2	2	2
	HIGH		0	0	0
overall					
Range 1: R1	sad/tired-unpleasant	18			
Range 2: R2	happy/pleased-pleasant	0			
Range3 :R3	excited-aroused	0			
V=50 & A=50	LOW		2	14	2
	MED		4	14	0
	HIGH		7	11	0
overall					
Range 1: R1	sad/tired-unpleasant	3			
Range 2: R2	happy/pleased-pleasant	15			
Range3 :R3	excited-aroused	0			
V=100 & A=100	LOW		1	1	2
	MED		8	3	5
	HIGH		10	14	11
overall					
Range 1: R1	sad/tired-unpleasant	1			
Range 2: R2	happy/pleased-pleasant	6			
Range3 :R3	excited-aroused	11			

Table6. 9: Response of participants for PAD model G3

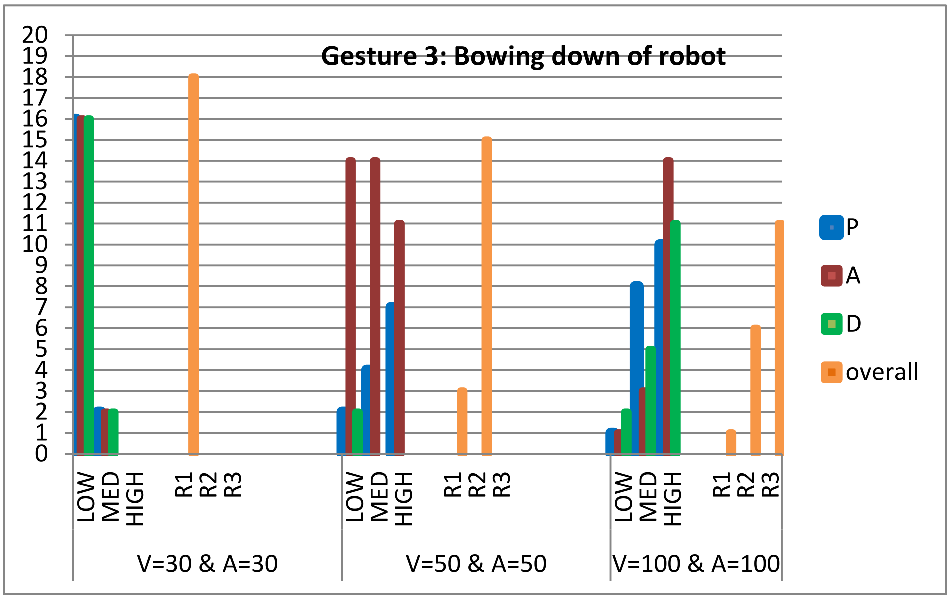

Figure6. 15: PAD model graph for 3 sets of parameters for G3

The graph in Fig. 6.15 shows that for bowing of robot according to PAD scale 18/18 people have marked the gesture in category R1 represented by orange bar, falling under the emotions of sad/tired-unpleasant. At medium level of velocity and acceleration 15/18 people marked it in R2 as Pleasant --- happy/Joyful shown by orange bar. For highest values of velocity and acceleration majority i.e. 11/18 perceived it as excited-aroused shown by orange bar.

6.5 Discussion of results

The statistical results concluded are shown below for all the gestures at all set of velocities and acceleration for the three models. The percentage represents the number of people that have marked particular emotion in that specific set of quadrant.

- Gesture1: Point-point motion at V=250 and A=10:

Russell's model

Q1	0%
Q2	0%
Q3	**95%**
Q4	5%

Tellegen-Watson-Clark model

Q1	0%
Q2	5%
Q3	11%
Q4	**83%**

PAD model

R1	**100%**
R2	0%
R3	0%

- For Gesture1: Point-point motion at V=800 and A=50:

Russell's model

Q1	22%
Q2	33%
Q3	6%
Q4	**39%**

Tellegen-Watson-Clark model

Q1	11%
Q2	**61%**
Q3	5%
Q4	22%

PAD model

R1	17%
R2	**61%**
R3	22%

- For Gesture1: Point-point motion at V=2000 and A=300:

Russell's model

Q1	**67%**
Q2	27%
Q3	0%
Q4	6%

Tellegen-Watson-Clark model

Q1	**50%**
Q2	5%
Q3	33%
Q4	11%

PAD model

R1	5%
R2	**67%**
R3	28%

Considering the first parameter for gesture1 of all the three models that is at V=250 and A=10, the result shows that this particular motion of the robot in terms of emotions perceived by majority of the participants comes under the following categories for all the models. The percentage shown represents the highest number of participants that marked in the particular quadrant.

Gesture1: Point-point motion at V=250 and A=10

- ✓ Russell's model : Q3-**95%**: Tired/Sleepy --- Sad/Miserable
- ✓ Tellegen-Watson-Clark model: Q4-**83%**: Unpleasant --- Sad/Tired
- ✓ PAD model: Range1-**100%**: Sad/Tired-Unpleasant

The results from all the three models come under the same category of being unpleasant, sad, tired etc. For the PAD model, most of the people marked pleasure, arousal and dominance as "low" for this set of parameters. This also makes sense that if the emotions shown by the embodiment are sad and unpleasant then all of the three factors will fall in low category. The percentage of people that marked in the categories is shown. The remaining percentage of the people is divided among the rest of categories for the gesture. Now considering the second set of parameters for all the three models of gesture1 that is point-point motion at V=800 and A=50, the following results are obtained:

Gesture1: Point-point motion at V=800 and A=50

- ✓ Russell's model : Q4-**39%**: Calm/Content --- Pleased
- ✓ Tellegen-Watson-Clark model: Q2-**61%**: Pleasant --- Happy/Joyful
- ✓ PAD model: Range2-**61%**: Happy/Pleased-Pleasant

The percentage shown represents the highest number of participants that have marked in the particular quadrant. So it is quite clear that all the three models categorise the second set of parameters as happy, pleasant and joyful. For the PAD model, most of the people marked pleasure, arousal and dominance as "medium" for this set of parameters. Now considering the third set of parameters that is at A=1000 and V=300 for gesture1 of all three models, the results are:

Gesture1: Point-point motion at V=2000 and A=200

- ✓ Russell's model :Q1-**67%**: Excited/Delighted ---- Aroused
- ✓ Tellegen-Watson-Clarkmodel:Q1-**50%:**Alert/Delighted---Amazed/Surprized
- ✓ PAD model: Range2-**67%**: Happy/Pleased --- Pleasant

The rest of the percentage is divided among all of the remaining categories, showing a very small percentage falling in each of them. However, for this gesture only the result shown by the PAD model differs from rest of the models. The other two models place the emotion under the category of being excited, delightful, and alert. According to the PAD model the perceived emotion comes under being happy or pleased. However the people marked pleasure, arousal and dominance as "high" for this set of parameters.

Similarly, shown below are the results for gesture2 (i.e. waving of the robotic arm) for all the three set of parameters for all models.

- Gesture2: Waving of robot at V=100 and A=15:

Russell's model

Q1	0%
Q2	11%
Q3	**83%**
Q4	5%

Tellegen-Watson-Clark model

Q1	5%
Q2	0%
Q3	12%
Q4	**83%**

PAD model

R1	**95%**
R2	5%
R3	0%

- For Gesture2: Waving of robot at V=100 and A=5:

Russell's model

Q1	6%
Q2	33%
Q3	22%
Q4	**39%**

Tellegen-Watson-Clark model

Q1	28%
Q2	**61%**
Q3	11%
Q4	0%

PAD model

R1	17%
R2	**78%**
R3	5%

- For Gesture2: Waving of robot at V=100 and A=1.5:

Russell's model

Q1	**72%**
Q2	28%
Q3	0%
Q4	0%

Tellegen-Watson-Clark model

Q1	**67%**
Q2	33%
Q3	0%
Q4	0%

PAD model

R1	0%
R2	22%
R3	**78%**

Gesture2: Waving of robot at V=100 and A=15

- ✓ Russell's model : Q3-**83%**: Tired/Sleepy --- Sad/Miserable
- ✓ Tellegen-Watson-Clark model-**83%**: Q4: Unpleasant --- Sad/Tired
- ✓ PAD model: Range1-**95%**: Sad/Tired --- Unpleasant

Gesture2: Waving of robot at V=100 and A=5

- ✓ Russell's model : Q4-**39%**: Calm/Content --- Pleased
- ✓ Tellegen-Watson-Clark model: Q2-**61%:** Pleasant --- Happy/Joyful
- ✓ PAD model: Range2-**78%**: Happy/Pleased --- Pleasant

Gesture2: Waving of robot at V=100 and A=1.5

- ✓ Russell's model : Q1-**72%**: Excited/Delighted ---- Aroused
- ✓ Tellegen-Watson-Clarkmodel:Q1-**67%**:Alert/Delighted---Amazed/Surprized
- ✓ PAD model: Range3-**78%:** Excited --- Aroused

This shows that for gesture2 the results for all the three set of parameters falls under the same category from all the models. Moreover these results are similar and support the ones obtained for Gesture1. Most of the people marked individual parameters of PAD scale as "low, low, low", "medium, medium, medium" and "high, high, high" for the three sets of parameters respectively representing the three emotions of being sad, happy and excited .

The results obtained for gesture 3 that is bowing down of the robotic arm for all three set of parameters is given below:

- Gesture3: Bowing down of robot at V=30 and A=30:

Russell's model

Q1	0%
Q2	5%
Q3	**83%**
Q4	11%

Tellegen-Watson-Clark model

Q1	5%
Q2	11%
Q3	12%
Q4	**72%**

PAD model

R1	**100%**
R2	0%
R3	0%

- Gesture3: Bowing down of robot at V=30 and A=30:

Russell's model

Q1	0%
Q2	5%
Q3	**83%**
Q4	11%

Tellegen-Watson-Clark model

Q1	5%
Q2	11%
Q3	12%
Q4	**72%**

PAD model

R1	**100%**
R2	0%
R3	0%

- For Gesture3: Bowing down of robot at V=50 and A=50:

Russell's model

Q1	11%
Q2	17%
Q3	22%
Q4	**50%**

Tellegen-Watson-Clark model

Q1	12%
Q2	**78%**
Q3	5%
Q4	5%

PAD model

R1	17%
R2	**83%**
R3	0%

- For Gesture3: Bowing down of robot at V=100 and A=100:

Russell's model

Q1	**61%**
Q2	11%
Q3	0%
Q4	28%

Tellegen-Watson-Clark model

Q1	**61%**
Q2	39%
Q3	0%
Q4	0%

PAD model

R1	5%
R2	33%
R3	**61%**

Gesture3: Bowing down of robot at V=30 and A=30

- ✓ Russell's model : Q3-**83%**: Tired/Sleepy --- Sad/Miserable
- ✓ Tellegen-Watson-Clark model: Q4-**72%**: Unpleasant --- Sad/Tired
- ✓ PAD model: Range1-**100%**: Sad/Tired --- Unpleasant

Gesture3: Bowing down of robot at V=50 and A=50

- ✓ Russell's model : Q4-**50%**: Calm/Content --- Pleased
- ✓ Tellegen-Watson-Clark model: Q2-**78%**: Pleasant --- Happy/Joyful
- ✓ PAD model: Range2-**83%**: Happy/Pleased --- Pleasant

Gesture3: Bowing down of robot at V=100 and A=100

- ✓ Russell's model : Q1-**61%**: Excited/Delighted ---- Aroused
- ✓ Tellegen-Watson-Clark-model:Q1-**61%**:Alert/Delighted--Amazed/Surprized
- ✓ PAD model: Range3-**61%**: Excited --- Aroused

The first set parameter of velocity and acceleration is perceived as being sad, unpleased etc. whereas the second and third are perceived as being happy and excited respectively. The individual marking for pleasure, arousal and dominance on the PAD scale is (low, low, low) for the first set of parameters which represents being sad, for happy and pleasure mood the individual parameters are marked as (high, low-medium, low) and for being alert and excited the individual P, A and D is marked as (high, high, high).

6.6 Summary of the chapter

This chapter focuses on the techniques and methods that were followed in order to perform the experiments with 18 different participants. It explains how the participants have marked the questionnaire for perceived emotions on three different scales. Later the results for these experiments are collected in the form of bar graphs. The statistical results of each gesture for all three scales are also discussed in this chapter. The concluded results shows that majority of the participants at low velocity and acceleration, for all the three gestures, have marked the perceived emotions in the category of being sad, unpleasant or tired. Whereas at medium level of velocity and acceleration the perceived emotion for all three gestures, according to all three scales, was pleasant, happy or pleased. However for high values of velocity and acceleration the perceived emotional behaviour falls under the category of alert, delighted, amazed or excited.

The next chapter will discuss the conclusions that are drawn from these results. It will highlight the major findings and limitation of this research. It will also focus on the possible future work that can be done.

CHAPTER 7

CONCLUSIONS AND RECOMMENDATIONS

7.1 Conclusion

From the results produced it can be concluded the slow motion is perceived as sad, unhappy and unpleasant by the participants, the medium level motion parameters for velocity and acceleration is perceived as happy, joyful and calm by the participants and the emotion that participants have associated with the fast motion is of being excited, alert and aroused. These motion parameters are therefore considered important for the change in user's perception of emotions (Saerbeck and Bartneck, 2010). Therefore with the change of speed and acceleration the emotional mood changes from being sad to happy to excited. This develops a link between the change in user perception of emotions by varying the motion parameters of velocity and acceleration (Ian et al., 2005).

This kind of robotic embodiment that is considered as machine robot is capable of conveying emotions without any android features such as face etc. (Beck et al., 2013). Moreover it is observed that the noise produced by the robot changes with change of emotional behaviour (Eun et al., 2009). When the robot was perceived to be sad or unhappy the noise associated with it was very low. However as the perceived emotion changed from sad to happy and then to excited as the noise associated with robotic embodiment increased exponentially.

This research gives rise to several questions that remain to be answered e.g. in the field of care and medication, are slow movements of a robot perceived as a sad gesture or a careful gesture by the patient? For industrial purposes can these emotional robots have the same efficiency and productivity rate as the ones used now? Further research and investigation is therefore needed in this area in order to incorporate these emotional robots in various important fields of life effectively.

7.2 Recommendations regarding hardware

The following improvements can be made in this project regarding the hardware:

- ✓ Use FPGA with a higher space capacity and more DMA channels for the transfer of data between RT and FPGA VIs
- ✓ Use a NI 9403 C Series 32-Ch, 5 V/TTL Bidirectional Digital I/O Module to read all joint encoders
- ✓ A gripper provided by FESTO and many other companies can be attached at the end of Robolink to introduce more functionally and for extending the core concept of project

7.3 Recommendations regarding LabVIEW programming

The code on the FPGA as well as RT side can be improved further by:

- ✓ Code on FPGA side should be reduced by either shifting it to RT VI or by reducing it so to have space for new concepts of programming
- ✓ NI 9403 module could be introduced in the code for keeping the track of the joint positions

7.4 Research limitations

It is important to highlight that the poses and gestures were deliberately selected to be expressive for the user. However it was important from the aspect of developing a movement that should be expressive and communicative to the user (Beck et al., 2013). This might had an effect on the results found in this research.

Moreover the participants should be blinded from the data for changing values of motion parameters on the questionnaire. This can be considered biased in finding a relationship between velocity and acceleration, and envisaged emotion.

The sequence of motion parameters as well as gestures should also be randomized as this might be helpful in predicting the next emotion in line.

Another potential bias associated with this robotic embodiment is the noise that it makes during its motion. This noise rises with the increase in values of motion parameters. At low values of motion parameters the noise associated is less. As the values of velocity and acceleration increases the noise gets louder. Therefore this might help the user to identify the perceived emotions.

7.5 Future work

This study did not consider the effect of changing the embodiment in same robot category that is of machine robot, to see if the change of embodiment affects the results or not. Therefore same experiments shall be performed on different embodiment to see the effect.

Introduction of new gestures and emotions in the embodiment can also increase the scope of research. Although the results are quite reasonable, the sample size of participants is quite small. It should be increased for the generalizability of results. Additionally the robot should be equipped with some kind of soundproof material for the reduction of noise.

This research shall be performed on android robot to see if the perception of user differs by changing the robot to android one. This will also check that whether the research supports Uncanny Valley theory or not.

References

1. Anandan, T., 2013. The End of Separation: Man and Robot as Collaborative Coworkers on the Factory Floor. Robotic online. URL: http://www.robotics.org/content-detail.cfm/Industrial-Robotics-Featured-Articles/The-End-of-Separation-Man-and-Robot-as-Collaborative-Coworkers-on-the-Factory-Floor/content_id/4140.
2. Bartneck, C., Reichenbach, J., Carpenter, J., 2006. Use of Praise and Punishment in Human-Robot Collaborative Teams, in: The 15th IEEE International Symposium on Robot and Human Interactive Communication, 2006. ROMAN 2006. Presented at the 15th IEEE International Symposium on Robot and Human Interactive Communication, 2006. ROMAN 2006, pp. 177–182.
3. Beck, A., Hiolle, A. & Cañamero, L., 2013. Using Perlin Noise to Generate Emotional Expressions in a Robot. CogSci 2013 THE ANNUAL MEETING OF THE COGNITIVE SCIENCE SOCIETY, pp.1845–1850. URL: http://mindmodeling.org/cogsci2013/papers/0343/paper0343.pdf.
4. Bizzi , E. et al., 1984. Posture control and trajectory formation during arm movement. , 4(11), pp.2738–2744. URL: http://web.mit.edu/bcs/bizzilab/publications/bizzi1994.pdf.
5. Blythe, P.W., Todd, P.M., Miller, G.F., 1999. How motion reveals intention: Categorizing social interactions, in: Simple Heuristics That Make Us Smart, Evolution and Cognition. Oxford University Press, New York, NY, US, pp. 257–285.
6. Boris , K., 2007. Pointer oriented object detection method, involves defining class of objects as action and realizing and processing pointer on vocabulary of computer system in natural speech during initialization of objects. URL: http://www.google.com/patents/DE102006052141A1?cl=en.
7. Braitenberg, V., 1984. Vehicles: Experiments in Synthetic Psychology First., USA: MIT press paperback edition 1986. URL: http://books.google.co.uk/books?id=7KkUAT_q_sQC&printsec=frontcover&source=gbs_ge_summary_r&cad=0#v=onepage&q&f=false.

8. Breazeal, C., 2003. Toward sociable robots. Robotics and Autonomous Systems 42, 167–175.
9. Coan, J.A., Allen, J.J., 2007. Handbook of Emotion Elicitation and Assessment. Oxford University Press.
10. Coolcore, 2009. CoolCore the Low Power IP Core Company. URL http://www.coolcore.co.uk/Home.html (accessed 7.29.13).
11. Dautenhahn, K. et al., 2009. KASPAR - a minimally expressive humanoid robot for human-robot interaction research. , (3-4), pp.369–397. URL: http://homepages.feis.herts.ac.uk/~comqkd/Dautenhahn-etal-Revised-CompleteDocument-web.pdf.
12. Dautenhahn, K., 2007. Socially intelligent robots: dimensions of human--robot interaction. Philosophical Transactions of the Royal Society B: Biological Sciences, 362, pp.679–704. Available at: http://www.ncbi.nlm.nih.gov/pmc/articles/PMC2346526/pdf/rstb20062004.pdf.
13. Dautenhahn, K., 1999. ROBOTS AS SOCIAL ACTORS:AURORA AND THE CASE OF AUTISM. In Third Cognitive Technology Conference CT'99, August, San Francisco. URL: http://www.gel.usherbrooke.ca/crj/Documentation/ctkerstin.pdf.
14. Dick, P.K., 2013. android project. Philip K. Dick Android project. URL http://www.pkdandroid.org/ (accessed 7.26.13).
15. Ertugrul, N., 2000. Towards Virtual Laboratories a Survey of LabVIEW-based teaching/learning tools and future trends. International Journal of Engineering Education, 2000 pp. 1–10.
16. Eun, S.J. et al., 2009. Sound Production for the Emotional Expression of Socially Interactive Robots. In Advances in Human-Robot Interaction. URL: http://cdn.intechopen.com/pdfs/6453/InTech Sound_production_for_the_emotional_expression_of_socially_interactive_robots.pdf.
17. Flanagan, J.R. & Ostry, D.J., 1990. Trajectories of human multi-joint arm movements: Evidence of joint level planning . In The First International Symposium on Experimental Robotics I. URL: http://brain.phgy.queensu.ca/flanagan/papers/FlaOst_ERO_90.pdf.

18. Folea, S., 2011. LabVIEW-practical applications and solutions. InTech, URL http://www.intechopen.com/books/practical-applications-and-solutions-using-labview-software (accessed 7.26.13).
19. Fong, T., Nourbakhsh, I. & Dautenhahn, K., 2003. A survey of socially interactive robots. , Volume 42(Issues 3–4), p.Pages 143–166. Available at: http://infoscience.epfl.ch/record/30017/files/CMU-RI-TR-02-29.pdf.
20. Fontys, 2013. IGUS robotic arm. Mechatronica. URL: http://lectoraatmechatronica.wikispaces.com/Igus-robotic-arm (accessed 7.26.13).
21. Forlizzi, J. & DiSalvo, C., 2006. Service Robots in the Domestic Environment: A Study of the Roomba Vacuum in the Home. In HRI ’06 Proceedings of the 1st ACM SIGCHI/SIGART. Human Robot Interaction. pp. 258–265. URL: http://133.11.9.3/~takeo/course/2007/media/papers/roomba_at_home.pdf.
22. Gaertner, S. et al., 2010. Generation of Human-like Motion for Humanoid Robots Based on Marker-based Motion Capture Data. In Robotics (ISR), 2010 41st International Symposium on and 2010 6th German Conference on Robotics (ROBOTIK). Munich, Germany, pp. 1 – 8. URL: http://ieeexplore.ieee.org/xpl/articleDetails.jsp?reload=true&arnumber=5756898&tag=1.
23. Gaveau, J., Papaxanthis, C., 2011. The Temporal Structure of Vertical Arm Movements. Open I beta. URL http://openi.nlm.nih.gov/detailedresult.php?img=3134452_pone.0022045.g002&req=4 (accessed 8.2.13).
24. Gizmag, team, 2002. Tiny lamprey-inspired robot could locate diseases inside human body . URL http://www.gizmag.com/lamprey-robot-disease-detection-epsrc/22016/ (accessed 7.26.13).Goodrich, M.A., Schultz, A.C., 2007.
25. Goodrich, M.A., Schultz, A.C., 2007. Human-robot interaction-A survey. Foundations and Trends R © in Human–Computer Interaction Vol. 1, No. 3 (2007) 203–275.
26. Haddadin, S. et al., 2011. Towards the Robotic Co-Worker. In 14TH International Symposium of Robotics Research. ISRR. Lucerne, Switzerland, pp. 261–282. URL: http://www.phriends.eu/isrr_09b.pdf.

27. Heider, F., Simmel, M., 1944. An Experimental Study of Apparent Behavior. The American Journal of Psychology 57, 243.
28. Höök, K., 2013. Affective Computing. The Encyclopedia of Human-Computer Interaction, 2nd Ed. URL /encyclopedia/affective_computing.html (accessed 7.29.13).
29. Ian , B., Debayan , G. & Fei , H., 2005. Effects of low level changes in motion on human perception of robots. In Development and Learning, 2005. Proceedings. . The 4th International Conference on Development and Learning. pp. 1–5. URL: http://work.debayangupta.com/smooth/BGH.pdf.
30. IGUS, 2013. Robolink. URL http://www.igus.eu/_wpck/pdf/global/DE-EN_robolink_04-2013_s.pdf (accessed 7.26.13).
31. IGUS, 2013. IGUS plastics for longer life. IGUS. URL http://www.igus.co.uk/wpck/default.aspx?PageNr=7904&C=US&L=en (accessed 7.26.13).
32. IGUS, 2012a. Robolink joint kit-documentation. URL http://www.igus.eu/_wpck/pdf/global/Documentation_robolink_en.pdf (accessed 7.26.13).IGUS, 2012b.
33. IGUS, 2012b. Stepper motor. URL http://www.igus.eu/_wpck/pdf/global/Motordatasheet_EN.pdf (accessed 7.26.13).
34. Jason , M.O., 2007. A theory for comparing robot systems. University of Illinois. URL: http://www.cse.sc.edu/~jokane/pubs/OKa07.html.
35. Jie Cao, H.W., 2008. PAD Model Based Facial Expression Analysis. Springer-Verlag Berlin Heidelberg pp.450–459. URL http://hcsi.cs.tsinghua.edu.cn/accenter/paper/ac2005/assist/Papers2008/09-PAD%20Model%20Based%20Facial%20Expression%20Analysis.pdf (accessed 7.29.13).
36. Kensinger, E.A., 2004. Remembering emotional experiences: The contribution of valence and arousal. Reviews in the Neurosciences pp. 241–253. URL https://www2.bc.edu/~kensinel/Kensinger_RevNeurosci04.pdf
37. Koeppe, R. et al., 2003. Robot-Robot and Human-Robot Cooperation in Commercial Robotics Applications. In Robotics Research, The Eleventh

International Symposium. ISRR. Siena, Italy.URL: http://link.springer.com/chapter/10.1007%2F11008941_22#page-1.

38. Kuhlman, R., 2013. Introduction to the LabVIEW FPGA Module.URL https://ni.adobeconnect.com/_a56821929/p28532990/?launcher=false&fcsContent=true&pbMode=normal (accessed 7.29.13).

39. Li, X., Zhou, H., Song, S., Ran, T., Fu, X., 2005. The Reliability and Validity of the Chinese Version of Abbreviated PAD Emotion Scales, in: Tao, J., Tan, T., Picard, R.W. (Eds.), Affective Computing and Intelligent Interaction, Lecture Notes in Computer Science. Springer Berlin Heidelberg, pp. 513–518.

40. Matsumaru, K., 2009. Discrimination of emotion from movement and addition of emotion in movement to improve human-coexistence robot's personal affinity. In Robot and Human Interactive Communication, 2009. RO-MAN 2009. The 18th IEEE International Symposium on. Toyama, pp. 387 – 394.URL: http://ieeexplore.ieee.org/xpl/articleDetails.jsp?arnumber=5326345&tag=1.

41. Mehrabian, A., 1977. Nonverbal Communication. Transaction Publishers. URL:http://books.google.co.uk/books?hl=en&lr=&id=XtYALu9CGwC&oi=fnd&pg=PR7&dq=nonverbal+communication+by+albert+mehrabian&ots=5xNeQi8kow&sig=G3O1zsT8yRfuio3oweb1XbkYvSw#v=onepage&q=nonverbal%20communication%20by%20albert%20mehrabian&f=false (accessed 7.29.13).

42. Mehrabian, A., 1980. Basic Dimensions for a General Psychological Theory: Implications for Personality, Social, Environmental, and Developmental Studies. Oelgeschlager, Gunn & Hain.

43. Mehrabian, A., 1996. Pleasure-arousal-dominance: A general framework for describing and measuring individual differences in Temperament. Current Psychology 14, 261–292.

44. Menzel, P., 2013. Kismet. Kismet. URL http://www.ai.mit.edu/projects/humanoid-robotics-group/kismet/kismet.html (accessed 7.26.13).

45. Mori, M., 2005. The Uncanny Valley. URL http://www.androidscience.com/theuncannyvalley/proceedings2005/uncannyvalley.html (accessed 7.26.13).NASA, 2013. Robonaut.

46. NASA. URL robonaut.jsc.nasa.gov/default.asp (accessed 7.26.13).

47. NI, 2013. About virtual instrumentation. National Instruments. URL http://www.ni.com/white-paper/2964/en/ (accessed 7.29.13).

48. NI, 2010. Operating instructions and specifications CompactRIO cRIO-9072/3/4 National Instruments. URL http://www.ni.com/pdf/manuals/374639e.pdf (accessed 7.29.13).

49. NI, 2012. Integrated 400MHz Real-Time Controller and 2M gate FPGA. National Instruments. URL http://sine.ni.com/nips/cds/print/p/lang/en/nid/203964 (accessed 7.29.13).

50. NI, 2012e. Advanced Motion Using NI CompactRIO. National Instruments. URL http://zone.ni.com/wv/app/doc/p/id/wv-873 (accessed 7.29.13).

51. NI, 2013f. Building an NI Motion Control System. National Instruments. URL http://www.ni.com/white-paper/12127/en/ (accessed 7.29.13).

52. NI, 2011b. CompactRIO Integrated Systems with Real-Time Controller and Reconfigurable Chassis. National Instruments. URL http://sine.ni.com/ds/app/doc/p/id/ds-204/lang/en (accessed 7.29.13).

53. NI, 2013e. FPGA Design, Development and Programming Tutorial. National Instruments. URL http://www.ni.com/white-paper/3358/en/ (accessed 7.29.13).

54. NI, 2013d. FPGA Fundamentals. National Instruments. URL http://www.ni.com/white-paper/6983/en/ (accessed 7.29.13).

55. NI, 2013. Hands-On: Introduction to LabVIEW Real-Time. URL ftp://ftp.ni.com/pub/branches/uk/nidays2008/track_6/intro_to_lv_realtime.pdf (accessed 7.29.13).

56. NI, 2013b. Increase your organization productivity with LabVIEW. National Instruments. URL http://www.ni.com/white-paper/3494/en/ (accessed 7.29.13).

57. NI, 2011a. LabVIEW for measurement and data analysis. National Instruments. URL http://www.ni.com/white-paper/3566/en/ (accessed 7.26.13).

58. NI, 2012b. Measurement and automation explorer help .National Instruments. URL http://digital.ni.com/manuals.nsf/websearch/A20E4510ACC3BADE862579FF00789571 (accessed 7.29.13).

59. NI, 2012d. NI 9401, 8 Ch, 5 V/TTL High-Speed Bidirectional Digital I/O Module. National Instruments. URL http://sine.ni.com/nips/cds/print/p/lang/en/nid/208809 (accessed 7.29.13).

60. NI, 2012c. NI 9501. National Instruments. URL http://sine.ni.com/ds/app/doc/p/id/ds-292/lang/en (accessed 7.29.13).

61. NI, 2012a. NI cRIO 9074. National Instruments. URL http://sine.ni.com/nips/cds/print/p/lang/en/nid/203964 (accessed 7.26.13).

62. NI, 2013c. NI LabVIEW Real-Time Module. National Instruments. URL http://www.ni.com/labview/realtime/ (accessed 7.29.13).

63. NI, 2012f. Overview of the LabVIEW Robotics Module. National Instruments. URL http://www.google.co.uk/url?sa=t&rct=j&q=&esrc=s&source=web&cd=2&ved=0CDYQFjAB&url=http%3A%2F%2Fwww.ni.com%2Fwhite-paper%2F11564%2Fen%2Fpdf&ei=gkXtUei6PILTPOePgLgD&usg=AFQjCNGs8l4u4paGnD2cZWTpUev7a06PjQ&bvm=bv.49478099,d.d2k (accessed 7.29.13).

64. NI, 2013a. What is CompactRIO. National Instruments. URL http://www.ni.com/compactrio/whatis/ (accessed 7.29.13).

65. NI, 2013b. Designing Serial Arms (Robotics Module). National Instruments. URL:http://zone.ni.com/reference/en-XX/help/372983D-01/lvrobogsm/robo_arm_definition/.

66. Nishida, T., Jain, L.C., Faucher, C., 2010. Modelling Machine Emotions for Realizing Intelligence - Foundations and Applications. URL http://www.springer.com/engineering/computational+intelligence+and+complexity/book/978-3-642-12603-1 (accessed 9.06.13).

67. Posada-Gomez, R., Osvaldo, O., Martinez, A., Portillo-Rodriguez, O., Alor-Hernandez, G., 2011. Digital Image Processing Using LabView, in: Folea, S. (Ed.), Practical Applications and Solutions Using LabVIEW Software. InTech.

68. Posner, J., Russell, J.A., Peterson, B.S., 2005. The circumplex model of affect: An integrative approach to affective neuroscience, cognitive development, and psychopathology. Dev Psychopathol 17, 715–734.

69. Qassem, M.A., Abuhadrous, I. & Elaydi, H., 2010. Modeling and Simulation of 5 DOF educational robot arm. In Advanced Computer Control (ICACC), 2010 2nd International Conference. Shenyang, pp. 569 – 574. URL: http://ieeexplore.ieee.org/xpl/login.jsp?tp=&arnumber=5487136&url=http%3A%2F%2Fieeexplore.ieee.org%2Fxpls%2Fabs_all.jsp%3Farnumber%3D5487136

70. Remington, N.A., Fabrigar, L.R., Visser, P.S., 2000. Re-examining the circumplex model of affect. Journal of Personality and Social Psychology 79, 286–300.

71. Russell, J.A., 1980. A circumplex model of affect. Journal of Personality and Social Psychology 39, 1161–1178.

72. Russell, J.A., Lewicka, M., Niit, T., 1989. A cross-cultural study of a circumplex model of affect. Journal of Personality and Social Psychology 57, 848–856.

73. Saerbeck, M., Van Breemen, A.J.N., 2007. Design guidelines and tools for creating believable motion for personal robots, in: The 16th IEEE International Symposium on Robot and Human Interactive Communication, 2007. RO-MAN 2007. Presented at the 16th IEEE International Symposium on Robot and Human interactive Communication, 2007. RO-MAN 2007, pp. 386–391.

74. Saerbeck, M., Bartneck, C., 2010. Perception of affect elicited by robot motion, in: Proceedings of the 5th ACM/IEEE International Conference on Human-robot Interaction, HRI '10. IEEE Press, Piscataway, NJ, USA, pp. 53–60.

75. Sandin, P.E., 2003. Robot Mechanisms and Mechanical Devices Illustrated. McGraw-hill companies.

76. Tellegen, A., Watson, D., Clark, L.A., 1999. On the Dimensional and Hierarchical Structure of Affect. Psychological Science 10, 297–303.

77. Thalmann, D., Ahn, J., Silvestre, Q., 2010. Asymmetrical Facial Expressions based on an Advanced Interpretation of Two-dimensional Russells Emotional Model. proceedings of ENGAGE 2010.

78. Thrun, S., Bennewitz, M., Burgard, W., Cremers, A.B., Dellaert, F., Fox, D., Hahnel, D., Rosenberg, C., Roy, N., Schulte, J., Schulz, D., 1999. MINERVA: a second-generation museum tour-guide robot, in: 1999 IEEE International Conference on Robotics and Automation, 1999. Proceedings. Presented at the

1999 IEEE International Conference on Robotics and Automation, 1999. Proceedings, pp. 1999–2005 vol.3.

79. Travis, J., Kring, J., 2013. LabView for everyone, 3rd ed. Prentice Hall PTR.

80. Trohidis, K., Tsoumakas, G., Kalliris, G., Vlahavas, I., 2011. Multi-label classification of music by emotion. EURASIP Journal on Audio, Speech, and Music Processing 2011, 4.

81. Tuomas, Eerola & Jonna, K. Vuoskoski, 2011. A comparison of the discrete and dimensional models of emotion in music. , 39, pp.18–49. URL: http://pom.sagepub.com/content/39/1/18.abstract.

82. Uno, A., 2009. RIBA robot nurse bear. Pink tentacle. URL http://pinktentacle.com/2009/08/riba-robot-nurse-bear/ (accessed 7.26.13).

83. Watson, D., Clark, L.A., Tellegen, A., 1988. Development and validation of brief measures of positive and negative affect: The PANAS scales. Journal of Personality and Social Psychology 54, 1063–1070.

84. Wondolowski, C., Davis, D.K., 1991. The Lived Experience of Health in the Oldest Old: A Phenomenological Study. Nurs Sci Q 4, 113–118.

85. Yang, dan, Lee, W., 2004. Disambiguating music emotion using software agents. Presented at the 5th International Conference on Music Information Retrieval, Universitat Pompeu Fabra, Barcelona, Spain, pp. 10–14.

Appendices

Appendix A: Drawings for IGUS robotic arm

Appendix B: Tube length of joints

Appendix C: Technical data for tube lengths

Appendix D: Datasheet of integrated Hall IC's and configuration of sensor lines

Appendix E: Technical data for stepper motors

Appendix F: Complete specifications for drive unit

Appendix G: Technical Datasheet of NI 9501

Appendix H: Technical Datasheet of cRIO 9074

Appendix I: Technical Datasheet of NI 9401

Appendix J: Properties of CompactRIO 9074

Appendix K: Connection of motors with 9501

Appendix L: Wiring of chassis and cRIO

Appendix M: Mechanical parts and joint types of Robolink

Appendix N: Ethical approval and consent form

Appendix O: LabVIEW Code (CDROM)

Appendix A: Drawings for IGUS robotic arm

robolink® Joint kit – Documentation (#1; 2012-09)

Dimensioned drawings

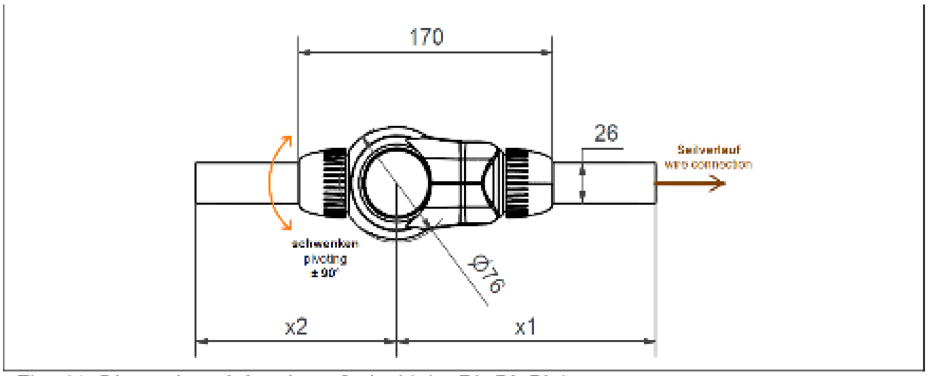

Fig. 41: Dimensioned drawing - Swivel joint RL-50-PL1

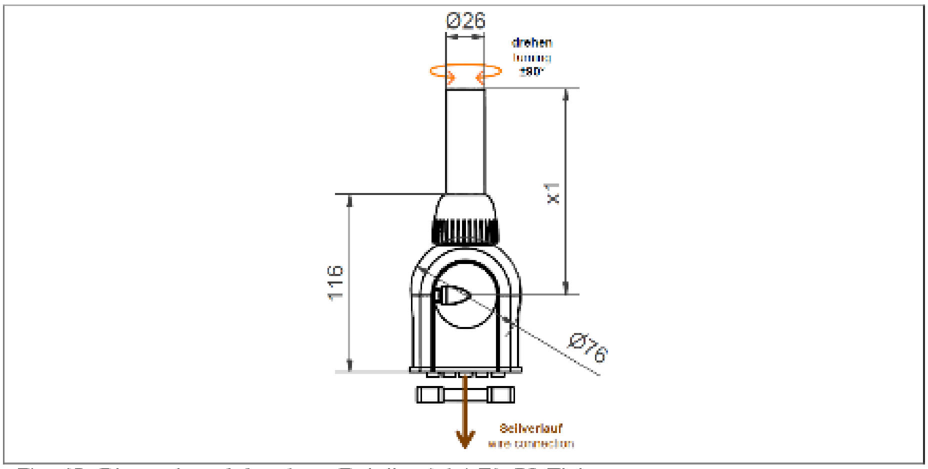

Fig. 42: Dimensioned drawing - Rotating joint RL-50-TL1

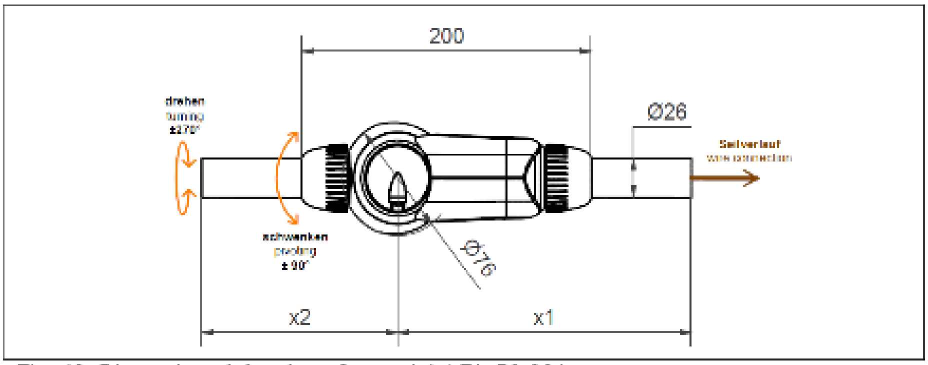

Fig. 43: Dimensioned drawing - 2 axes joint RL-50-001

igus® GmbH | Martin Raak | Tel. +49 (0)2203 9649 409 | mraak@igus.de 25

Exploded drawings / parts lists

Fig. 44: Exploded drawing / parts list - Swivel joint RL-50-PL1

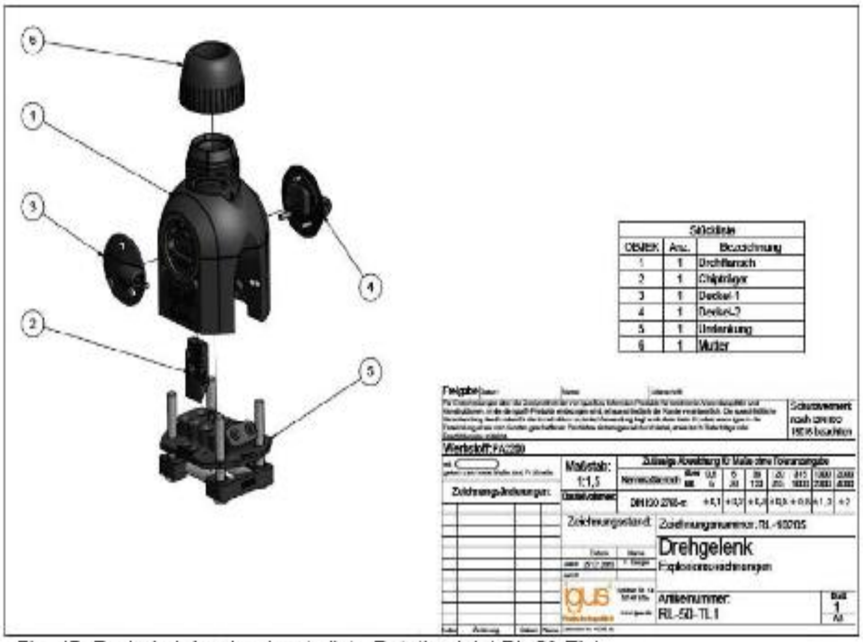

Fig. 45: Exploded drawing / parts list - Rotating joint RL-50-TL1

[illegible]		
[illegible]	Anz.	Bezeichnung
1	1	Gabel
2	1	Kugel
3	1	[illegible]
4	1	Deckel-1
5	1	Deckel-2
6	2	Mutter

Fig. 46: Exploded drawing / parts list - 2 axes joint RL-50-001 (-002)

Appendix B: Tube length of joints

robolink® Joint kit – Documentation (#1; 2012-09)

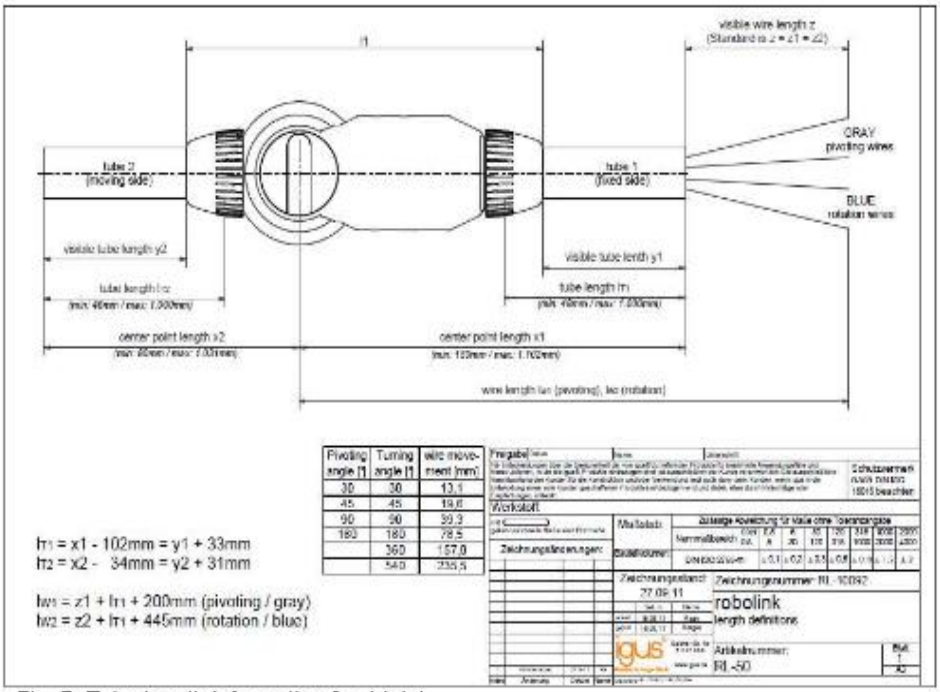

Fig. 7: Tube length information for 1 joint

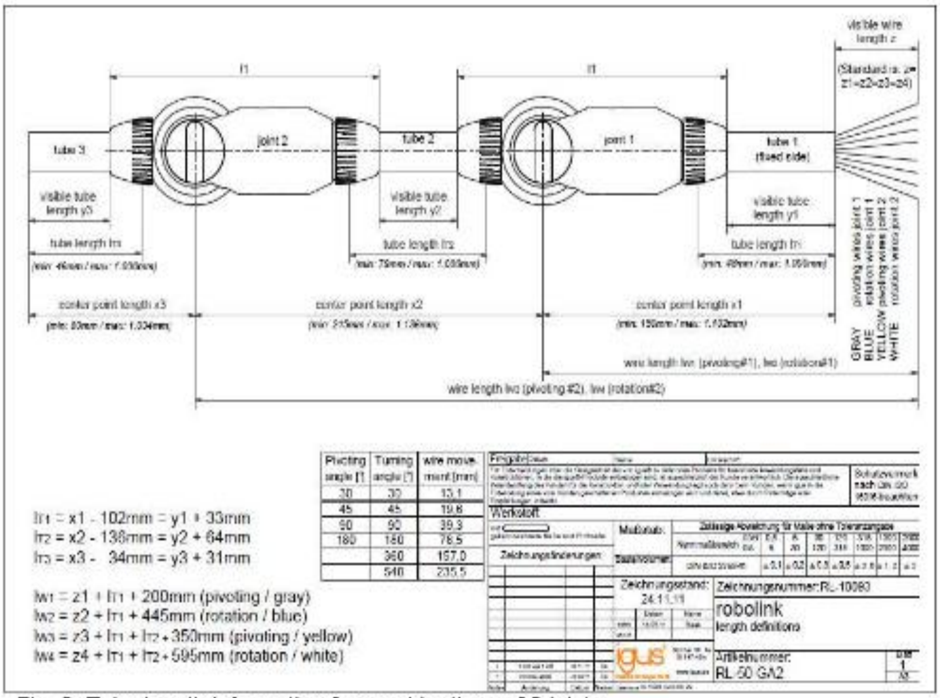

Fig. 8: Tube length information for combinations of 2 joints

igus® GmbH | Martin Raak | Tel. +49 (0)2203 9649 409 | mraak@igus.de 5

Appendix C: Technical data for tube lengths

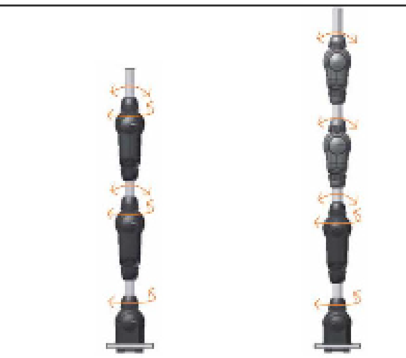

-26, -27, -28, -29 -30, -31

Fig. 13: Articulated arms with 5 DOF

The 31 articulated arm permutations are numbered. The following technical data corresponds to the system numbers shown (01—31), (at 100 mm tube length each):

DOF	Pos.	Version	LT [mm] (Stand.)	x1*) [mm]	x2*) [mm]	x3*) [mm]	x4*) [mm]	x tot. [mm]*)	weight [gr]*)	max. stat. Load [N] *)	max. dyn. Load [N] *)**)
1	1	RL-50-DOF1-01	100	173	134	-	-	307	290	89	62
	2	RL-50-DOF1-02	100	134	-	-	-	134	270	89	62
2	3	RL-50-DOF2-03	100	202	134	-	-	336	400	89	62
	4	RL-50-DOF2-04	100	202	134	-	-	336	400	89	62
	5	RL-50-DOF2-05	100	173	207	134	-	514	555	33	15
	6	RL-50-DOF2-06	100	207	134	-	-	341	535	89	62
3	7	RL-50-DOF3-07	100	202	207	134	-	543	665	33	15
	8	RL-50-DOF3-08	100	202	207	134	-	543	665	33	15
	9	RL-50-DOF3-09	100	173	236	134	-	543	665	30	12
	10	RL-50-DOF3-10	100	173	236	134	-	543	665	30	12
	11	RL-50-DOF3-11	100	173	207	207	134	721	815	18	5
	12	RL-50-DOF3-12	100	236	134	-	-	370	645	89	62
	13	RL-50-DOF3-13	100	236	134	-	-	370	645	89	62
	14	RL-50-DOF3-14	100	207	207	134	-	548	800	33	15
4	15	RL-50-DOF4-15	100	202	236	134	-	572	775	30	12
	16	RL-50-DOF4-16	100	202	236	134	-	572	775	30	12
	17	RL-50-DOF4-17	100	202	236	134	-	572	775	30	12
	18	RL-50-DOF4-18	100	202	236	134	-	572	775	30	12
	19	RL-50-DOF4-19	100	202	207	207	134	750	930	18	5
	20	RL-50-DOF4-20	100	202	207	207	134	750	930	18	5
	21	RL-50-DOF4-21	100	236	207	134	-	577	910	33	15
	22	RL-50-DOF4-22	100	236	207	134	-	577	910	33	15
	23	RL-50-DOF4-23	100	207	236	134	-	577	910	30	12
	24	RL-50-DOF4-24	100	207	236	134	-	577	910	30	12
	25	RL-50-DOF4-25	100	207	207	207	134	755	1.060	18	5

DOF	Pos.	Version	LT [mm] (Stand.)	x1*) [mm]	x2*) [mm]	x3*) [mm]	x4*) [mm]	x tot. [mm]*)	weight [gr]*)	max. stat. Load [N] *)	max. dyn. Load [N] *)**)
5	26	RL-50-DOF5-26	100	238	238	134	-	606	1.020	30	12
	27	RL-50-DOF5-27	100	236	236	134	-	606	1.020	30	12
	28	RL-50-DOF5-28	100	238	238	134	-	606	1.020	30	12
	29	RL-50-DOF5-29	100	236	236	134	-	606	1.020	30	12
	30	RL-50-DOF5-30	100	236	207	207	134	784	1.170	18	5
	31	RL-50-DOF5-31	100	236	207	207	134	784	1.170	18	5

*) only applies to geometric configurations with standard tube length = 100mm

**) at 30 RPMs and 0.1 sec. ramp time

Table 1: Specification for articulated arms with 1-5 DOF

All articulated arms can be optionally equipped with angle sensors (=> Section - Angle sensors). The shown end-plates (for rotating joints) or end-flanges (for 2 axes and swivel joints) are not part of the delivery scope, but can be ordered as accessories.
When the articulated arm is equipped with a rotating joint, RL-50-TL1, in the first position, the assembled wires already exit the arm in pairs.

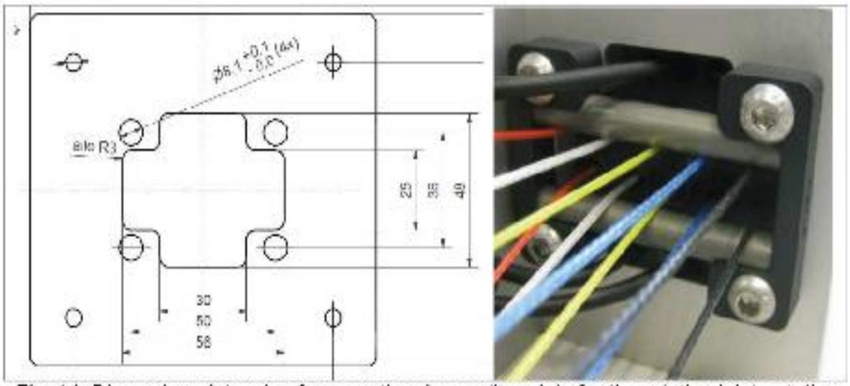

Fig. 14: Dimensioned drawing for an optional mounting plate for the rotating joint, rotating joint view from below

When the articulated arm is equipped with a 2 axes or a swivel joint in the first position, the use of a wire splitting unit (RL-WSU8-001) is generally recommended starting at 3 DOF for a controlled distribution of the drive wires.

The 3D STEP data for all articulated arms is available for download at: www.igus.de/robolink/support&service.

Appendix D: Datasheet of integrated Hall IC's and configuration of sensor lines

9 GENERAL DEVICE SPECIFICATIONS

9.1 Absolute Maximum Ratings (Non Operating)

Stresses beyond those listed under "Absolute Maximum Ratings" may cause permanent damage to the device.

Parameter	Symbol	Min	Max	Unit	Note
Supply	VDD	-0.3	7	V	
Input pin voltage	V_{in}	VSS-0.5	VDD+0.5	V	
Input current (latchup immunity)	I_{scr}	-100	100	mA	Norm: JESD78
ESD		+/-2		kV	Norm: MIL 883 E method 3015
Package thermal resistance	Θ_{JA}		114.5	°C /W	Still Air / Single Layer PCB
Storage temperature	T_{strg}	-55	150	°C	
Soldering conditions	T_{body}		260	°C	Norm: IPC/JEDEC J-STD-020C
Humidity non-condensing		5	85	%	

9.2 Operating Conditions

Parameter	Symbol	Min	Typ	Max	Unit	Note
Positive supply voltage	AVDD	4.5	5.0	5.5	V	
Digital supply voltage	DVDD					
Negative supply voltage	VSS	0.0	0.0	0.0	V	
Power supply current, AS5304	IDD	25		35	mA	A/B/Index, AO unloaded!
Power supply current, AS5306		20		30		
Ambient temperature	T_{amb}	-40		125	°C	
Junction temperature	T_J	-40		150	°C	
Resolution	LSB		25 15		µm	AS5304 AS5306
Integral nonlinearity	INL			1	LSB	Ideal input signal (ErrMax - ErrMin) / 2
Differential nonlinearity	DNL			±0.5	LSB	No missing pulses, optimum alignment
Hysteresis	Hyst	1	1.5	2	LSB	

9.3 System Parameters

Parameter	Symbol	Min	Max	Unit	Note
Power up time	T_{PwrUp}		500	µs	Amplitude within valid range / Interpolator locked, A B Index enabled
Propagation delay	T_{Prop}		20	µs	Time between change of input signal to output signal

9.4 A / B / C Push/Pull or Open Drain Output

Push Pull Mode is set for AS530xA, Open Drain Mode is set for AS530xB versions.

Parameter	Symbol	Min	Typ	Max	Unit	Note
High level output voltage	V_{OH}	0.8 VDD			V	Push/Pull mode
Low level output voltage	V_{OL}			0.4 + VSS	V	
Current source capability	I_{LOH}	12	14		mA	Push/Pull mode
Current sink capability	I_{LOL}	13	15		mA	
Short circuit limitation current	I_{Short}		25	39	mA	Reduces maximum operating temperature
Capacitive load	C_L		20		pF	See Figure 13
Load resistance	R_L		820		Ω	See Figure 13
Rise time	t_R			1.2	µs	Push/Pull mode
Fall time	t_F			1.2	µs	

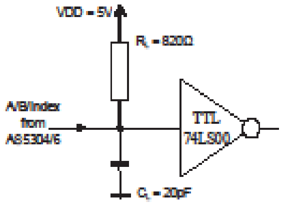

Figure 13: Typical digital load

9.5 CAO Analogue Output Buffer

Parameter	Symbol	Min	Typ	Max	Unit	Note
Minimum output voltage	$V_{OutRange}$	0.5	1	1.2	V	Strong field, min. AGC
Maximum output voltage	$V_{OutRange}$	3.45	4	4.3	V	Weak field, max. AGC
Offset	V_{Offs}			±10	mV	
Current sink / source capability	I_L	5			mA	
Average short circuit current	I_{Short}	6		40	mA	Reduces maximum Operating Temperature
Capacitive load	C_L		10		pF	
Bandwidth	BW		5		KHz	

9.6 Magnetic Input

Parameter	Symbol	Min	Typ	Max	Unit	Note
Magnetic pole length	L_{P_PP}		2.0		mm	AS5304
			1.2			AS5306
Magnetic pole pair length	T_{PP}		4.0		mm	AS5304
			2.4			AS5306
Magnetic amplitude	A_{mag}	5		60	mT	
Operating dynamic input range		1:12		1:24		
Magnetic offset	Off_{mag}			±0.5	mT	
Magnetic temperature drift	T_{dmag}			-0.2	%/K	
Input frequency	f_{mag}	0		5	kHz	

Table 1: AS5304 ordering guide

Device	Resolution	Magnet Pole Length	Digital Outputs
AS5304A	25µm	2mm	Push Pull
AS5304B	25µm	2mm	Open Drain

Table 2: AS5306 ordering guide

Device	Resolution	Magnet Pole Length	Digital Outputs
AS5306A	15µm	1.2mm	Push Pull
AS5306B	15µm	1.2mm	Open Drain

Configuration sensor lines for pivoting movement

+5V	Red
GND	Black
Hall-Sensor	White
Encoder Index	Green
Encoder Channel A	Blue
Encoder Channel B	Yellow

Configuration sensor lines for rotating movement

+5V	Red/Blue
GND	Brown
Hall-Sensor	Grey
Encoder Index	Grey/Rose
Encoder Channel A	Violet
Encoder Channel B	Rose

Appendix E: Technical data for stepper motors

stepper motor MOT-AN-S . . .

technical data					
flange dimension		**42(NEMA17)**	**56(NEMA23)**	**60(NEMA23XL)**	**86 (NEMA34)**
motor					
max voltage	[VDC]	60	60	60	60
nominal voltage	[VDC]	24-48	24-48	24-48	24-48
nominal current	[A]	1,8	4,2	4,2	6,4
holding torque	[Nm]	0,5	2,0	3,5	5,9
detent torque	[Nm]	0,022	0,068	0,075	0,210
step angle	°	1,8	1,8	1,8	1,8
resistance / phase	[Ω]	1,75±10%	0,50±10%	0,65±10%	0,33±10%
inductance / phase	[mH]	3,30±20%	1,90±20%	3,20±20%	3,00±20%
moment of inertia / rotor	[kgcm²]	0,08	0,48	0,84	2,70
max load axial	[N]	7	15	15	65
max load radial	[N]	20	52	63	200

encoder		
operating voltage	[VDC]	5
impulse / turn	[1/min]	500
zero impulse / index		yes
line-driver		RS422 protocol

brake					
operating voltage	[VDC]	24±10%			
wattage	[W]	8	10	10	11
holding torque	[Nm]	0,4	1,0	1,0	2,0
moment of inertia	[kgcm²]	0,01	0,02	0,02	0,07

weight					
product weight	[kg]	0,32	1,12	1,56	3,20
with encoder	[kg]	0,34	1,14	1,58	3,30
with encoder and brake	[kg]	0,58	1,36	1,82	3,80

operating data		
ambient temperature	[°C]	-10 ... +50
max temperature rise	[°C]	80
insulation class		B
humidity (not condensing)	[%]	85
protection class engine case		IP65 (shaft seal IP52)
CE		EMV guideline

www.igus.de MOT-AN-S_EN_201111#1

stepper motor MOT-AN-S . . .

pin assignment stepper motor
flange dimension 42(NEMA17), 56(NEMA23), 60(NEMA23XL)   flange dimension 86(NEMA34)

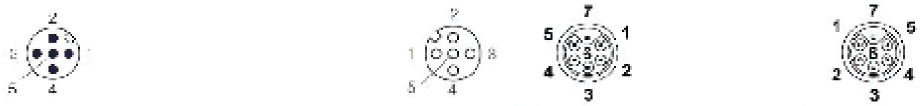

motor bipolar			motor cable
M12 5-pole		wires	M12 5-pole
pin	signal	color	color
1	A'	brown	brown
2	A	white	white
3	B	blue	blue
4	B'	black	black
5	PE	-	green/yellow
housing	schielding	-	-

motor bipolar		motor cable
M17 7-pole		M17 7-pole
pin	signal	number
1	A/	1
2	A	2
3	B	3
4	B/	4
5	brake 24V	5
6	brake 0V	6
7	PE	green/yellow
housing	schielding	schielding

pin assignment encoder
flange dimension 42(NEMA17), 56(NEMA23), 60(NEMA23XL)   flange dimension 86(NEMA34)

encoder		encoder cable
M12 8-pole		M12 8-pole
pin	signal	color
1	A	white
2	A'	brown
3	B	green
4	B'	yellow
5	0V	gray
6	N'	pink
7	N	blue
8	5V DC	red
housing	schielding	schielding

encoder		encoder cable
M17 12-pole		M17 12-pole
pin	signal	color
1	A	brown
2	A/	green
3	B	blue
4	B/	violett
5	0V	white 0,5
6	N/	gray
7	N	pink
8	5V DC	brown 0,5
9	-	-
10	-	-
11	-	-
12	-	-
housing	schielding	schielding

pin assignment brake/initiator
flange dimension 42(NEMA17), 56(NEMA23), 60(NEMA23XL)

brake		brake cable
M8 3-pole		M8 3-pole
pin	signal	color
1	brake (24V)	brown
3	0V	blue
4	-	black

initiator		initiator cable
M8 3-pole		M8 3-pole
pin	signal	color
1	VCC	brown
3	0V	blue
4	load	black

www.igus.de   MOT-AN-S_EN_201111#1

stepper motor MOT-AN-S . . .

characteristic

flange dimension 42 (NEMA17)
MOT-AN-S-060-005-042-...

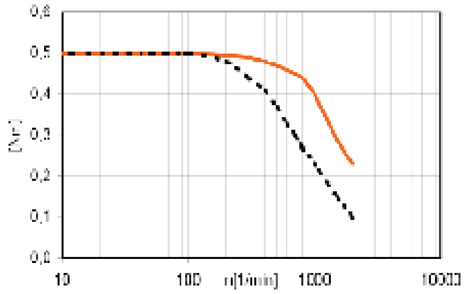

flange dimension 56 (NEMA23)
MOT-AN-S-060-020-056-...

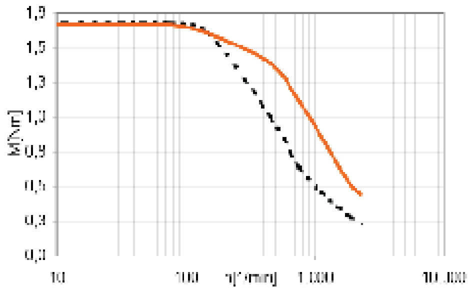

flange dimension 60 (NEMA23XL)
MOT-AN-S-060-035-060-...

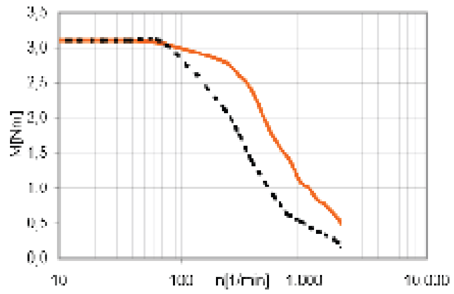

flange dimension 86 (NEMA34)
MOT-AN-S-060-059-086-...

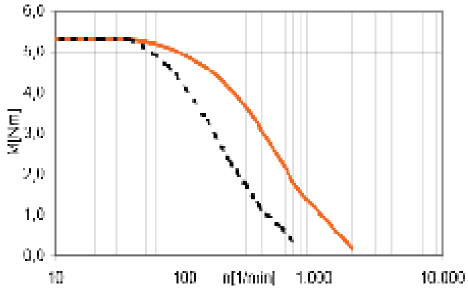

------ 24VDC ———— 48 VDC characteristic based on quarter step mode

www.igus.de MOT-AN-S_EN_201111#1

stepper motor MOT-AN-S . . .

dimension
MOT-AN-S-060-...-L-A-AAAA
MOT-AN-S-060-...-M-A-AAAA

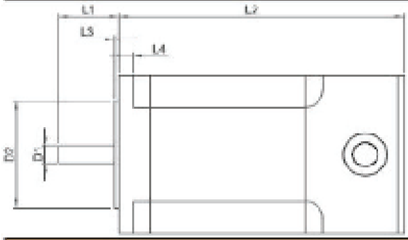

MOT-AN-S-060-...-M-C-AAAC

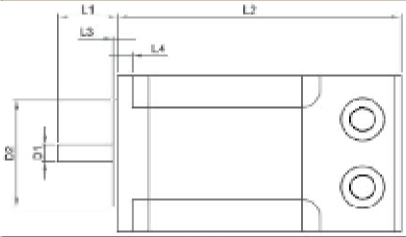

MOT-AN-S-060-...-M-D-AAAD

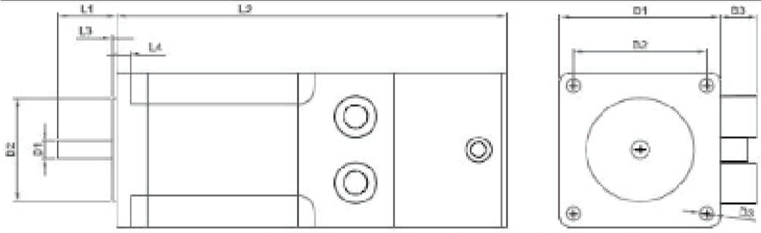

Typ	B1 [mm]	B2 [mm] ±0,2	B3 [mm]	D1 Ø [mm] -0,013	D2 Ø [mm] ±0,025	D3 Ø [mm]	L1 [mm] ±1	L2 [mm] ±1	L3 [mm]	L4 [mm]
MOT-AN-S-060-006-042-L-A-AAAA	42,3	31,00	/	5,00	22,00	M3	24,0	48	2,0	/
MOT-AN-S-060-006-042-M-A-AAAA	42,3	31,00	13	5,00	22,00	M3	24,0	70	2,0	/
MOT-AN-S-060-006-042-M-C-AAAC	42,3	31,00	13	5,00	22,00	M3	24,0	70	2,0	/
MOT-AN-S-060-006-042-M-D-AAAD	42,3	31,00	13	5,00	22,00	M3	24,0	115	2,0	/
MOT-AN-S-060-020-056-L-A-AAAA	56,4	47,14	/	6,35	38,10	5,0	20,6	76	1,6	5
MOT-AN-S-060-020-056-M-A-AAAA	56,4	47,14	13	6,35	38,10	5,0	20,6	98	1,6	5
MOT-AN-S-060-020-056-M-C-AAAC	56,4	47,14	13	6,35	38,10	5,0	20,6	98	1,6	5
MOT-AN-S-060-020-056-M-D-AAAD	56,4	47,14	13	6,35	38,10	5,0	20,6	138	1,6	5
MOT-AN-S-060-035-080-L-A-AAAA	60,0	47,14	/	8,00	38,10	4,5	20,6	88	1,6	7
MOT-AN-S-060-035-080-M-A-AAAA	60,0	47,14	13	8,00	38,10	4,5	20,6	110	1,6	7
MOT-AN-S-060-035-080-M-C-AAAC	60,0	47,14	13	8,00	38,10	4,5	20,6	110	1,6	7
MOT-AN-S-060-035-080-M-D-AAAD	60,0	47,14	13	8,00	38,10	4,5	20,6	150	1,6	7
MOT-AN-S-060-059-086-M-A-AAAA	85,8	69,50	37	14,00	73,02	5,6	37,0	118	2,0	9
MOT-AN-S-060-059-086-M-C-AAAC	85,8	69,50	37	14,00	73,02	5,6	37,0	118	2,0	9
MOT-AN-S-060-059-086-M-D-AAAD	85,8	69,50	37	14,00	73,02	5,6	37,0	170	2,0	9

www.igus.de MOT-AN-S_EN_201111#1

stepper motor MOT-AN-S . . .

cable part number	outer jacket	typ	cable length	plug
flange dimension 42(NEMA17), 56(NEMA23), 60(NEMA23XL)				
motor cable				
MAT9043737	TPE	CF9-CF.INI	3	straight
MAT9043738	TPE	CF9-CF.INI	5	straight
MAT9043740	TPE	CF9-CF.INI	10	straight
MAT9043742	TPE	CF9-CF.INI	3	angulate
MAT9043743	TPE	CF9-CF.INI	5	angulate
MAT9043745	TPE	CF9-CF.INI	10	angulate
encoder cable				
MAT90432594-3	PVC	CF240	3	straight
MAT90432594-5	PVC	CF240	5	straight
MAT90432594-10	PVC	CF240	10	straight
MAT90436430-3	PVC	CF240	3	angulate
MAT90436430-5	PVC	CF240	5	angulate
MAT90436430-10	PVC	CF240	10	angulate
flange dimension 86(NEMA34)				
motor cable				
MAT90439520-3	PUR	CF78.UL	3	straight
MAT90439520-5	PUR	CF78.UL	5	straight
MAT90439520-10	PUR	CF78.UL	10	straight
encoder cable				
MAT90439519-3	PVC	CF211	3	angulate
MAT90439519-5	PVC	CF211	5	angulate
MAT90439519-10	PVC	CF211	10	angulate
flange dimension 42(NEMA17), 56(NEMA23), 60(NEMA23XL)				
brake-/initiator cable				
MAT9043716	TPE	CF9-CF.INI	3	straight
MAT9043717	TPE	CF9-CF.INI	5	straight
MAT9043719	TPE	CF9-CF.INI	10	straight
MAT9043724	TPE	CF9-CF.INI	3	angulate
MAT9043725	TPE	CF9-CF.INI	5	angulate
MAT9043727	TPE	CF9-CF.INI	10	angulate

plug straight

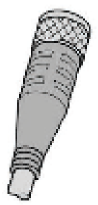

plug angulate

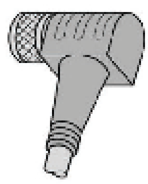

www.igus.de MOT-AN-S_EN_201111#1

stepper motor MOT-AN-S . . .

component part			
motor flange			
part number	**flange dimension/motor**	**linear table**	**material**
MF-1123-NEMA17	42(NEMA17)	SAW-0630	polymer, black
MF-2040-NEMA17	42(NEMA17)	SLW-/SLWE-/SAW-1040 SHT-/SHTC-/SHTS-12	aluminium, black anodized
MF-2040-NEMA23	56 & 60(NEMA23&23XL)	SLW-/SLWE-/SAW-1040 SHT-/SHTC-/SHTS-12	aluminium, black anodized
MF-0630-NEMA17-S	42(NEMA17)	ZLW-0630	aluminium, clear anodized
MF-0630-NEMA23-S	56 & 60(NEMA23&23XL)	ZLW-0630	aluminium, clear anodized
MF-1040-NEMA17-S	42(NEMA17)	ZLW-1040	aluminium, clear anodized
MF-1040-NEMA23-S	56 & 60(NEMA23&23XL)	ZLW-1040	aluminium, clear anodized
MF-1040-NEMA34-L	86(NEMA34)	ZLW-1040	aluminium, clear anodized
MF-2260-NEMA23-S	56 & 60(NEMA23&23XL)	ZAW-1040	aluminium, clear anodized
MF-1660-NEMA34-S	86(NEMA34)	ZLW-1660	aluminium, black anodized

spacer			
part number	**flange dimension/motor**	**linear table**	**material**
STY-104001	42(NEMA17) 56 & 60(NEMA23&23XL)	SLW-/SLWE-1040	aluminium, clear anodized
STY-121001	42(NEMA17) 56 & 60(NEMA23&23XL)	SHT-/SHTC-/SHTS-12 SHT-12-PL	aluminium, blue-grey anodized
STY-201601	56 & 60(NEMA23&23XL)	SHT-/SHTC-/SHTS-20	aluminium, blue-grey anodized

coupling		
part number	**linear table**	**flange dimension/motor**
COU-AR-K-050-000-25-26-B-AAAB	ZLW-0630-B ZLW-1040-B	42(NEMA17)
COU-AR-K-050-080-25-26-B-AAAA	ZLW-0630-S	42(NEMA17)
COU-AR-K-050-100-32-32-B-AAAA	ZLW-1040 SLW-/SLWE-/SAW-1040 SHT-/SHTC-/SHTS-12	42(NEMA17)
COU-AR-K-050-080-25-26-B-AAAA	SAW-0630 ZLW-0630-S	42(NEMA17)
COU-AR-K-063-000-25-26-B-AAAB	ZLW-0630-B ZLW-1040-B ZAW-1040-B	56(NEMA23)
COU-AR-K-063-080-25-26-B-AAAA	ZLW-0630-S	56(NEMA23)
COU-AR-K-063-100-32-32-B-AAAA	SLW-/SLWE-/SAW-1040 SHT-/SHTC-/SHTS-12 ZLW-1040-S ZAW-1040-S	56(NEMA23)
COU-AR-K-063-120-32-32-B-AAAA	SHT-20	56(NEMA23)
COU-AR-K-080-000-25-26-B-AAAB	ZLW-0630-B ZLW-1040-B ZAW-1040-B	60(NEMA23XL)
COU-AR-K-080-100-32-32-B-AAAA	SLW-/SLWE-/SAW-1040 SHT-/SHTC-/SHTS-12 ZLW-1040-S ZAW-1040-S	60(NEMA23XL)
COU-AR-K-140-100-32-32-B-AAAA	ZLW-1040-S	86(NEMA34)
COU-AR-K-140-140-32-32-B-AAAA	ZLW-1660-S	86(NEMA34)

www.igus.de MOT-AN-S_EN_201111#1

stepper motor MOT-AN-S . . .

component part		
initiator		
part number		typ
INI-AB-I-025-A-AA		n.o. (PNP)
INI-AB-I-025-B-AA		n.c. (PNP)

initiator bracket		
part number	linear table	material
ZSY-104021	ZLW-0630, ZLW-1040, ZAW,SAW-0630, SAW-1040	aluminium, black anodized

technical data initiator		
supply voltage	[VDC]	10...30
switching current max.	[mA]	100
no-load current	[mA]	10
ambient temperature	[°C]	-25 ...+70
switching frequency max.	[Hz]	3000
utilisation category		DC12
ingress protection		IP67
reacting distance	Sn	2,5

www.igus.de MOT-AN-S_EN_201111#1

Appendix F: Complete specifications for drive unit

Drive units

Drive modules can be optionally assembled in drive units. In this case, the entire wire feed mechanism is assembled at the factory. A completed module then consists of a customized articulated arm, and a pre-assembled and tested drive unit. igus® offers drive units starting at 3 DOF. Drive units for 1 and 2 DOF are available upon request.

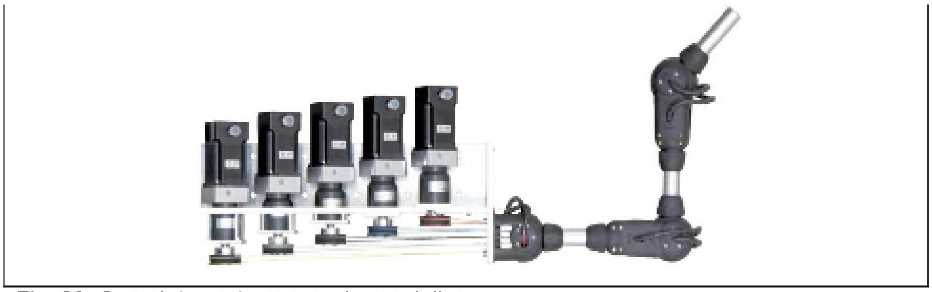

Fig. 39: Complete system = maximum delivery scope

The following options are user selectable for these systems:

- Articulated arm with 3-5 DOF per specification (=> Section - Articulated arms)
- With or without angle sensors in the joints (=> Section - Sensors)
- Tube lengths per specification (standard = 100mm, max. = 1,000 mm),
- NEMA17 or NEMA23 motors, connector or strand conductor version,
- Grippers or suction cups per specification (=> Section - Actuators).

Other options (not available from stock):

- Step motors with encoder and/or brake,
- Other reduction gearing,
- Special designs.
-

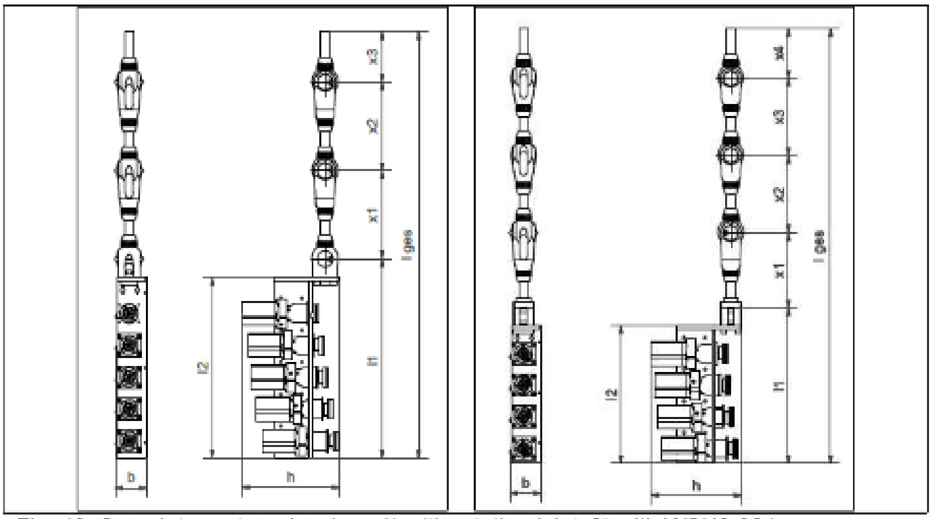

Fig. 40: Complete system drawings 1) with rotating joint, 2) with WSU8-001

Complete units have the following specifications:

DOF	Pos.	NEMA17 version	l1 [mm]	l2 [mm]	b [mm]	h [mm]	l ges. [mm]*)	weight [gr]*)
3	7	RL-50-DOF3-07-AEK3-17	258	210	80	240	801	5.415
	8	RL-50-DOF3-08-AEK3-17	258	210	80	240	801	5.415
	9	RL-50-DOF3-09-AEK3-17	258	210	80	240	801	5.415
	10	RL-50-DOF3-10-AEK3-17	258	210	80	240	801	5.415
	11	RL-50-DOF3-11-AEK3-17	258	210	80	240	979	5.565
	12	RL-50-DOF3-12-AEK3-17	260	210	80	240	630	4.995
	13	RL-50-DOF3-13-AEK3-17	260	210	80	240	630	4.995
	14	RL-50-DOF3-14-AEK3-17	260	210	80	240	808	5.150
4	15	RL-50-DOF4-15-AEK4-17	358	310	80	240	930	6.875
	16	RL-50-DOF4-16-AEK4-17	358	310	80	240	930	6.875
	17	RL-50-DOF4-17-AEK4-17	358	310	80	240	930	6.875
	18	RL-50-DOF4-18-AEK4-17	358	310	80	240	930	6.875
	19	RL-50-DOF4-19-AEK4-17	358	310	80	240	1.108	7.030
	20	RL-50-DOF4-20-AEK4-17	358	310	80	240	1.108	7.030
	21	RL-50-DOF4-21-AEK4-17	360	310	80	240	937	6.610
	22	RL-50-DOF4-22-AEK4-17	360	310	80	240	937	6.610
	23	RL-50-DOF4-23-AEK4-17	360	310	80	240	937	6.610
	24	RL-50-DOF4-24-AEK4-17	360	310	80	240	937	6.610
	25	RL-50-DOF4-25-AEK4-17	360	310	80	240	1.115	6.760
5	26	RL-50-DOF5-26-AEK5-17	460	410	80	240	1.066	8.070
	27	RL-50-DOF5-27-AEK5-17	460	410	80	240	1.066	8.070
	28	RL-50-DOF5-28-AEK5-17	460	410	80	240	1.066	8.070
	29	RL-50-DOF5-29-AEK5-17	460	410	80	240	1.066	8.070
	30	RL-50-DOF5-30-AEK5-17	460	410	80	240	1.244	8.220
	31	RL-50-DOF5-31-AEK5-17	460	410	80	240	1.244	8.220

*) only applies to geometric configurations with standard tube length = 100mm

Table 4: Complete system specification with NEMA17 motors

DOF	Pos.	NEMA23 version	l1 [mm]	l2 [mm]	b [mm]	h [mm]	l ges. [mm]*)	weight [gr]*)
3	7	RL-50-DOF3-07-AEK3-23	308	260	80	240	851	8.965
	8	RL-50-DOF3-08-AEK3-23	308	260	80	240	851	8.965
	9	RL-50-DOF3-09-AEK3-23	308	260	80	240	851	8.965
	10	RL-50-DOF3-10-AEK3-23	308	260	80	240	851	8.965
	11	RL-50-DOF3-11-AEK3-23	308	260	80	240	1.029	9.115
	12	RL-50-DOF3-12-AEK3-23	310	260	90	275	680	8.545
	13	RL-50-DOF3-13-AEK3-23	310	260	90	275	680	8.545
	14	RL-50-DOF3-14-AEK3-23	310	260	90	275	858	8.700
4	15	RL-50-DOF4-15-AEK4-23	358	310	80	240	930	11.475
	16	RL-50-DOF4-16-AEK4-23	358	310	80	240	930	11.475
	17	RL-50-DOF4-17-AEK4-23	358	310	80	240	930	11.475
	18	RL-50-DOF4-18-AEK4-23	358	310	80	240	930	11.475
	19	RL-50-DOF4-19-AEK4-23	358	310	80	240	1.108	11.630
	20	RL-50-DOF4-20-AEK4-23	358	310	80	240	1.108	11.630
	21	RL-50-DOF4-21-AEK4-23	420	370	90	275	997	11.210
	22	RL-50-DOF4-22-AEK4-23	420	370	90	275	997	11.210
	23	RL-50-DOF4-23-AEK4-23	420	370	90	275	997	11.210
	24	RL-50-DOF4-24-AEK4-23	420	370	90	275	997	11.210
	25	RL-50-DOF4-25-AEK4-23	420	370	90	275	1.175	11.360
5	26	RL-50-DOF5-26-AEK5-23	530	480	90	275	1.136	13.720
	27	RL-50-DOF5-27-AEK5-23	530	480	90	275	1.136	13.720
	28	RL-50-DOF5-28-AEK5-23	530	480	90	275	1.136	13.720
	29	RL-50-DOF5-29-AEK5-23	530	480	90	275	1.136	13.720
	30	RL-50-DOF5-30-AEK5-23	530	480	90	275	1.314	13.870
	31	RL-50-DOF5-31-AEK5-23	530	480	90	275	1.314	13.870

*) only applies to geometric configurations with standard tube length = 100mm

Table 5: Complete system specification with NEMA23 motors

Colour coding of rope

Motor order & joints	Joints	Rope colours
Motor1: joint1	Rotational	Red
Motor2: joint3	Rotational	White
Motor3: joint3	Pivot	Yellow
Motor4: joint2	Rotational	Blue
Motor5: joint2	Pivot	Black

Rope channels to implement movements

The internal diameter of the rope is 50mm. Rope channel for the pivoting and rotation movement are as follow (IGUS, 2013.):

- 90°=π x d/4=~ 39mm
- 180°=π x d/2=~ 79mm
- 360°=π x d=~ 160mm

Dimension of multi-axis joint

The dimensions of multi-axis joint of robolink that is used in this project are as shown below in the figure (Fontys, 2013):

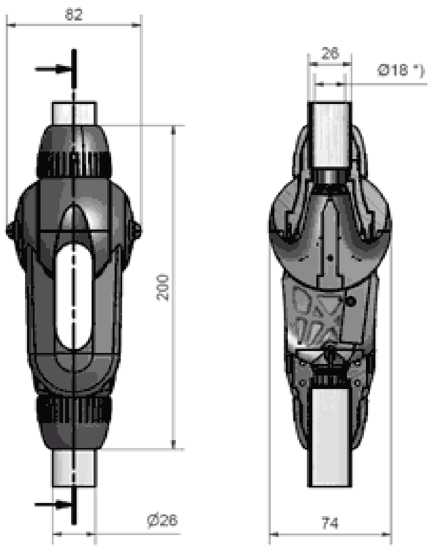

Appendix G: Technical Datasheet of NI 9501

NI 9501 Requires: 1 Connectivity Accessories ;	779767-01	**Connectivity Accessories:** screwTerminal - NI 9932 Strain relief, operator protection (qty 1)	779017-01

Back to Top

Support and Services

System Assurance Programs

NI system assurance programs are designed to make it even easier for you to own an NI system. These programs include configuration and deployment services for your NI PXI, CompactRIO, or Compact FieldPoint system. The NI Basic System Assurance Program provides a simple integration test and ensures that your system is delivered completely assembled in one box. When you configure your system with the NI Standard System Assurance Program, you can select from available NI system driver sets and application development environments to create customized, reorderable software configurations. Your system arrives fully assembled and tested in one box with your software preinstalled. When you order your system with the standard program, you also receive system-specific documentation including a bill of materials, an integration test report, a recommended maintenance plan, and frequently asked question documents. Finally, the standard program reduces the total cost of owning an NI system by providing three years of warranty coverage and calibration service. Use the online product advisors at ni.com/advisor to find a system assurance program to meet your needs.

Calibration

NI measurement hardware is calibrated to ensure measurement accuracy and verify that the device meets its published specifications. To ensure the ongoing accuracy of your measurement hardware, NI offers basic or detailed recalibration service that provides ongoing ISO 9001 audit compliance and confidence in your measurements. To learn more about NI calibration services or to locate a qualified service center near you, contact your local sales office or visit ni.com/calibration.

Technical Support

Get answers to your technical questions using the following National Instruments resources.

- **Support** - Visit ni.com/support to access the NI KnowledgeBase, example programs, and tutorials or to contact our applications engineers who are located in NI sales offices around the world and speak the local language.
- **Discussion Forums** - Visit forums.ni.com for a diverse set of discussion boards on topics you care about.
- **Online Community** - Visit community.ni.com to find, contribute, or collaborate on customer-contributed technical content with users like you.

Repair

While you may never need your hardware repaired, NI understands that unexpected events may lead to necessary repairs. NI offers repair services performed by highly trained technicians who quickly return your device with the guarantee that it will perform to factory specifications. For more information, visit ni.com/repair.

Training and Certifications

The NI training and certification program delivers the fastest, most certain route to increased proficiency and productivity using NI software and hardware. Training builds the skills to more efficiently develop robust, maintainable applications, while certification validates your knowledge and ability.

- **Classroom training in cities worldwide** - the most comprehensive hands-on training taught by engineers.
- **On-site training at your facility** - an excellent option to train multiple employees at the same time.
- **Online instructor-led training** - lower-cost, remote training if classroom or on-site courses are not possible.
- **Course kits** - lowest-cost, self-paced training that you can use as reference guides.
- **Training memberships** and training credits - to buy now and schedule training later.

Visit ni.com/training for more information.

Extended Warranty

NI offers options for extending the standard product warranty to meet the life-cycle requirements of your project. In addition, because NI understands that your requirements may change, the extended warranty is flexible in length and easily renewed. For more information, visit ni.com/warranty.

OEM

NI offers design-in consulting and product integration assistance if you need NI products for OEM applications. For information about special pricing and services for OEM customers, visit ni.com/oem.

Alliance

Our Professional Services Team is comprised of NI applications engineers, NI Consulting Services, and a worldwide National Instruments Alliance Partner program of more than 700 independent consultants and integrators. Services range from start-up assistance to turnkey system integration. Visit ni.com/alliance.

Back to Top

Detailed Specifications

The following specifications are typical for the temperature range –40 to 70 °C unless otherwise noted. All voltages are relative to COM unless otherwise noted.

Input/Output Characteristics	
Motor DC power supply (Vsup)	+9 to +30 VDC
Max step pulse rate	5 MHz
Minimum phase inductance	1 mH

Type	Bipolar chopper
Chopping frequency	20 kHz
Current per phase	3 A RMS (4.24 A peak)
Current reduction	0%, 25%, or 50%
Microstepping selections	×2, 4, 8, 16, 32, 64, 128, 256 (software-selectable)
Vsup capacitance	750 µF
MTBF	Contact NI for Bellcore MTBF specifications.

Drive Protection

Undervoltage	<8 V

⚠ **Caution** Vsup greater than 40 V will result in damage to the module.

Overvoltage	>32 V
Motor terminal (Phase A±/Phase B±) short to ground	Yes
Motor terminal (Phase A±/Phase B±) short to Vsup	Yes

Power Requirements

Power consumption from chassis	
Active mode	500 mW max
Sleep mode	2.5 mW max
Thermal dissipation (at 70 °C)	
Active mode	1.5 W max
Sleep mode	2.5 mW max

Physical Characteristics

If you need to clean the module, wipe it with a dry towel.

Note For two-dimensional drawings and three-dimensional models of the C Series module and connectors, visit ni.com/dimensions and search by module number.

Screw terminal wiring	12 to 24 AWG copper conductor wire with 10 mm (0.39 in.) of insulation stripped from the end
Torque for screw terminals	0.5 to 0.6 N · m (4.4 to 5.3 lb · in.)
Ferrules	0.25 mm^2 to 2.5 mm^2
Weight	144 g (5.1 oz)

Safety

Safety Voltages

Connect only voltages that are within the following limits.

Channel-to-COM	0 to +30 VDC max, Measurement Category I
Isolation	
Channel-to-channel	None
Channel-to-earth ground	
Continuous	60 VDC, Measurement Category I
Withstand	1000 V_{rms}, verified by a 5 s dielectric withstand test

Measurement Category I is for measurements performed on circuits not directly connected to the electrical distribution system referred to as *MAINS* voltage. MAINS is a hazardous live electrical supply system that powers equipment. This category is for measurements of voltages from specially protected secondary circuits. Such voltage measurements include signal levels, special equipment, limited-energy parts of equipment, circuits powered by regulated low-voltage sources, and electronics.

⚠ **Caution** Do *not* connect the NI 9501 to signals or use for measurements within Measurement Categories II, III, or IV.

Power Supply Requirements

Caution You must use a UL Listed ITE power supply marked *LPS* with the NI 9501.

Safety Standards

This product is designed to meet the requirements of the following standards of safety for electrical equipment for measurement, control, and laboratory use:
IEC 61010-1, EN 61010-1
UL 61010-1, CSA 61010-1

Note For UL and other safety certifications, refer to the product label or the *Online Product Certification* section.

Electromagnetic Compatibility

This product meets the requirements of the following EMC standards for electrical equipment for measurement, control, and laboratory use:
EN 61326-1 (IEC 61326-1): Class A emissions; Industrial Immunity
EN 55011 (CISPR 11): Group 1, Class A emissions
AS/NZS CISPR 11: Group 1, Class A emissions
FCC 47 CFR Part 15B: Class A emissions
ICES-001: Class A emissions

Note For EMC declarations and certifications, refer to the *Online Product Certification* section.

Note For EMC compliance, operate this device with shielded cabling.

CE Compliance CE

This product meets the essential requirements of applicable European Directives, as amended for CE marking, as follows:
2006/95/EC; Low-Voltage Directive (safety)
2004/108/EC; Electromagnetic Compatibility Directive (EMC)

Online Product Certification

To obtain product certifications and the DoC for this product, visit ni.com/certification, search by model number or product line, and click the appropriate link in the Certification column.

Shock and Vibration

To meet these specifications, you must panel mount the system and affix ferrules to the end of the screw terminal wires.

Operating vibration	
Random (IEC 60068-2-64)	5 g_{rms}, 10 to 500 Hz
Sinusoidal (IEC 60068-2-6)	5 g, 10 to 500 Hz
Operating shock (IEC 60068-2-27)	30 g, 11 ms half sine, 50 g, 3 ms half sine, 18 shocks at 6 orientations

Environmental

National Instruments C Series modules are intended for indoor use only, but may be used outdoors if installed in a suitable enclosure. Refer to the manual for the chassis you are using for more information about meeting these specifications.

Operating temperature (IEC 60068-2-1, IEC 60068-2-2)	–40 to 70 °C
Storage temperature (IEC 60068-2-1, IEC 60068-2-2)	–40 to 85 °C
Ingress protection	IP 40
Operating humidity (IEC 60068-2-56)	10 to 90% RH, noncondensing
Storage humidity (IEC 60068-2-56)	5 to 95% RH, noncondensing
Maximum altitude	2,000 m
Pollution Degree (IEC 60664)	2

Environmental Management

NI is committed to designing and manufacturing products in an environmentally responsible manner. NI recognizes that eliminating certain hazardous substances from our products is beneficial not only to the environment but also to NI customers.

For additional environmental information, refer to the *NI and the Environment* Web page at ni.com/environment. This page contains the environmental regulations and directives with which NI complies, as well as other environmental information not included in this document.

Waste Electrical and Electronic Equipment (WEEE)

EU Customers At the end of the product life cycle, all products *must* be sent to a WEEE recycling center. For more information about WEEE recycling centers, National Instruments WEEE initiatives, and compliance with WEEE Directive 2002/96/EC on Waste Electrical and Electronic Equipment, visit ni.com/environment/weee.htm.

电子信息产品污染控制管理办法（中国 RoHS）

中国客户 National Instruments 符合中国电子信息产品中限制使用某些有害物质指令 (RoHS)。

5/6 www.ni.com

Appendix H: Technical Datasheet of cRIO 9074

NATIONAL INSTRUMENTS

Technical Sales
United States
(866) 531-6285
info@ni.com

Print | E-mail this Page | Open Document as PDF

Requirements and Compatibility | Ordering Information | Detailed Specifications | Pinouts/Front Panel Connections
For user manuals and dimensional drawings, visit the product page resources tab on ni.com.

Last Revised: 2011-05-18 10:19:47.0

CompactRIO Integrated Systems with Real-Time Controller and Reconfigurable Chassis

NI cRIO-907x

- Integrated CompactRIO systems with a reconfigurable FPGA chassis and embedded real-time controller
- Lower-cost systems for high-volume OEM applications
- Up to 2M gate reconfigurable FPGA
- 4 or 8 slots for C Series I/O modules
- Up to 400 MHz real-time processor
- Up to 256 MB DRAM memory, 512 MB of nonvolatile storage
- Up to two 10/100BASE-TX Ethernet ports with built-in FTP/HTTP servers and LabVIEW remote panel Web server
- RS232 serial port and available USB port for peripheral devices

Overview

NI cRIO-907x integrated systems combine an industrial real-time controller and reconfigurable field-programmable gate array (FPGA) chassis for industrial machine control and monitoring applications. The NI cRIO-9074 integrated system features an industrial 400 MHz real-time processor and an eight-slot chassis with an embedded, reconfigurable 2M gate FPGA chip. The new NI cRIO-9076 integrated system contains a 400 MHz real-time processor, a four-slot chassis with an embedded, reconfigurable LX45 FPGA chip, and a high-speed USB port. Both systems feature built-in nonvolatile memory and a fault tolerant file system. The new four-slot NI cRIO-9075 and NI cRIO-9076 systems provide a cost-optimized solution for high volume deployments and OEM applications.

Back to Top

Requirements and Compatibility

OS Information
VxWorks

Driver Information
NI-RIO

Software Compatibility
LabVIEW
LabVIEW FPGA Module
LabVIEW Professional Development System
LabVIEW Real-Time Module

Back to Top

Comparison Tables

Product	Module Slots	Processor Speed (MHz)	FPGA	DRAM (MB)	Internal Nonvolatile Storage (MB)	10/100BASE-TX Ethernet Port	RS232 Serial Port	Power Supply Input Range	USB Port
NI cRIO-9072	8	266	Spartan-3 1M	64	128	yes	yes	19 to 30 VDC	no
NI cRIO-9073	8	266	Spartan-3 2M	64	128	yes	yes	19 to 30 VDC	no
NI cRIO-9074	8	400	Spartan-3 2M	128	256	yes (Dual)	yes	19 to 30 VDC	no

Product	Module Slots	Processor Speed (MHz)	FPGA	DRAM (MB)	Internal Nonvolatile Storage (MB)	10/100BASE-TX Ethernet Port	RS232 Serial Port	Power Supply Input Range	USB Port
NI cRIO-9075	4	400	Spartan-6 LX25	128	256	yes	yes	9 to 30 VDC	no
NI cRIO-9076	4	400	Spartan-6 LX45	256	512	yes	yes	9 to 30 VDC	yes

Back to Top

Application and Technology

System Configuration

These NI CompactRIO real-time controllers combine a four- or eight-slot reconfigurable chassis into an integrated system. The user-defined FPGA circuitry in the chassis controls each I/O module and passes data to the controller through a local PCI bus using built-in communication functions.

Product	FPGA	Logic Cells	Multipliers	RAM (Kb)
NI cRIO-9073	Spartan-3 2M	46080	40	720
NI cRIO-9074	Spartan-3 2M	46080	40	720
NI cRIO-9075	Spartan-6 LX25	24051	38	936
NI cRIO-9076	Spartan-6 LX45	43661	58	2088

FPGA Resource Comparison

These systems also accept up to eight NI C Series I/O modules. A variety of I/O modules are available including voltage, current, thermocouple, RTD, accelerometer, and strain gage inputs; up to ±60 V simultaneous sampling analog I/O; 12, 24, and 48 V industrial digital I/O; 5 V/TTL digital I/O; counter/timers; pulse generation; and high voltage/current relays.

The 10/100 Mbits/s Ethernet port allows for programmatic communication over the network and the cRIO-9074 features dual Ethernet ports, which allows for the use of one port for network communication to a host PC or enterprise system and the other port for expansion I/O (easily connect another CompactRIO system or another Ethernet-based device for additional I/O). The new cRIO-9076 also features a USB 2.0 port for data storage and connection to peripheral devices.

NI CompactRIOs have the ability to by synchronized with an SNTP time server on a network and the cRIO-9072, cRIO-9073, and cRIO-9074 also feature a built-in backup battery to maintain operation for the Real-Time Clock when external power is removed. The cRIO-9075 and cRIO-9076 do not contain a backup battery for the Real-Time Clock.

Embedded Software

You can synchronize embedded code execution to an FPGA-generated interrupt request (IRQ) or an internal millisecond real-time clock source. The LabVIEW Real-Time ETS OS provides reliability and simplifies the development of complete embedded applications that include time-critical control and acquisition loops in addition to lower-priority loops for postprocessing, data logging, and Ethernet/serial communication. Built-in elemental I/O functions such as the FPGA Read/Write function provide a communication interface to the highly optimized reconfigurable FPGA circuitry. Data values are read from the FPGA in integer format and are then converted to scaled engineering units in the controller.

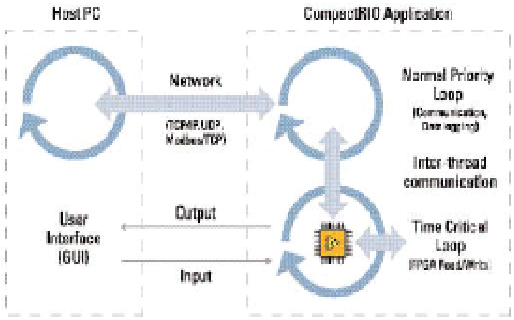

CompactRIO Software Architecture

Note: NI Scan Engine is not supported on the cRIO-9075 and cRIO-9076.

Built-In Servers

In addition to programmatic communication via TCP/IP, UDP, Modbus/TCP, IrDA, and serial protocols, the CompactRIO controllers include built-in servers for Virtual Instrument Software Architecture (VISA), HTTP, and FTP. The VISA server provides remote download and communication access to the reconfigurable I/O (RIO) FPGA over Ethernet. The HTTP server provides a Web browser user interface to HTML pages, files, and the user interface of embedded LabVIEW applications through a Web browser plug-in. The FTP server provides access to logged data or configuration files.

Back to Top

Ordering Information

For a complete list of accessories, visit the product page on ni.com.

Products	Part Number	Recommended Accessories	Part Number
NI cRIO-9072			
cRIO-9072 8-Slot Integrated 266 MHz Real-Time Ctrlr, 1M Gate FPGA Requires:	779998-01	**Connector Block:** Screw Terminal - NI 9978 4-pos screw terminal power supply plugs (quantity 5)	196938-01
NI cRIO-9073			
cRIO-9073 8-Slot Integrated 266 MHz Real-Time Ctrlr, 2M Gate FPGA Requires:	780471-01	**Connector Block:** Shielded - NI PS-15 Power Supply, 24 VDC, 5 A, 100-120/200-240 VAC Input ***Also Available: Screw Terminal*	781093-01
		Connector Block: Screw Terminal - NI 9979 Strain relief kit for 4-pos power connector	196939-01
NI cRIO-9076			
cRIO-9076 4-Slot Integrated 400 MHz Real-Time Ctrlr, LX45 FPGA Requires: 1 Connectivity Accessory	781716-01	**Connectivity Accessory:** Shielded - NI PS-15 Power Supply, 24 VDC, 5 A, 100-120/200-240 VAC Input	781093-01
NI cRIO-9075			
cRIO-9075 4-Slot Integrated 400 MHz Real-Time Ctrlr, LX25 FPGA Requires: 1 Connectivity Accessory	781715-01	**Connectivity Accessory:** Shielded - NI PS-15 Power Supply, 24 VDC, 5 A, 100-120/200-240 VAC Input	781093-01
NI cRIO-9074			
cRIO-9074 8-Slot Integrated 400 MHz Real-Time Ctrlr, 2M Gate FPGA Requires: 1 Connectivity Accessory	779999-01	**Connectivity Accessory:** Shielded - NI PS-15 Power Supply, 24 VDC, 5 A, 100-120/200-240 VAC Input	781093-01

Back to Top

Software Recommendations

LabVIEW Professional Development System for Windows

- Advanced software tools for large project development
- Automatic code generation using DAQ Assistant and Instrument I/O Assistant
- Tight integration with a wide range of hardware
- Advanced measurement analysis and digital signal processing
- Open connectivity with DLLs, ActiveX, and .NET objects
- Capability to build DLLs, executables, and MSI installers

NI LabVIEW FPGA Module

- Create your own I/O hardware without VHDL coding or board design
- Graphically configure FPGAs on NI reconfigurable I/O (RIO) hardware targets
- Define your own control algorithms with loop rates up to 300 MHz
- Execute multiple tasks simultaneously and deterministically
- Implement custom timing and triggering logic, digital protocols, and DSP algorithms
- Incorporate existing HDL code and third-party IP including Xilinx CORE Generator functions

NI LabVIEW Real-Time Module

- Design deterministic real-time applications with LabVIEW graphical programming
- Download to dedicated NI or third-party hardware for reliable execution and a wide selection of I/O
- Take advantage of built-in PID control, signal processing, and analysis functions
- Automatically take advantage of multicore CPUs or set processor affinity manually
- Includes real-time operating system (RTOS), development and debugging support, and board support
- Purchase individually or as part of an NI Developer Suite bundle

Back to Top

Support and Services

System Assurance Programs

NI system assurance programs are designed to make it even easier for you to own an NI system. These programs include configuration and deployment services for your NI PXI, CompactRIO, or Compact FieldPoint system. The NI Basic System Assurance Program provides a simple integration test and ensures that your system is delivered completely assembled in one box. When you configure your system with the NI Standard System Assurance Program, you can select from available NI system driver sets and application development environments to create customized, reorderable software configurations. Your system arrives fully assembled and tested in one box with your software preinstalled. When you order your system with the standard program, you also receive system-specific documentation including a bill of materials, an integration test report, a recommended maintenance plan, and frequently asked question documents. Finally, the standard program reduces the total cost of owning an NI system by providing three years of warranty coverage and calibration service. Use the online product advisors at ni.com/advisor to find a system assurance program to meet your needs.

Calibration

NI measurement hardware is calibrated to ensure measurement accuracy and verify that the device meets its published specifications. To ensure the ongoing accuracy of your measurement hardware, NI offers basic or detailed recalibration service that provides ongoing ISO 9001 audit compliance and confidence in your measurements. To learn more about NI calibration services or to locate a qualified service center near you, contact your local sales office or visit ni.com/calibration.

Technical Support

Get answers to your technical questions using the following National Instruments resources.

- **Support** - Visit ni.com/support to access the NI KnowledgeBase, example programs, and tutorials or to contact our applications engineers who are located in NI sales offices around the world and speak the local language.
- **Discussion Forums** - Visit forums.ni.com for a diverse set of discussion boards on topics you care about.
- **Online Community** - Visit community.ni.com to find, contribute, or collaborate on customer-contributed technical content with users like you.

Repair

While you may never need your hardware repaired, NI understands that unexpected events may lead to necessary repairs. NI offers repair services performed by highly trained technicians who quickly return your device with the guarantee that it will perform to factory specifications. For more information, visit ni.com/repair.

Training and Certifications

The NI training and certification program delivers the fastest, most certain route to increased proficiency and productivity using NI software and hardware. Training builds the skills to more efficiently develop robust, maintainable applications, while certification validates your knowledge and ability.

- **Classroom training in cities worldwide** - the most comprehensive hands-on training taught by engineers.
- **On-site training at your facility** - an excellent option to train multiple employees at the same time.
- **Online instructor-led training** - lower-cost, remote training if classroom or on-site courses are not possible.
- **Course kits** - lowest-cost, self-paced training that you can use as reference guides.
- **Training memberships** and training credits - to buy now and schedule training later.

Visit ni.com/training for more information.

Extended Warranty

NI offers options for extending the standard product warranty to meet the life-cycle requirements of your project. In addition, because NI understands that your requirements may change, the extended warranty is flexible in length and easily renewed. For more information, visit ni.com/warranty.

OEM

NI offers design-in consulting and product integration assistance if you need NI products for OEM applications. For information about special pricing and services for OEM customers, visit ni.com/oem.

Alliance

Our Professional Services Team is comprised of NI applications engineers, NI Consulting Services, and a worldwide National Instruments Alliance Partner program of more than 700 independent consultants and integrators. Services range from start-up assistance to turnkey system integration. Visit ni.com/alliance.

Back to Top

Detailed Specifications

The following specifications are typical for the – 20 to 55 °C operating temperature range unless otherwise noted.

Network	
Network interface	10BaseT and 100BaseTX Ethernet
Compatibility	IEEE 802.3
Communication rates	10 Mbps, 100 Mbps, auto-negotiated
Maximum cabling distance	100 m/segment
RS-232 Serial Port	
Maximum baud rate	115,200 bps
Data bits	5, 6, 7, 8
Stop bits	1, 2
Parity	Odd, Even, Mark, Space
Flow control	RTS/CTS, XON/XOFF, DTR/DSR

SMB Connector (cRIO-9074 Only)	
Output Characteristics	
Minimum high-level output voltage	
With –100 µA output current	2.9 V
With –16 mA output current	2.4 V
With –24 mA output current	2.3 V
Maximum low-level output voltage	
With 100 µA output current	0.10 V
With 16 mA output current	0.40 V
With 24 mA output current	0.55 V
Driver type	CMOS
Maximum sink/source current	±24 mA
Maximum 3-state output leakage current	±5 µA
Input Characteristics	
Minimum input voltage	0 V
Minimum low-level input voltage	0.94 V
Maximum high-level input voltage	2.43 V
Maximum input voltage	5.5 V
Typical input capacitance	2.5 pF
Typical resistive strapping	1 kΩ to 3.3 V
Memory	
cRIO-9072, cRIO-9073	
Nonvolatile	128 MB
System memory	64 MB
cRIO-9074	
Nonvolatile	256 MB
System memory	128 MB
Reconfigurable FPGA	
cRIO-9072	
Number of logic cells	17,280
Available embedded RAM	432 kbits
cRIO-9073, cRIO-9074	
Number of logic cells	46,080
Available embedded RAM	720 kbits
Internal Real-Time Clock	
Accuracy	200 ppm; 35 ppm at 25 °C
Power Requirements	
Caution You must use a National Electric Code (NEC) UL Listed Class 2 power supply with the cRIO-9072/3/4.	
Recommended power supply	48 W, 24 VDC
Power consumption	20 W maximum
Power supply input range	19 to 30 V
Physical Characteristics	
If you need to clean the controller, wipe it with a dry towel.	
Screw-terminal wiring	0.5 to 2.5 mm 2 (24 to 12 AWG) copper conductor wire with 10 mm (0.39 in.) of

	Insulation stripped from the end
Torque for screw terminals	0.5 to 0.6 N · m (4.4 to 5.3 lb · in.)
Weight	929 g (32.7 oz)

Safety Voltages

Connect only voltages that are within these limits.

V terminal to C terminal	35 V max, Measurement Category I

Measurement Category I is for measurements performed on circuits not directly connected to the electrical distribution system referred to as MAINS voltage. MAINS is a hazardous live electrical supply system that powers equipment. This category is for measurements of voltages from specially protected secondary circuits. Such voltage measurements include signal levels, special equipment, limited-energy parts of equipment, circuits powered by regulated low-voltage sources, and electronics.

Caution Do not connect the system to signals or use for measurements within Measurement Categories II, III, or IV.

Safety Standards

This product is designed to meet the requirements of the following standards of safety for electrical equipment for measurement, control, and laboratory use:
IEC 61010-1, EN 61010-1
UL 61010-1, CSA 61010-1

Note For UL and other safety certifications, refer to the product label or the *Online Product Certification* section.

Electromagnetic Compatibility

This product meets the requirements of the following EMC standards for electrical equipment for measurement, control, and laboratory use:
EN 61326 (IEC 61326): Class A emissions; Industrial Immunity
EN 55011 (CISPR 11): Group 1, Class A emissions
AS/NZS CISPR 11: Group 1, Class A emissions
FCC 47 CFR Part 15B: Class A emissions
ICES-001: Class A emissions

Note For the standards applied to assess the EMC of this product, refer to the *Online Product Certification* section.

Note For EMC compliance, operate this product according to the documentation.

CE Compliance

This product meets the essential requirements of applicable European Directives, as amended for CE marking, as follows:
2006/95/EC; Low-Voltage Directive (safety)
2004/108/EC; Electromagnetic Compatibility Directive (EMC)

Online Product Certification

Refer to the product Declaration of Conformity (DoC) for additional regulatory compliance information. To obtain product certifications and the DoC for this product, visit ni.com/certification, search by module number or product line, and click the appropriate link in the Certification column.

Environmental Management

National Instruments is committed to designing and manufacturing products in an environmentally responsible manner. NI recognizes that eliminating certain hazardous substances from our products is beneficial not only to the environment but also to NI customers.

For additional environmental information, refer to the *NI and the Environment* Web page at ni.com/environment. This page contains the environmental regulations and directives with which NI complies, as well as other environmental information not included in this document.

Waste Electrical and Electronic Equipment (WEEE)

EU Customers At the end of the product life cycle, all products *must* be sent to a WEEE recycling center. For more information about WEEE recycling centers, National Instruments WEEE initiatives, and compliance with WEEE Directive 2002/96/EC on Waste Electrical and Electronic Equipment, visit ni.com/environment/weee.htm.

Battery Replacement and Disposal

This device contains a long-life coin cell battery. If you need to replace it, use the Return Material Authorization (RMA) process or contact an authorized National Instruments service representative.

After replacement, recycle the old battery. For additional information, visit ni.com/environment.

Hazardous Locations

U.S. (UL)	Class I, Division 2, Groups A, B, C, D, T4; Class I, Zone 2, AEx nL IIC T4
Canada (C-UL)	Class I, Division 2, Groups A, B, C, D, T4; Class I, Zone 2, Ex nL IIC T4
Europe (DEMKO)	Ex nL IIC T4 (part numbers beginning with 192172F and 198944 only)

Environmental

The cRIO-9072/3/4 is intended for indoor use only, but it may be used outdoors if mounted in a suitably rated enclosure.

Operating temperature (IEC 60068-2-1, IEC 60068-2-2)	– 20 to 55 °C

Note To meet this operating temperature range, follow the guidelines in the installation instructions for your CompactRIO system.

Storage temperature (IEC 60068-2-1, IEC 60068-2-2)	– 40 to 85 °C
	IP 40

Ingress protection	
Operating humidity (IEC 60068-2-56)	10 to 90% RH, noncondensing
Storage humidity (IEC 60068-2-56)	5 to 95% RH, noncondensing
Maximum altitude	2,000 m
Pollution Degree (IEC 60664)	2

Shock and Vibration

To meet these specifications, you must panel mount the CompactRIO system and affix ferrules to the ends of the power terminal wires.

Operating shock (IEC 60068-2-27)	30 g, 11 ms half sine 50 g, 3 ms half sine, 18 shocks at 6 orientations
Operating vibration, random (IEC 60068-2-64)	5 g_{rms}, 10 to 500 Hz
Operating vibration, sinusoidal (IEC 60068-2-6)	5 g, 10 to 500 Hz

Cabling

The following table shows the standard Ethernet cable wiring connections for both normal and crossover cables.

Ethernet Cable Wiring Connections			
Pin	Connector 1	Connector 2 (Normal)	Connector 2 (Crossover)
1	white/orange	white/orange	white/green
2	orange	orange	green
3	white/green	white/green	white/orange
4	blue	blue	blue
5	white/blue	white/blue	white/blue
6	green	green	orange
7	white/brown	white/brown	white/brown
8	brown	brown	brown

Back to Top

Pinouts/Front Panel Connections

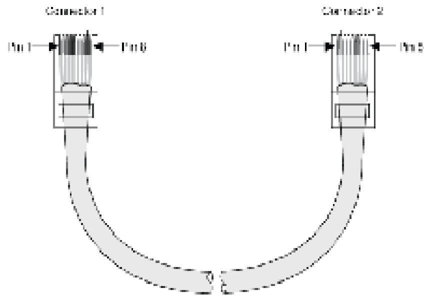

Ethernet Connector Pinout

Back to Top

Appendix I: Technical Datasheet of NI 9401

NATIONAL INSTRUMENTS

Technical Sales
United States
(866) 531-6285
info@ni.com

Print | E-mail this Page | Open Document as PDF

Requirements and Compatibility | Ordering Information | Detailed Specifications | Pinouts/Front Panel Connections

For user manuals and dimensional drawings, visit the product page resources tab on ni.com.

Last Revised: 2010-02-10 17:19:41.0

NI 9401

8 Ch, 5 V/TTL High-Speed Bidirectional C Series Digital I/O Module

- 8-channel, 100 ns ultrahigh-speed digital I/O
- 5 V/TTL, sinking/sourcing digital I/O
- Bidirectional, configurable by nibble (4 bits)
- Industry-standard 25-pin D-Sub connector
- Hot-swappable operation
- -40 to 70 °C operating range

Overview

The NI 9401 is an eight-channel, 100 ns bidirectional digital input C Series module for any NI CompactDAQ or CompactRIO chassis. You can configure the direction of the digital lines on the NI 9401 for input or output by nibble (four bits). Thus, you can program the NI 9401 for three configurations – eight digital inputs, eight digital outputs, or four digital inputs and four digital outputs. With reconfigurable I/O (RIO) technology (CompactRIO only), you can use the NI LabVIEW FPGA Module to program the NI 9401 for implementing custom, high-speed counter/timers, digital communication protocols, pulse generation, and much more. Each channel is compatible with 5 V/TTL signals and features 1,000 Vrms transient isolation between the I/O channels and the backplane.

The NI 9934 (or other 25-pin D-Sub connector) is required for use with the NI 9401 module. The module includes a screw-terminal connector with strain relief as well as a D-Sub solder cup backshell for creating custom cable assemblies.

Back to Top

Requirements and Compatibility

OS Information	Driver Information	Software Compatibility
Real-Time OS	NI-DAQmx	LabVIEW
Windows	NI-RIO	LabWindows/CVI
		Measurement Studio
		SignalExpress
		Visual Studio
		Visual Studio .NET

Back to Top

Comparison Tables

Product Name	Signal Levels	Number of Channels	Connectivity	Speed	Special Features
NI 9401	TTL	8	25-Pin D-Sub	100 ns	Bidirectional, nibble configurable
NI 9402	LV TTL	4	BNC	50 ns	Bidirectional shift on the fly by channel
NI 9403	TTL	32	37-Pin D-Sub	7 µs	Bidirectional, configurable by line

Back to Top

1/6 www.ni.com

Application and Technology

High-performance digital output and switching modules for NI CompactDAQ systems, CompactRIO embedded systems, and R Series expansion chassis provide extended voltage ranges and high-current-switching capacity for direct control of a wide array of industrial and automotive actuators. Each module features an integrated connector junction box with screw-terminal or cable options for flexible, low-cost signal wiring. All modules feature CompactRIO extreme industrial certifications and ratings including -40 to 70 °C operating temperatures and 50 g shock.

When used in CompactRIO, NI C Series digital output modules connect directly to reconfigurable I/O (RIO) field-programmable gate array (FPGA) hardware to create high-performance embedded systems. The reconfigurable FPGA hardware within CompactRIO provides a variety of options for timing, triggering, synchronization, digital waveform generation, or digital communication. For instance, with CompactRIO, you can implement a circuit to generate pulse-width modulation (PWM) outputs for controlling motors, heaters, or fans as well as to perform pulse code modulation encoding (PCME) for wireless telemetry applications.

The C Series hardware family features more than 50 measurement modules and several chassis and carriers for deployment. With this variety of modules, you can mix and match measurements such as temperature, acceleration, flow, pressure, strain, acoustic, voltage, current, digital, and more to create a custom system. Install the modules in one of several carriers to create a single module USB, Ethernet, or Wi-Fi system, or combine them in chassis such as NI CompactDAQ and CompactRIO to create a mixed-measurement system with synchronized measurements. You can install up to eight modules in a simple, complete NI CompactDAQ USB data acquisition system to synchronize all of the analog output, analog input, and digital I/O from the modules. For a system without a PC, CompactRIO holds up to eight modules and features a built-in processor, RAM, and storage for an embedded data logger or control unit. For higher-speed control, CompactRIO chassis incorporate a field-programmable gate array (FPGA) that you can program with LabVIEW software to achieve silicone-speed processing on I/O data from C Series modules.

Back to Top

Ordering Information

For a complete list of accessories, visit the product page on ni.com.

Products	Part Number	Recommended Accessories	Part Number
NI 9401 Counter FrontMount Acc			
NI 9401 with Front-Mount Accessories Requires: 1 Terminal Block ;	779351-01	**Terminal Block:** screwTerminal - NI 9924, Front-mount 25-pin D-SUB to screw terminals	781922-01

Back to Top

Support and Services

System Assurance Programs

NI system assurance programs are designed to make it even easier for you to own an NI system. These programs include configuration and deployment services for your NI PXI, CompactRIO, or Compact FieldPoint system. The NI Basic System Assurance Program provides a simple integration test and ensures that your system is delivered completely assembled in one box. When you configure your system with the NI Standard System Assurance Program, you can select from available NI system driver sets and application development environments to create customized, reorderable software configurations. Your system arrives fully assembled and tested in one box with your software preinstalled. When you order your system with the standard program, you also receive system-specific documentation including a bill of materials, an integration test report, a recommended maintenance plan, and frequently asked question documents. Finally, the standard program reduces the total cost of owning an NI system by providing three years of warranty coverage and calibration service. Use the online product advisors at ni.com/advisor to find a system assurance program to meet your needs.

Calibration

NI measurement hardware is calibrated to ensure measurement accuracy and verify that the device meets its published specifications. To ensure the ongoing accuracy of your measurement hardware, NI offers basic or detailed recalibration service that provides ongoing ISO 9001 audit compliance and confidence in your measurements. To learn more about NI calibration services or to locate a qualified service center near you, contact your local sales office or visit ni.com/calibration.

Technical Support

Get answers to your technical questions using the following National Instruments resources.

- **Support** - Visit ni.com/support to access the NI KnowledgeBase, example programs, and tutorials or to contact our applications engineers who are located in NI sales offices around the world and speak the local language.
- **Discussion Forums** - Visit forums.ni.com for a diverse set of discussion boards on topics you care about.
- **Online Community** - Visit community.ni.com to find, contribute, or collaborate on customer-contributed technical content with users like you.

Repair

While you may never need your hardware repaired, NI understands that unexpected events may lead to necessary repairs. NI offers repair services performed by highly trained technicians who quickly return your device with the guarantee that it will perform to factory specifications. For more information, visit ni.com/repair.

Training and Certifications

The NI training and certification program delivers the fastest, most certain route to increased proficiency and productivity using NI software and hardware. Training builds the skills to more efficiently develop robust, maintainable applications, while certification validates your knowledge and ability.

- **Classroom training in cities worldwide** - the most comprehensive hands-on training taught by engineers.
- **On-site training at your facility** - an excellent option to train multiple employees at the same time.
- **Online instructor-led training** - lower-cost, remote training if classroom or on-site courses are not possible.
- **Course kits** - lowest-cost, self-paced training that you can use as reference guides.
- **Training memberships** and training credits - to buy now and schedule training later.

Visit ni.com/training for more information.

Extended Warranty

NI offers options for extending the standard product warranty to meet the life-cycle requirements of your project. In addition, because NI understands that your requirements may change, the extended warranty is flexible in length and easily renewed. For more information, visit ni.com/warranty.

OEM

NI offers design-in consulting and product integration assistance if you need NI products for OEM applications. For information about special pricing and services for OEM customers, visit ni.com/oem.

Alliance

Our Professional Services Team is comprised of NI applications engineers, NI Consulting Services, and a worldwide National Instruments Alliance Partner program of more than 700 independent consultants and integrators. Services range from start-up assistance to turnkey system integration. Visit ni.com/alliance.

Back to Top

Detailed Specifications

The following specifications are typical for the range –40 to 70 °C unless otherwise noted. All voltages are relative to COM unless otherwise noted.

Input/Output Characteristics	
Number of channels	8 DIO channels
Default power-on line direction	Input
Input/output type	TTL, single-ended
Digital logic levels	
Input	
Voltage	5.25 V max
High, V_{IH}	2 V min
Low, V_{IL}	0.8 V max
Output	
High, V_{OH}, 5.25 V max	
Sourcing 100 µA	4.7 V min
Sourcing 2 mA	4.3 V min
Low, V_{OL}	
Sinking 100 µA	0.1 V max
Sinking 2 mA	0.4 V max
Maximum input signal switching frequency by number of input channels, per channel	
8 input channels	9 MHz
4 input channels	16 MHz
2 input channels	30 MHz
Maximum output signal switching frequency by number of output channels with an output load of 1 mA, 50 pF, per channel	
8 output channels	5 MHz
4 output channels	10 MHz
2 output channels	20 MHz
I/O propagation delay	100 ns max
I/O pulse width distortion	10 ns typ
Input current (0 V ≤ V_{in} ≤ 4.5 V)	±250 µA typ
Input capacitance	30 pF typ
Input rise/fall time	500 ns max
Overvoltage protection, channel-to-COM	±30 V max on one channel at a time; however, continued use at this level will degrade the life of the module.
MTBF	1,244,763 hours at 25 °C; Bellcore Issue 2, Method 1, Case 3, Limited Part Stress Method

Note Contact NI for Bellcore MTBF specifications at other temperatures or for MIL-HDBK-217F specifications.

Power Requirements	
Power consumption from chassis	
Active mode	580 mW max
Sleep mode	1 mW max
Thermal dissipation (at 70 °C)	
Active mode	580 mW max
Sleep mode	1 mW max

Physical Characteristics	
Weight	145 g (5.1 oz)

Safety

If you need to clean the module, wipe it with a dry towel.

Maximum Voltage [1]

Connect only voltages that are within the following limits.

Channel-to-COM	±30 V max on one channel at a time, Measurement Category I

Isolation Voltages

Channel-to-channel	None
Channel-to-earth ground	
Continuous	60 VDC, Measurement Category I
Withstand	1,000 V_{rms}, verified by a 5 s dielectric withstand test

Measurement Category I is for measurements performed on circuits not directly connected to the electrical distribution system referred to as MAINS [2] voltage. This category is for measurements of voltages from specially protected secondary circuits. Such voltage measurements include signal levels, special equipment, limited-energy parts of equipment, circuits powered by regulated low-voltage sources, and electronics.

Caution Do *not* connect the NI 9401 to signals or use for measurements within Measurement Categories II, III, or IV.

Safety Standards

This product is designed to meet the requirements of the following standards of safety for electrical equipment for measurement, control, and laboratory use:
IEC 61010-1, EN 61010-1
UL 61010-1, CSA 61010-1

Note For UL and other safety certifications, refer to the product label or the *Online Product Certification* section.

Hazardous Locations

U.S. (UL)	Class I, Division 2, Groups A, B, C, D, T4; Class I, Zone 2, AEx nC IIC T4
Canada (C-UL)	Class I, Division 2, Groups A, B, C, D, T4; Class I, Zone 2, Ex nC IIC T4
Europe (DEMKO)	EEx nC IIC T4

Environmental

National Instruments C Series modules are intended for indoor use only but may be used outdoors if installed in a suitable enclosure. Refer to the manual for the chassis you are using for more information about meeting these specifications.

Operating temperature (IEC 60068-2-1, IEC 60068-2-2)	– 40 to 70 °C
Storage temperature (IEC 60068-2-1, IEC 60068-2-2)	– 40 to 85 °C
Ingress protection	IP 40
Operating humidity (IEC 60068-2-56)	10 to 90% RH, noncondensing
Storage humidity (IEC 60068-2-56)	5 to 95% RH, noncondensing
Maximum altitude	2,000 m
Pollution Degree (IEC 60664)	2

Shock and Vibration

To meet these specifications, you must panel mount the system.

Operating vibration	
Random (IEC 60068-2-64)	5 g_{rms}, 10 to 500 Hz
Sinusoidal (IEC 60068-2-6)	5 g, 10 to 500 Hz
Operating shock (IEC 60068-2-27)	30 g, 11 ms half sine, 50 g, 3 ms half sine, 18 shocks at 6 orientations

Electromagnetic Compatibility

This product is designed to meet the requirements of the following standards of EMC for electrical equipment for measurement, control, and laboratory use:
EN 61326 EMC requirements; Industrial Immunity
EN 55011 Emissions; Group 1, Class A
CE, C-Tick, ICES, and FCC Part 15 Emissions; Class A

Note For EMC compliance, operate this device with shielded cables.

CE Compliance

This product meets the essential requirements of applicable European Directives, as amended for CE marking, as follows:
2006/95/EC; Low-Voltage Directive (safety)
2004/108/EC; Electromagnetic Compatibility Directive (EMC)

Note For the standards applied to assess the EMC of this product, refer to the *Online Product Certification* section.

Online Product Certification

Refer to the product Declaration of Conformity (DoC) for additional regulatory compliance information. To obtain product certifications and the DoC for this product, visit ni.com/certification, search by module number or product line, and click the appropriate link in the Certification column.

Environmental Management

National Instruments is committed to designing and manufacturing products in an environmentally responsible manner. NI recognizes that eliminating certain hazardous substances from our products is beneficial not only to the environment but also to NI customers.

For additional environmental information, refer to the *NI and the Environment* Web page at ni.com/environment. This page contains the environmental regulations and directives with which NI complies, as well as other environmental information not included in this document.

Waste Electrical and Electronic Equipment (WEEE)

EU Customers At the end of their life cycle, all products *must* be sent to a WEEE recycling center. For more information about WEEE recycling centers and National Instruments WEEE initiatives, visit ni.com/environment/weee.htm.

电子信息产品污染控制管理办法 （中国 RoHS）

中国客户 National Instruments 符合中国电子信息产品中限制使用某些有害物质指令 (RoHS)。
关于 National Instruments 中国 RoHS 合规性信息，请登录 ni.com/environment/rohs_china。
(For information about China RoHS compliance, go to ni.com/environment/rohs_china.)

[1] The maximum voltage that can be applied or output between any channel and COM without damaging the module or other devices.

[2] MAINS is defined as the (hazardous live) electrical supply system to which equipment is designed to be connected for the purpose of powering the equipment. Suitably rated measuring circuits may be connected to the MAINS for measuring purposes.

Back to Top

Pinouts/Front Panel Connections

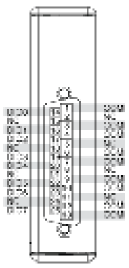

Back to Top

Appendix J: Properties of CompactRIO 9074

General properties of cRIO 9074

Product Name	cRIO-9074
Form Factor	CompactRIO
Product Type	Controller(Computing Device)
Part Number	779999-01
Operating System/Target	Real-Time
LabVIEW RT Support	Yes
CE Compliance	Yes

FPGA properties for cRIO 9074

FPGA	Spartan-3
Gates	2000000

Properties of chassis for cRIO 9074

Number of Slots	8
Integrated Controller	Yes
Input Voltage Range	19V, 30V
Recommended Power Supply: Power	48W
Recommended Power Supply: Voltage	24V
Power Consumption	20W

Physical specifications for cRIO

Length	28.97 cm
Width	8.81 cm
Height	5.89 cm
Weight	929 gram
Minimum Operating Temperature	-20 °C
Maximum Operating Temperature	55 °C
Maximum Altitude	2000 m

Appendix K: Connection of motors with 9501

In order to change the direction of motion for the joint, just reverse the cables for that specific joint. The table below tells about the sequence of motors for the each joint of this platform and also represents the type of joint that's rotational or pivot.

Motor and joints representation

Motor number	Joint number	Type of joint
1	1	Rotational
2	3	Rotational
3	3	Pivot
4	2	Rotational
5	2	Pivot

Sequence of connection for motors with 9501

Motor number	Slot number for 9501 on chassis
1	1
2	5
3	4
4	3
5	2

Appendix L: Wiring of chassis and cRIO

Wiring power to chassis

The external power supply is required to be connected with the chassis of cRIO 9074. This will give power to all the chassis slots. It is also provided with the reverse-voltage protection. Following steps should be followed for connecting power supply with the chassis:

- The COMBICON connector shown should be tightened in the chassis with the help of screw provided at its both ends.

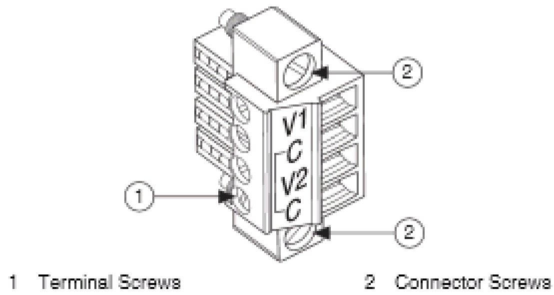

COMBICON (NI, 2010)

- Connect the positive (red) lead of power supply with the upper most terminal V1 and the negative (black) lead with the lower terminal C of the COMBICON.
- Insert the wires and tighten them with the screws available at the top of connector.

Power on cRIO 9074

When the chassis is first powered on, there will be two lights blinking, the power and the status lights. It is important to understand the LED indication on the chassis to avoid any problems during working.

LED indication on cRIO 9074

The LED indications are stated below:

LEDs indication for cRIO 9074 (NI, 2010)

- The power LED is lit when the cRIO 9074 is powered on indicating that the correct voltage is being supplied to the chassis
- The second LED is FPGA LED which is used for debugging of the application. To define these LED FPGA mode or NI RIO mode is used
- The third LED is the status LED. As the name tells that this LED indicates the status of the chassis. If this LED is off it means that it is under normal operation. The blinking of this LED indicates an error condition. The type of error then depends on the manner of blinking. The following table discusses the manner in which this LED flashes by relating it with the error condition.
- The user1 LED can be defined by the user depending upon the application. To define this, use RT LEDs in LabVIEW. However in our project this LED is not used.

Flashes Every Few Seconds	Indication
1	The chassis is un-configured. Use MAX to configure the chassis. Refer to the Measurement & Automation Explorer Help for information about configuring the chassis
2	The chassis has detected an error in its software. This usually occurs when an attempt to upgrade the software is interrupted. Reinstall software on the chassis. Refer to the Measurement & Automation Explorer Help for information about installing software on the chassis
3	The chassis is in safe mode because the SAFE MODE DIP switch is in the ON position or there is no software installed on the chassis
Continuously flashing	The chassis has detected an unrecoverable error. Contact National Instruments
continuously flashing or solid	The device may be configured for DHCP but unable to get an IP address because of a problem with the DHCP server. Check the network connection and try again. If the problem persists, contact National Instruments

LEDs indication for error condition (NI, 2012b)

Reset option for chassis

The table below tells about the reset options for the chassis available on cRIO 9074. This explains how it will behave on giving a reset. RIO devices setup utility is used for the reset option.

Chassis Reset Option	Behaviour
Do not auto load VI	Does not load the FPGA bit stream from flash memory
Auto load VI on device power up	Loads the FPGA bit stream from flash memory to the FPGA when the controller powers on
Auto load VI on device reboot	Loads the FPGA bit stream from flash memory to the FPGA when you reboot the controller either with or without cycling power.

Reset option for cRIO 9074 (NI, 2012b)

Configuring settings and obtaining IP for target

Various steps below indicate how to connect the hardware with the LabVIEW project (NI, 2012b):

1. Connecting with Ethernet/cross over cable:

The first step in connecting the hardware with the LabVIEW software is to connect the chassis to a network. This can be done by connecting the chassis with the Ethernet network using RJ-45 Ethernet port 1 on the front panel of the controller as shown in Fig 4.6. A crossover cable can also be used for connecting directly to a computer or laptop. The Ethernet cable is used for the communication of the host computer and the chassis. If they are not connected through some IP address they can communicate with each other through cross over cable. However for prior case the subnet for the host computer and the chassis should be same.

2. LabVIEW Real-time booting:

Before getting onto the configuration settings, it is important to make sure that the system is being booted in real time. There are several different boot modes that are available and are listed below:

- Normal boot mode
- IP reset
- Start-up application disabled
- Safe mode

- Uninstall mode

The real time target that is being used decides the booting of target. There are various helps documents available online for booting of the hardware system in real-time.

3. Configuring network by MAX:

The hardware/remote system that is being used must be assigned with a certain IP address for it to communicate with the host PC. For configuring network settings, the device is detected in Measurement and Automation Explorer (MAX). In MAX there is a tab of Remote System at the left side. By expanding that tab, the selection of particular remote system is done in order to configure it.

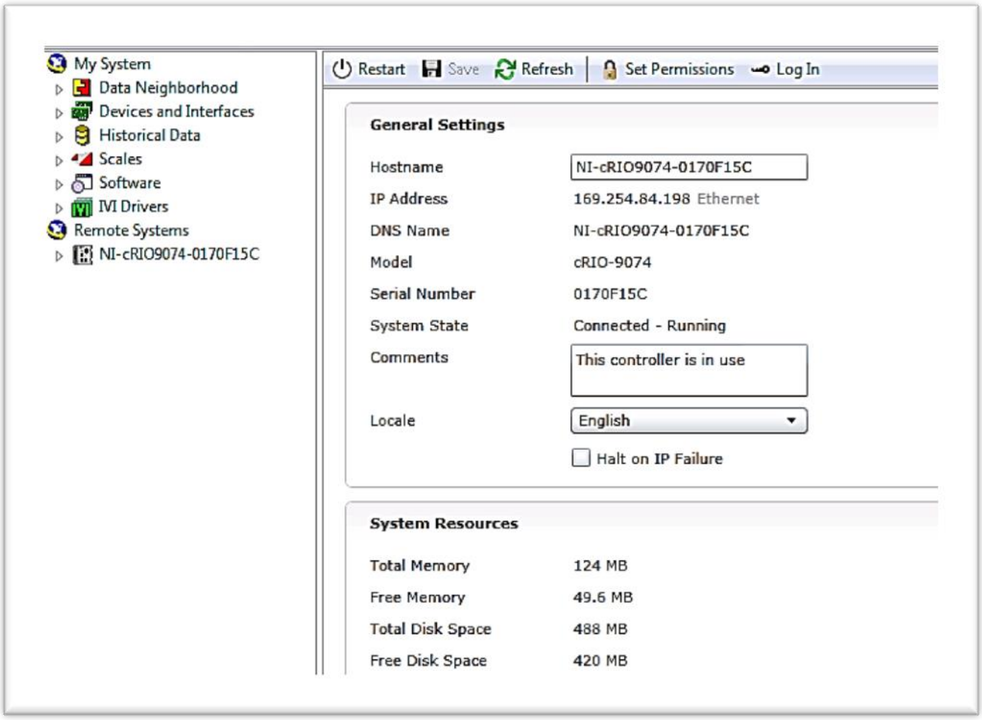

Measurement and automation explorer

It can be seen in the figure above that by expanding the remote targets; the particular device cRIO 9074 that is being used in the project is detected.

The IP address can be seen as 169.254.84.198. Once the IP is obtained the second thing is installing the software on the remote device. For this, expand the particular target on which the software has to installed, right click and select an option of add/remove software. Select the software that is required to be installed on the devices and start installing. After the installation is complete, on expanding software tab one can see different software installed as in figure below:

.

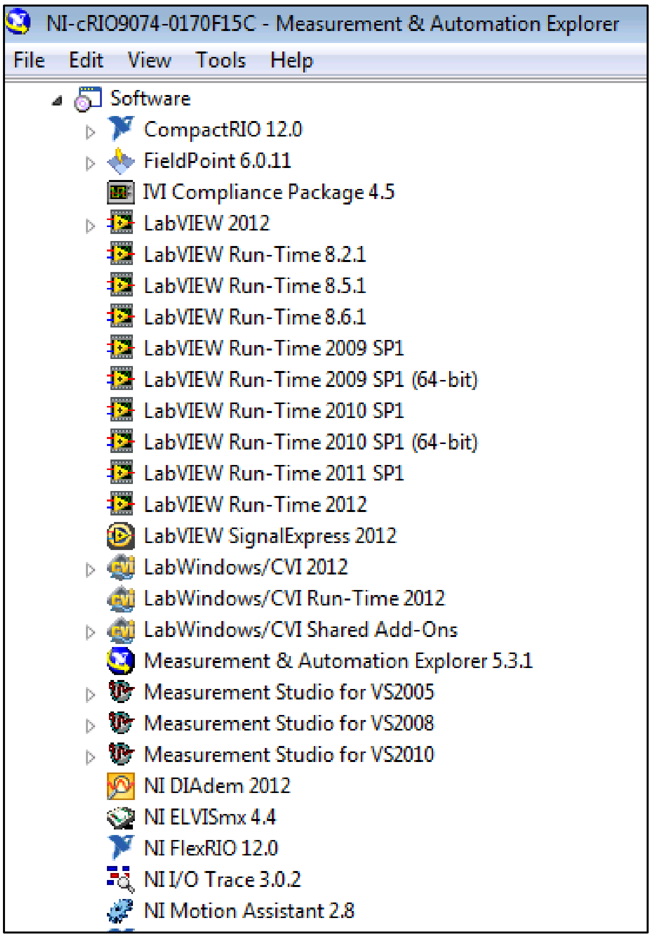

Different software's installed on remote device

Configuring LabVIEW project with hardware:

1. Once the software is installed on the target device, the chassis is mounted with all the input and output modules and the controller is powered up, the next step is adding the FPGA real-time device into the LabVIEW project to start with the graphical programming interface.

For this, create a new project in LabVIEW, and right click my computer under project explorer and select New>>Target and devices and shown in the figure below:

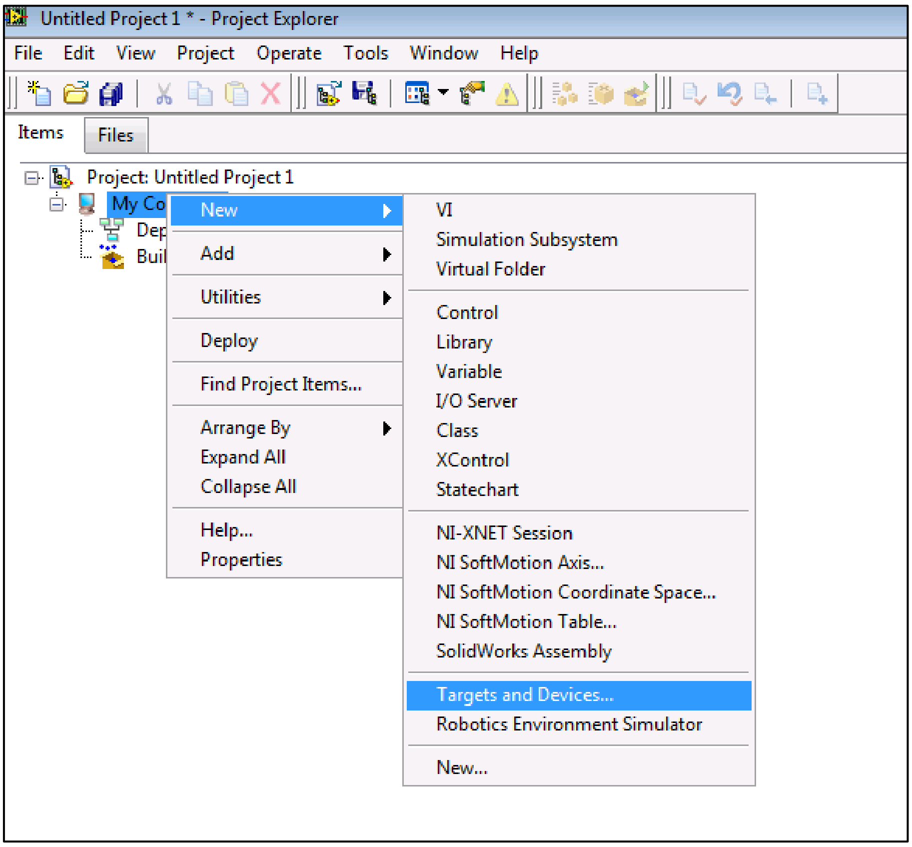

Adding target device in LabVIEW project

2. The installed FPGA devices will be shown when existing target/devices option is clicked. Expand the Real-Time CompactRIO option to find the particular controller under that as shown in the figure below:

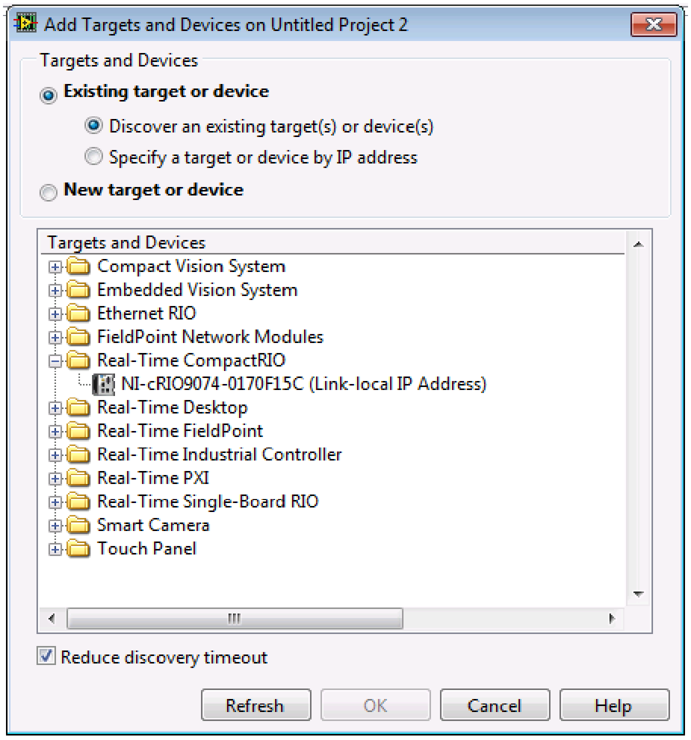

Existing target and devices

3. Select the specific controller and press ok. Another window will appear asking for the mode of interface. Select LabVIEW FPGA interface that enables to use C-series modules from LabVIEW FPGA VI's.

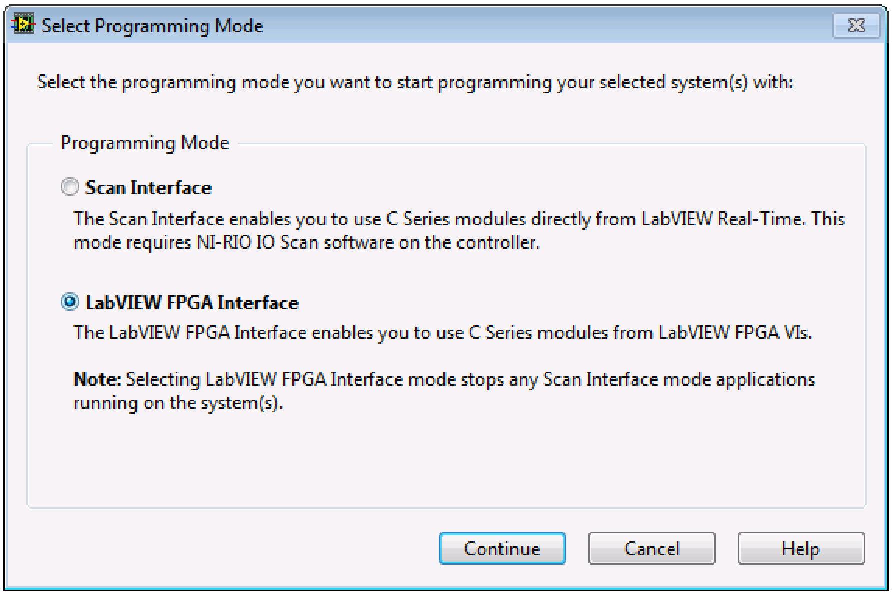

Selecting programming mode

4. On pressing continue after selecting the mode, the next step will be discovering of the chassis. The software will ask whether to discover or not. Then press discover C series modules as in figure:

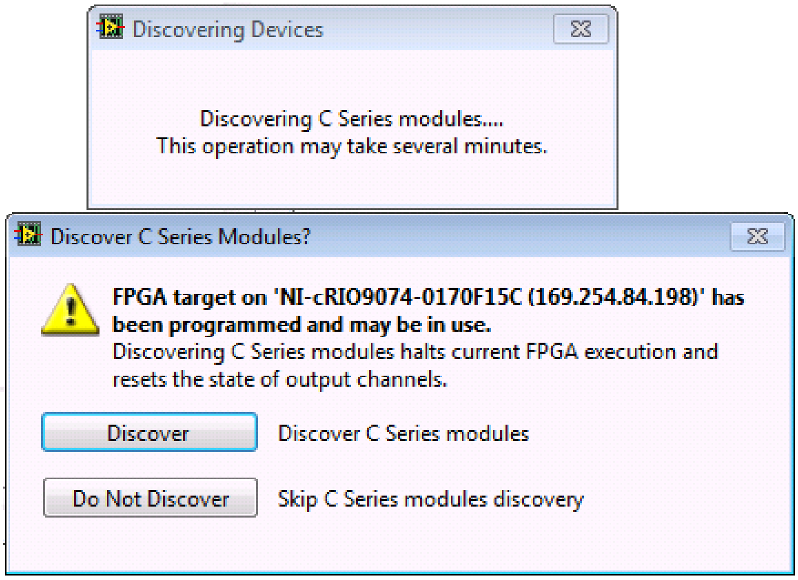

Discovering the modules

5. This process of discovering the modules will take few seconds. After that they will be automatically added in the main project as shown below:

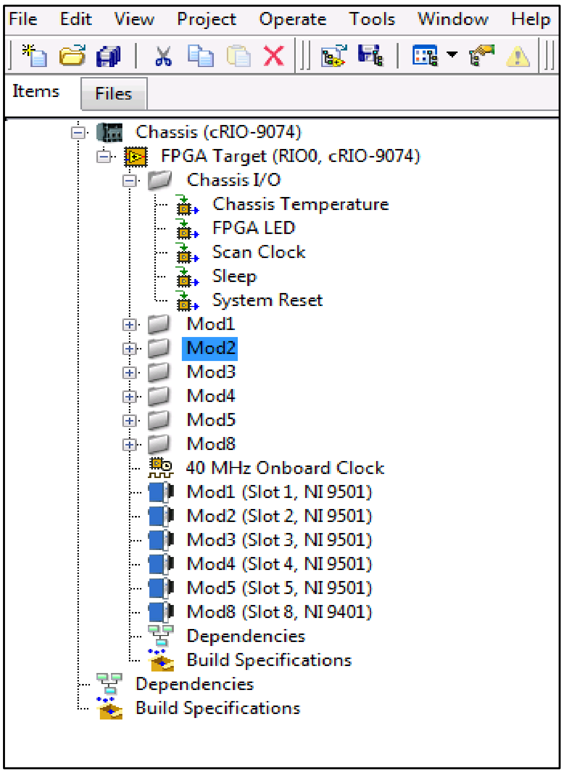

Modules in project file

6. At this stage the chassis, FPGA controller and all the drivers have been added into the project successfully. Now it is time to start with the programming of RT and FPGA VI's. Right click the chassis and click create new VI. That will be the RT VI. And for FPGA VI right click the FPGA target in the project and then build a new VI under that.

Appendix M: Mechanical parts and joint types of Robolink

Mechanical parts of Robolink

There are several different components of robotic arm that are also shown in fig: 3.1 above. These include (IGUS, 2012a):

- Joint types
- Articulated arm
- Angle sensors
- Actuators
- Draw wires
- Stepper motors
- Drive units
- Accessories
- Controls

The dimensional drawings and the exploded drawings of Igus robotic arm are attached in the appendix A. These parts are discussed below:

Joint types

There are four types of joint types that are offered by Igus with this robotic arm (IGUS, 2012a) namely: Swivel joint, rotating joint, Symmetric joint, Asymmetric joint. The specifications for each of them are discussed below:

Joint type	Version of joint	Range of joint
Swivel Joint	RL-50-PL1	+/- 90° swivel range
Rotating Joint	RL-50-TL1	+/- 90° rotating range
Symmetric Joint (2 axes joint)	RL-50-001	+/- 90° swivel range +/- 270° rotating range
Asymmetric Joint (2 axes joint)	RL-50-002	+130/- 50° swivel range +/- 270° rotating range

Type, version and joint limitation for IGUS robotic platform (IGUS, 2013)

These joints are provided with mechanical limits, but these can be removed. Rotating and pivoting joints, are shown below in the figures

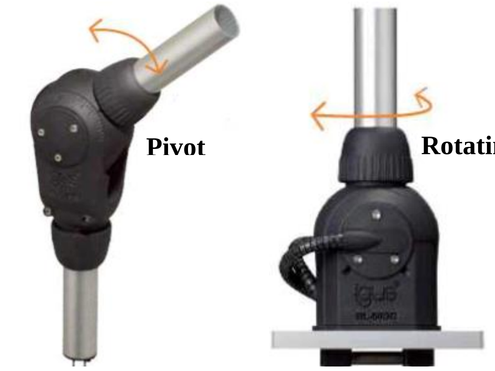

(a) Pivoting and Rotating joints (IGUS, 2012a)

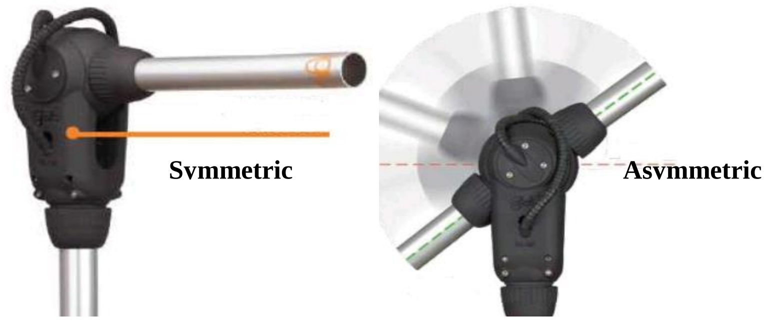

(b) Symmetric and Asymmetric joints (IGUS, 2012a)

Figure a) represents the symmetric 2 axis joint and Figure b) represents the Asymmetric 2 axis joint. The version of upper joint in Figure b) is RL-50-001, and the pivot angle allowed is +/-90°. For lower joint the version is RL-50-002 and the pivot angle allowed is +130°/-50°.

Articulated arms

With the help of these four joints, one can make one's own customized arm by choosing the link lengths and the type of material required for the link. There are basically three types of material available for the links:

- Aluminium tubes
- Fiberglass tubes
- Carbon-fibre tubes

Depending upon the utility the type is chosen. Standard tubes are made up of aluminium with a diameter of 26mm and the tube length can be customized by the user. The standard length of the link is 100mm and the tubes are hollow and with an

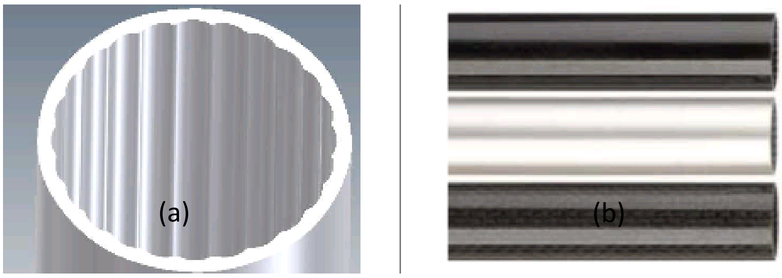

Inside of tube and Types of material (IGUS, 2012a)

interior contour. The purpose of this contour is to avoid the rotation on joint interface. Figure a) shows the interior contour of the connecting tubes used for the Robolink. Figure b) represents different types of materials that can be used for Robolink FGC, aluminium and CFC are shown respectively. Other specification like length of the tubes, visible tube length and rotating point distance are attached in the appendix B.

DOF of an articulated arm

The four types of joints results in 31 different types of configuration for the articulated arm. The versions can be configured for 1-5 degrees of freedom. The figures below represents articulated arms with different degrees of freedom.

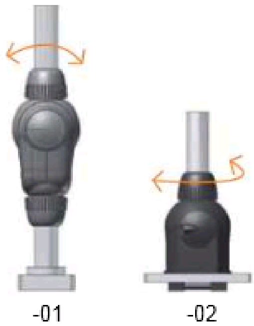

Articulated arm with 1 DOF (IGUS, 2012a)

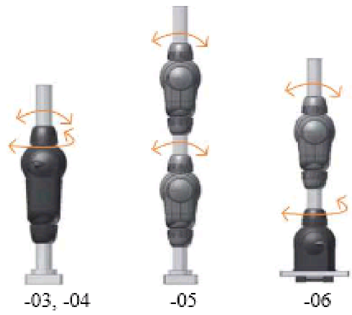

Articulated arm with 2 DOF (IGUS, 2012a)

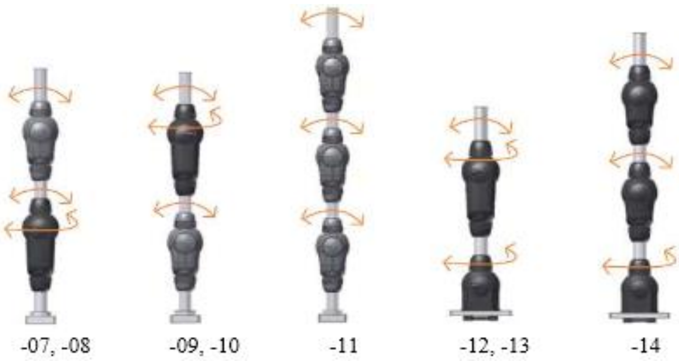

Articulated arm with 3 DOF (IGUS, 2012a)

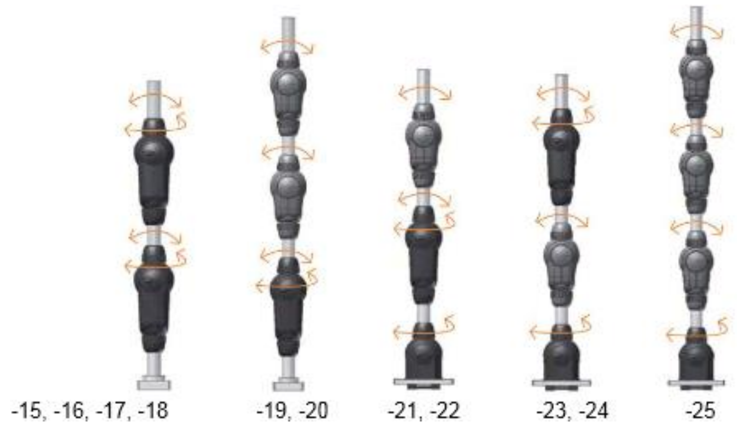

Articulated arm with 4 DOF (IGUS, 2012a)

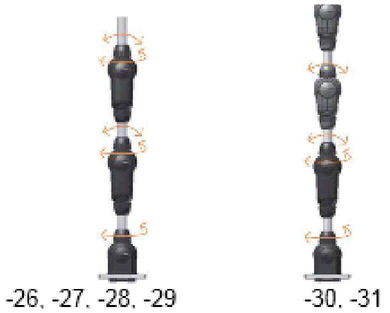

Articulated arm with 5 DOF (IGUS, 2012a)

The technical data for these articulated arms from 01-31with a link length of 100mm are attached in the appendix C. All articulated arms can be ordered with option of the angle sensors.

Angle sensors

The optional sensors provided with the Robolink are magnetic incremental encoders. Each axis has a magnetic ring and a Hall sensor associated with it. The specification of the magnetic rings is different for swivel and rotating motion. For the swivel motion it has 31 pole pairs and one additional South Pole, whereas for rotating motion it has 29 pole pairs in total and an additional pole. Figure below shows the magnetic ring and sensor unit for two axis joints:

Magnetic rings for swivelling and rotating respectively (IGUS, 2012a)

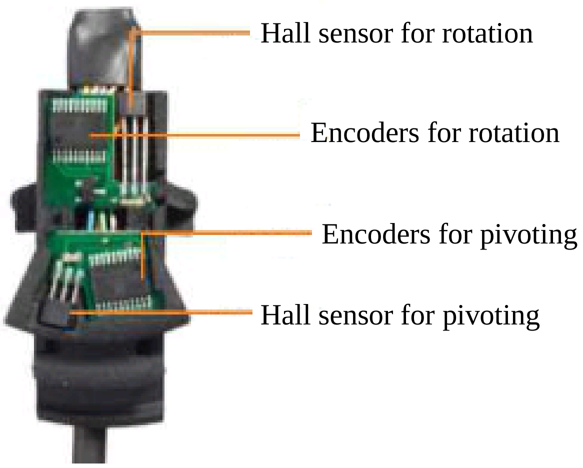

Sensor unit (IGUS, 2012a)

The resolution of this encoder per axis is as follow:

- Swivel motion 4960 counts per revolution, resolution 0.073 degrees
- Rotating motion 4640 counts per revolution, resolution 0.078 degrees

Each joint has incremental encoders. The specification of particular arm for pivoting and rotation are given below (Fontys, 2013):

- **Pivoting**
  - 31 pole pairs
  - 40 pulses/pole pairs
  - 160 positions/pole pairs
  - 1240 pulses/revolutions
  - 4690 positions/revolutions
- **Rotation**
  - 29 pole pairs
  - 40 pulses/pole pairs
  - 160 positions/pole pairs
  - 1160 pulses/revolutions
  - 4640 positions/revolutions
- **Accuracy**
  - For pivoting: 0.0726 degrees
  - For rotation: 0.0776 degrees

The main function of the incremental encoder is to convert the angular position of the joint into digital information. It provides information about the motion of the joint and further information about speed, distance and position can also be deduced. It has three digital outputs: A, B and Index. The pulses A and B are quadrature outputs, as they are 90° out of phase from each. Figure below shows A, B and index pulses for the encoder.

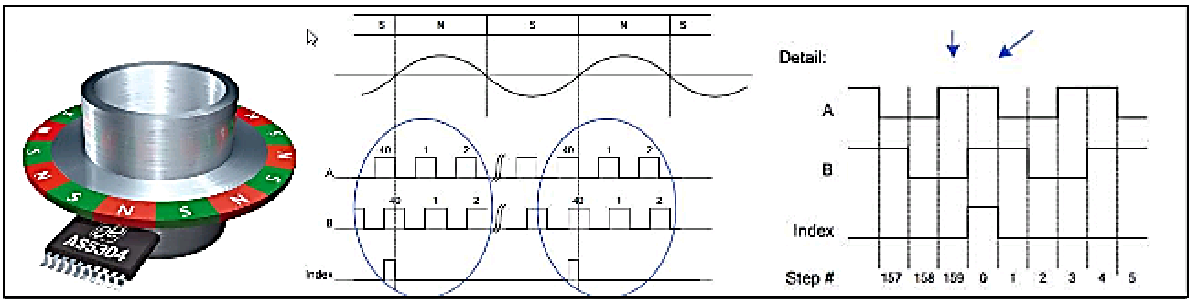

A/B and index signals for the encoder (IGUS, 2012a)

The datasheet for the Hall sensors and the configuration of sensor line that represents the colour coding of wires for pivoting as well as rotating joints is attached in appendix D.

End effectors

The Robolink system is not provided with end effectors, however one can connect various end effectors to the last link of the system if required. There are various pneumatic and electrical grippers recommended for this robotic arm. FESTO® and SCHUNK® provide pneumatic and electrical grippers for these arms. A standard adaptor is provided by IGUS® for these grippers. Figure below shows some of the popular gripper used.

Standard pneumatic grippers used (IGUS, 2012a)

In this project there is no gripper or effector. As the main focus of this project was on the behavioural movement of robot, no end effector was required.

Draw wires

The system of driving joint movement is by draw wires that are generally made from Dyneema® (IGUS, 2013). There is a special coating that ensures long life and less friction of these wires. The specifications of the wire used are as follow (IGUS, 2012a):

- 12-strand braiding
- Diameter=2mm
- Breaking strength=3.500N
- Operating elongation=1% approx.

These wires are held in the drive wheel with the help of a nipple crimped on to the end can be seen in figure below:

Assembled drive wheel with wire and wire with nipple (IGUS, 2012a)

This nipple is fitted into the drive wheels shown in fig (a) below, so as to hold it properly. The tension in the wires should be adequate to avoid play in the joint. Typically it is between 5-10N at idle (IGUS, 2012a). If the tension in the wires is too high, the working life is reduced because of wear and friction. The robotic arm is provided with the tools to adjust the tension of these wires.

The robotic arm consists of multiple joints that are combined together in series. All the joints are independent from each other because of the sequence through which wires are fed into these joints. There is a limitation for the number of joints that can be added in series, because only 4 wires can be fed through the lower joint. The pre-assembled structure for the wires passing through lower joint is shown in the figures below:

(a, b, c, d): Feeding of wires through joints (IGUS, 2012a).

Figure (a, b, c, d) shows the feeding of wires through the lower joint of articulated arm platform. Fig (a) shows that two wire pairs are being fed through the lower joint. Fig (b) shows upper connecting element for guiding the wire. Fig (c) shows Bowden cable segments for parallel feed-through and Fig (d) shows lower connecting element of the robotic arm (IGUS, 2012a).

Stepper motors

Igus® uses stepper motors as the drive system for this articulated arm. However alternate drive systems are also possible to control the motion of this platform. The features of the stepper motor used are as follow (IGUS, 2013.):

- Two phase hybrid stepper motors that are bipolar
- Comes with plug/stranded wires
- It has an option of encoder/brake

The stepper motors used for this project is: MOT-AN-S-060-020-056-L-LAAAA.

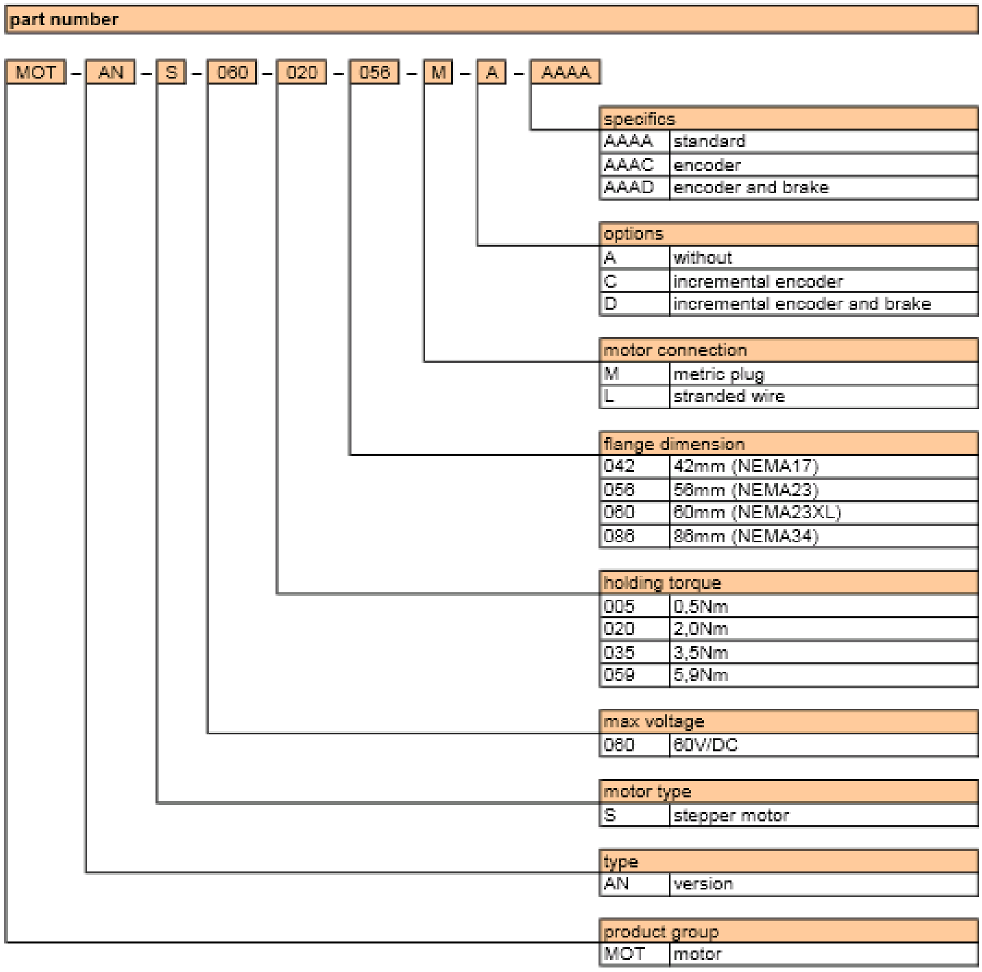

Product code layout for stepper motors (IGUS, 2013)

The stepper motor used for this project has version AN, maximum DC voltage of 60V, holding torque is 20Nm, and flange dimension is 56mm (NEMA 23) with motor connection of stranded wires. The technical drawings and data specifications are attached in the appendix E. Table below shows the key data for these motors

Motor	**NEMA 23**
Maximum voltage	60 VDC
Nominal voltage	24-48 VDC
Nominal current	4.2A
Holding torque	2 Nm
Distance over hubs	56mm

Specifications for stepper motor drives (IGUS, 2013.)

Fig. below shows the stepper motor used in the project with stranded conductor version. It has four coloured wires. Table below shows the colour coding of wires.

Stepper motors with four stranded wires (IGUS, 2012a)

Pins	Colour	Signals
1	Brown	A/
2	White	A
3	Blue	B
4	Black	B/

Colour representation of motor wires

Drive modules

The stepper motors used are equipped with a planetary gear and a tensionable drive wheel system by the manufacturers. The reason for this is to increase the torque of motors. Table below shows the configuration of gears used (IGUS, 2012b):

Complete drive module (IGUS, 2013)

Motors	Reduction gearing
NEMA 23	1:16

Gear ratio of stepper motors (IGUS, 2012b)

Drive units

There is an option of assembling the drive modules into drive units. This makes the whole mechanism assembled. This process of fitting is done at factory. This complete module consists of articulated arm and tested drive units by Igus®. The complete assembly is shown Fig. below:

Complete system (IGUS, 2012b)

There are some user selectable options that are available while ordering this complete system (IGUS, 2012b).

- Selection of DOF: 3-5 degrees of freedom can be selected depending upon the requirement
- Selection of angle sensors: joints of the system can be selected with or without the angle sensors.
- Adjustable link lengths: the length of the links can be selected from 100mm to 1000mm
- Selection of motors: two options for motor selections are available: NEMA17 or NEMA23
- End effectors can also be added depending upon the requirement like various grippers etc.

The units with the complete specifications are in appendix F.

Accessories/Spare parts

There are many other accessories that are provided by Igus® depending upon the requirement e.g. rope end fitting, tensionable drive wheels, flange shaft blocks, rope guides outside/inside, guide rollers, rope tensioners and many more.

Torque and force

Torque and force are important parameters to be considered as two different motions are made i.e. rotational and pivoting. At Igus® the data below is available (Fontys, 2013):

- For pivoting movement 12 Nm at force 600N on the rope
- For rotating movement 5Nm at force 300N on the rope

- Torque for pivoting movement +/-27.88 Nm
- For rotating movement +/-15 Nm

Rope management

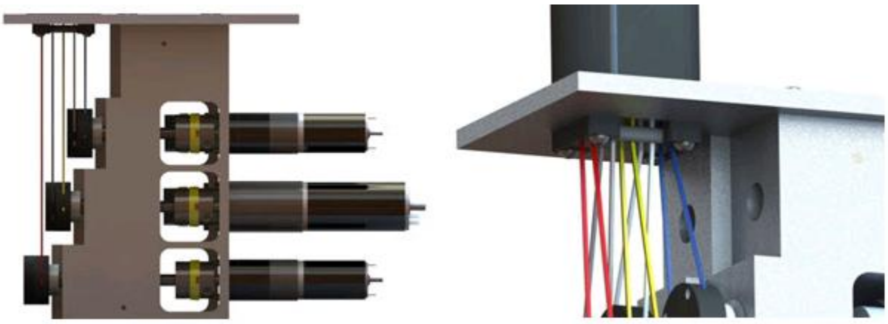

Rope guiding system used in arms (Fontys, 2013)

The whole system is driven by cables as discussed above. Figure above shows the guiding arrangement of the cables. Different colours of cables are used for each motor so that it is easy to distinguish that which joint is connected to which motor. The details of the rope channels are in appendix F

Pictorial representation of motor to drive wheel

Figure below shows the whole assembly from motors to drive wheel

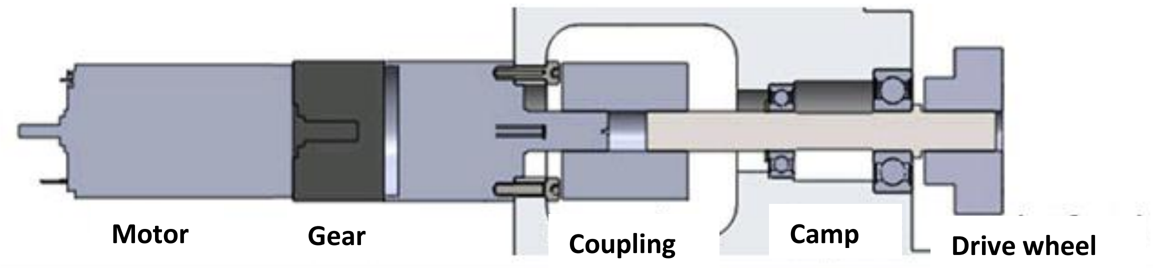

Motor to drive wheel (IGUS, 2013)

Appendix N: Ethical approval and consent form

Ethical approval

Middlesex University London

Form D: Declaration Form

This form should be given to your supervisor along with your project proposal. It must also be included in your Project Report.

Student Project: Ethical Approval Request

Name: **Sara Baber Sial**	Student ID: **M00423635**	Date:**12-07-2013**

Supervisor: **Dr. Aleksandar Zivanovic**

Title: **Communicating Simulated Emotional States of Robots by Expressive Movements**

Ethical Approval Statement:

Declaration A

(i) I have studied the Ethical Approval section.
(ii) I have established that my study does not require additional human participation.
(iii) I agree to re-apply for approval if the nature or goals of my project change.

☑

Declaration B

Project Goals involving human participation:

Observing the robot to see the change in motion with changing parameters.

Filling in the observed movements on various emotional models.

(i) I have studied the Ethical Approval section.
(ii) My study involves human participation through
- observation
- questioning.

(iii) Participants will be selected without coercion (see Chart 1).
(iv) I will obtain informed consent (see Chart 2) from each participant using Form C.
(v) I have arrangements in place for the protection of personal data (see Chart 3).
(vi) I agree to re-apply for approval if the nature or goals of my project change.

☑

Declaration C

My project does not fulfil the conditions for fast track Ethical Approval and I am applying separately to the Ethics Committee.

Note: to make an application to the Ethics Committee, you need to complete **Form E - Application for Ethical Approval** (download from http://tinyurl.com/sst-ethics)

☐

Student Signature.......[signature]....... Date 12-07-2013

Supervisor's Signature.......[signature]....... Date 12-07-2013.

Consent form

Middlesex University

Middlesex University School of Science and Technology

Research Informed Consent Form

This consent form, a copy of which has been given to you, is only part of the process of informed consent. It should give you the basic idea of what the research is about and what your participation will involve. If you would like more detail about something mentioned here, or information not included here, please ask. Please take the time to read this form carefully and to understand any accompanying information.

Research Project Title

Communicating Simulated Emotional States of Robots by Expressive Movements

Researcher

The team conducting this study are: Ms. Sara Baber Sial and Dr Aleksandar Zivanovic.

Experiment Purpose

The goal of the experiment is to explore how the participant's grasps different emotional states of the robotic arm based on its movements and gestures.

Participant Recruitment and Selection

University staff and students, healthy people.

Procedure

This experiment will take you about 15-20 minutes (including completing a simple questionnaire at the end of the experiment):

Experiment:

> The robotic arm will be moved several times with different emotions. The participants have to mark the emotional state they think the robot has at that particular time on three different models in the questionnaire. That gives the idea of how they perceive the motion of robot in terms of its behavior.

Data Collection

Participants will be assessed through a questionnaire using the methodology suggested by three different models that are: Russell's model of mood, Tellegen-Watson-Clark model and PAD scale, to measure the emotional state of embodiment.

Confidentiality

You must supply your name and sign this form so that the university can keep a record of your participation in this experiment. All results of this experiment are anonymous and your name does not form part of the data.

Likelihood of Discomfort

Very unlikely you will feed any discomfort. You will be just observing a robot and marking its gesture on the questionnaire without doing or touching anything.

Finding out about Results

If you would like to find out the results at the end of the project, please contact the researchers.

Agreement

Your signature on this form indicates that you have understood to your satisfaction the information regarding participation in the research project and agree to participate as a participant. In no way does this waive you legal rights nor release the investigators, sponsors, or involved institutions from their legal and professional responsibilities. You are free to not answer specific items or questions in interviews or on questionnaires. You are free to withdraw from the study at any time without penalty. Your continued participation should be as informed as your initial consent, so you should feel free to ask for clarification or new information throughout your participation. If you have further questions concerning matters related to this research, please contact the researchers.

________________________ _______________

Participant Date

________________________ _______________

Investigator/Witness Date

A copy of this consent form has been given to you to keep for your records and reference.